ING

Hypogene Evolution of the Toquepala Porphyry Copper-Molybdenum Deposit, Moquegua, Southeastern Peru

PAUL L. ZWENG — *Consulting Economic Geologist, Redwood City, California*
ALAN H. CLARK — *Department of Geological Sciences, Queen's University, Kingston, Ontario, Canada*

ABSTRACT

The Toquepala Porphyry Copper-Molybdenum Deposit of southern Peru developed during Paleocene to early Eocene time (52-56 Ma) as the terminal stage in the local evolution of the subaerial Upper Cretaceous to Paleogene Toquepala Group in a calc-alkaline to shoshonitic volcano-plutonic arc. The deposit is centered on an intrusive center defined by a succession of hypabyssal dacite (T, Main, L/M, and Late) porphyries, dacite agglomerate, latite porphyry stocks and dikes, and associated alteration and mineralization features related to four (early, tourmaline, main, and late) hydrothermal events.

Early stage alteration and mineralization largely preceded intrusion of the Main and L/M Porphyries. This stage is characterized by potassic and sodic alteration assemblages and by chalcopyrite-pyrite and rare bornite-chalcopyrite mineralization which contributed less than 5 percent of the copper to the orebody. A voluminous sulfide-barren tourmaline breccia pipe and scarce tourmaline-quartz veinlets formed during the tourmaline stage and after emplacement of all but the late dacite porphyries. Tourmaline breccia contains angular to rounded fragments altered to quartz-sericite and cemented in a tourmaline-quartz matrix. Reopening of tourmaline breccias and fracturing of wallrocks allowed main stage fluids to deposit essentially all of the molybdenite and most of the chalcopyrite in the deposit without wallrock alteration. Emplacement of the dacite agglomerate and latite porphyry followed formation of the hypogene orebody but was coeval with widespread quartz-sericite-pyrite andalusite alteration, more localized advanced argillic alteration, and high-sulfur assemblages of the late stage. Considerable ore was lost during this waning stage as large-scale phreatomagmatic eruptions associated with the intrusion of latite porphyry generated a 300-meter-wide pebble breccia pipe and pebble dike swarm.

Hydrothermal fluids of the first three stages were of moderate temperature (335–480° C) and high salinity (extreme in the tourmaline stage) and were boiling. A change from lithostatic to near-hydrostatic pressure conditions occurred near the end of the early stage, and all subsequent hydrothermal stages formed at epithermal-type pressures of 300 bars or less. Late stage fluids were significantly cooler (220-370° C) and lower in salinity and did not boil; they may record encroachment of oxygenated meteoric waters into a decaying juvenile hydrothermal system.

The four hydrothermal stages correspond closely to the early, transitional, and late stages documented by Gustafson and Hunt (1975) at El Salvador, Chile, indicating that both deposits followed broadly similar evolutionary trends. Differences between these deposits reflect the degree of development of each hydrothermal event: The early stage at Toquepala is poorly developed and contributed little copper, but three quarters of the total hypogene copper at El Salvador was deposited during that deposit's early stage. Similarly, the transitional stage at El Salvador is poorly developed, but the corresponding tourmaline and main stages at Toquepala produced large volumes of tourmaline breccia and the bulk of the hypogene orebody at that deposit.

Thermodynamic and mass-transfer calculations by Candela (1989a, b) and Cline and Bodnar (1991) suggest that the weak and copper-poor early stage at Toquepala may reflect the low pressure (300 bars) at which aqueous fluids exsolved from magma, reducing both their relative volume and their concentrations of chloride and copper. Later fluids exsolved before late stage time were much more voluminous and extracted greater quantities of copper, molybdenum, and boron from the melt. The greater amounts of copper precipitated during the early stage at El Salvador may reflect greater depth (600-1,000 bars), resulting in exsolution of greater volumes of copper- and chloride-rich fluids during initial retrograde boiling. Both Toquepala and El Salvador share comparable intensities of late stage features, suggesting that the difference in depth between these two systems did not have a profound effect on the waning stages of hydrothermal activity.

INTRODUCTION

Large bodies of hydrothermal breccia in which tourmaline is a major matrix constituent are a characteristic feature of the Central Andean Orogen. Occurring as isolated or gregarious pipes with copper and related mineralization (Sillitoe and Sawkins, 1971) and as early stages of the tin-polymetallic centers of the Bolivian-Peruvian tin belt (Grant and others, 1977), tourmaline breccias are also represented in numerous porphyry copper and copper-molybdenum deposits in Chile and Peru (Sillitoe, 1985) where they and associated tourmaline and tourmaline-quartz veinlets range from subsidiary components as at El Salvador (Gustafson and Hunt, 1975) to the dominant mineralization facies as at Disputada-Las Bronces (Warnaars and others, 1985). The intimate association of tourmaline breccias and stringers with molybdenite-rich B quartz veinlets at El Salvador (the transitional stage of Gustafson and Hunt, 1975) is a feature shared by other porphyry copper and copper-molybdenum deposits in this region and elsewhere. There is little documentation of the temporal relationships of tourmaline breccias in those porphyry deposits where they are best developed, however, and the development of detailed models for the deportment of boron and molybdenum relative to copper in the retrograde boiling environment has been inhibited (for example, Candela, 1989a, b).

The Toquepala Deposit of southeastern Peru (fig. 1) has

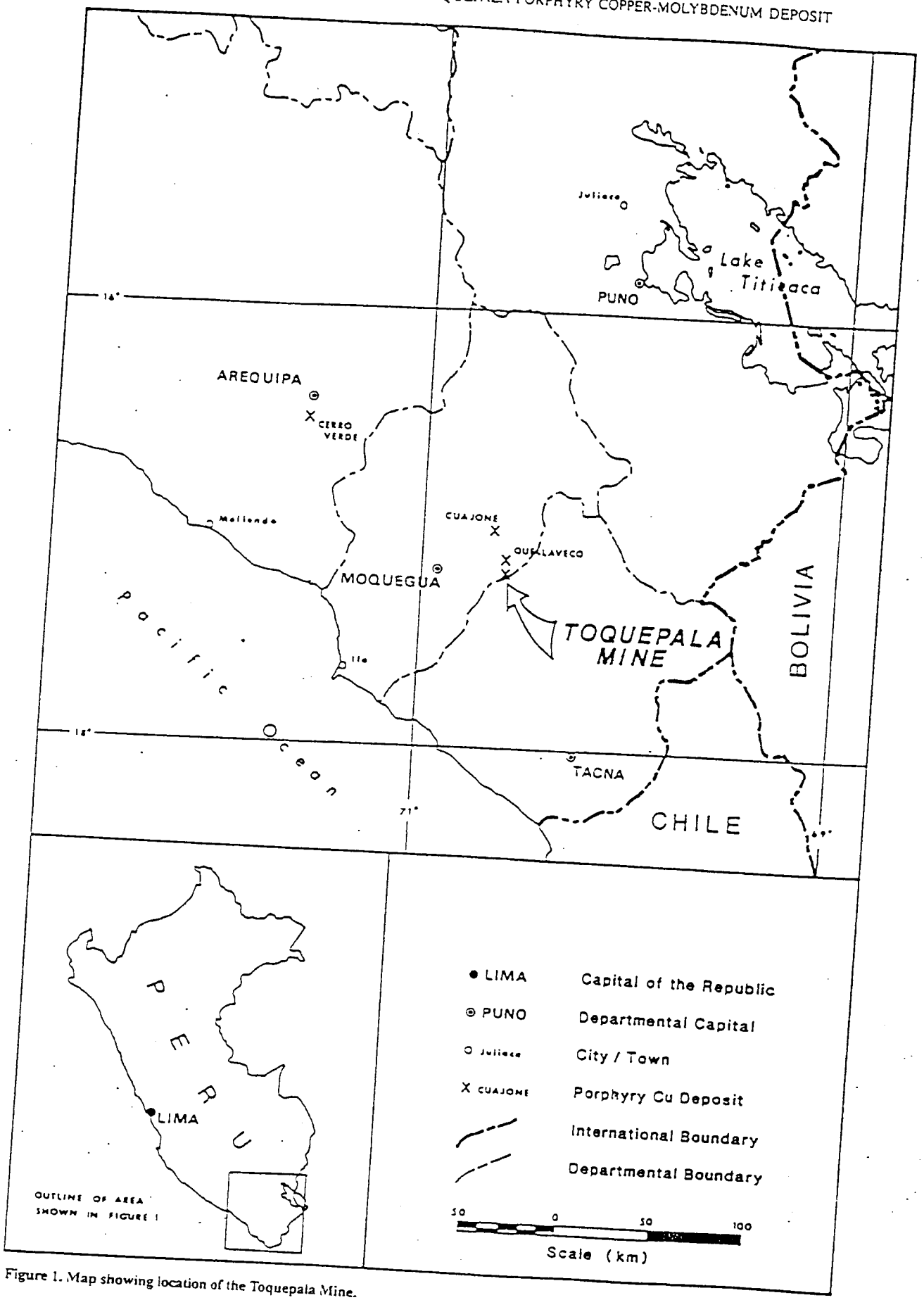

Figure 1. Map showing location of the Toquepala Mine.

Moreover, features observed in deep drill core provide a basis for clarification of the evolution of the upper half of the deposit. This is critical because late-stage veining and hydrolytic alteration together with intense argillic alteration directly associated with supergene sulfide enrichment of the orebody constitute an intense overprint in most exposures in the open pit, masking the nature and extent of early alteration-mineralization facies in the upper parts of the deposit. The more complete picture revealed by drilling necessitates significant modification of the model outlined by Richard and Courtright.

The regional setting of the Toquepala Deposit (Clark and others, 1990a), local post-mineralization geological and landform history (Tosdal and others, 1981, 1984), specific facies of hydrothermal brecciation (Clark, 1990), and age and geomorphological environment of important supergene sulfide enrichment in the district (Clark and others, 1990b) have been documented elsewhere.

Production at Toquepala over the period from 1960 to 1994 has aggregated over 465,000,000 tons of predominantly supergene-enriched sulfide ore with a mean grade of 1.07 percent copper and 0.034 percent MoS_2. The ores mined since 1988 have contained on average 0.83 percent copper and 0.030 percent MoS_2 (F.B. Stevenson, personal communication, 1994) and exhibit only minor supergene upgrading of hypogene sulfide assemblages. Inspection of deep drill cores reveals that molybdenite is enriched in the lower part of the deposit, and Toquepala may therefore exhibit an overall hypogene copper-molybdenum ratio corresponding to the molybdenum-rich limit of the porphyry copper field outlined by Sillitoe and others (1984). Approximately 30 to 40 tons of silver have been recovered annually from copper concentrates since 1987.

Bench elevations in the Toquepala Open Pit are expressed in meters above sea level and locations of observations or samples are reported in terms of geographic quadrant and date, thus "3160m-NW(1982)" refers to a feature exposed in 1982 in the northwestern area of the 3,160-meter bench. Locations of samples from drill core are recorded in meters above sea level.

GEOLOGICAL SETTING OF MINERALIZATION

The Toquepala Deposit and its broadly coeval (Clark and others, 1990a) companions Cuajone and Quellaveco (fig. 1) are

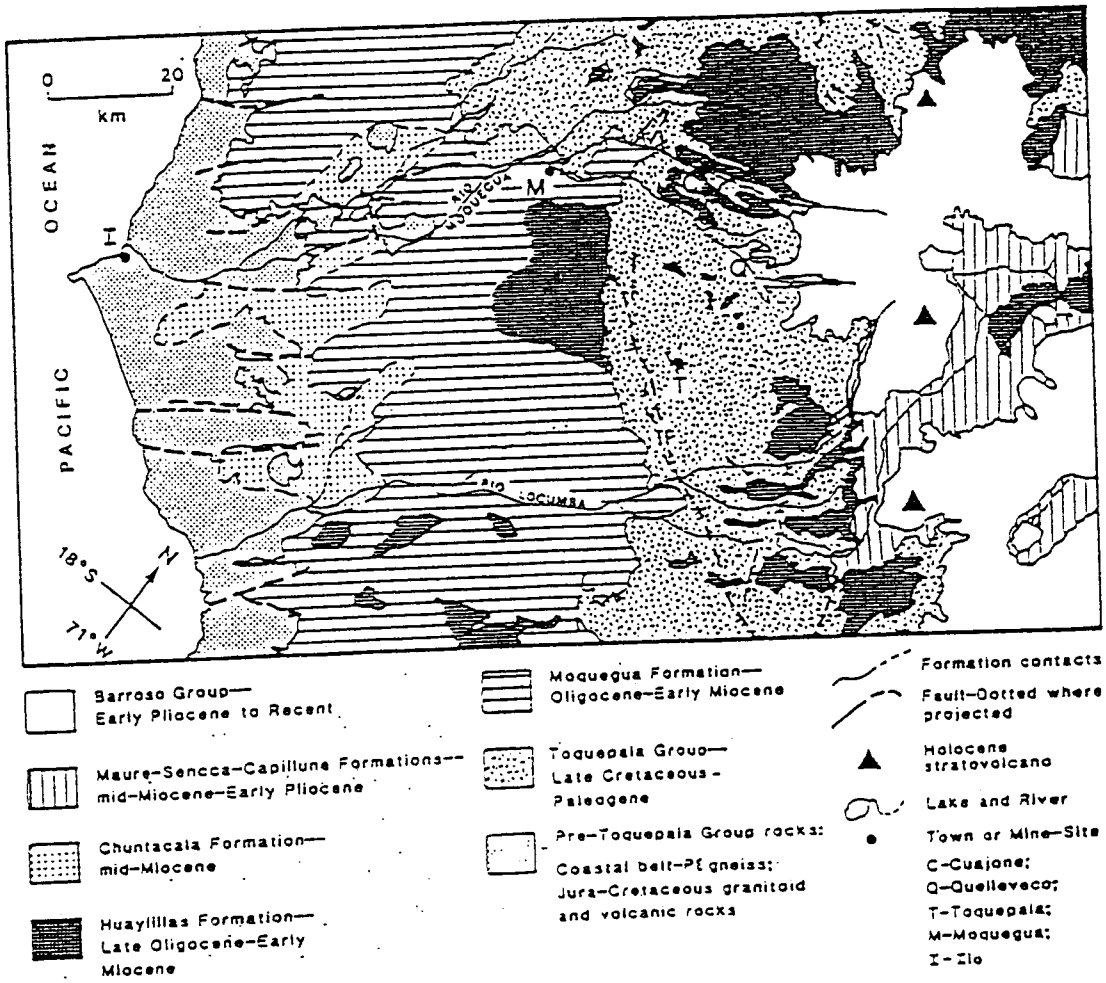

Figure 2. Simplified geology of the Pacific Slope of the Cordillera Occidental, southernmost Peru (modified from Tosdal and others, 1981). Toquepala Group includes granitoid intrusions of the Toquepala segment of the Peruvian Coastal Batholith.

exposed on the oceanward slopes of the Central Andean Cordillera Occidental (Western Cordillera) at altitudes of approximately 3,000 to 3,700 meters immediately southwest of the dormant and extinct Pliocene-Quaternary andesitic-dacitic stratovolcanoes which constitute the axis of the Cordillera. The geology of the mineralized district is described by Barúa (1961) and Bellido (1979) and clearly documented in the 1:100,000 geologic map of the Moquegua 30-minute quadrangle (Bellido and Landa, 1965). Porphyry copper and copper-molybdenum mineralization in the Toquepala-Cuajone Mining District constituted the terminal event in the evolution of a major continental volcano-plutonic arc the eruptive units of which are traditionally assigned to the Cretaceous-Paleogene Toquepala Group. Petrochemical studies of local pre-Neogene igneous rocks include those of James and others (1974), Barreiro and Clark (1984), Boily and others (1984, 1990), and Beckinsale and others (1985); Manrique and Plazolles (1975), Tosdal and others (1981), and Marocco and Noblet (1990) have defined the post-hypogene-mineralization Tertiary stratigraphic relationships in the district. Landform mapping by Tosdal and others (1984) provides a basis for clarification of Oligocene-Miocene geomorphologic and tectonic development of the area and hence of the controls on the supergene enrichment of the deposit (Clark and others, 1990b).

District Geology

The lowest strata of the Toquepala Group are exposed orthwest and southeast of the Toquepala-Cuajone Mining Dis-ict (fig. 2), where they rest unconformably upon folded sedi-ientary rocks of the Upper Jurassic to Lower Cretaceous Yura roup (Jenks, 1948; Wilson and García, 1962). Fringing and verlapping the volcanic-plutonic belt to the southwest (fig. 2) e the unfossiliferous continental clastic rocks and minor rhy-itic ignimbrites of the Oligocene Moquegua Formation (Bell-o and Guevara, 1963; Tosdal and others, 1981; Marocco and oblet, 1990) which accumulated during a protracted period of id-Tertiary erosion (Tosdal and others, 1984). Lower Miocene osdal and others, 1981, 1984) rhyodacitic and rhyolitic ignim-tic sheets of the Huaylillas Formation (Wilson and García, 62) mantle a subdued early Miocene topography known as "Altos de Camilaca Surface" (Tosdal and others, 1984) and erlie the Moquegua Formation and Toquepala Group. Several lated and areally restricted ignimbrite units exposed near the ajone Mine that were previously included in the Huaylillas mation (Bellido and Landa, 1965) have been assigned by Man-ie and Plazolles (1975) to the distinct and younger Chuntacala mation; Tosdal and others (1981) and Sébrier and others (1983) e shown these units to be widespread and of mid-Miocene . Exposed further to the northeast is a sequence of upper cene continental clastic sedimentary and volcanic rocks that er extensive areas of the inner Cordillera Occidental and e traditionally been assigned to the Maure, Sencca, and Cap-ie Formations (Mendívil, 1965; Tosdal and others, 1981). iated andesitic-dacitic stratovolcanoes of the Lower Plio-to Pleistocene Barroso Group (Mendívil, 1965; Tosdal and rs, 1981) and Pleistocene-Holocene Ampato Group (Klinck others, 1986) rise well above 5,000 meters above sea level form the crest of the Cordillera Occidental some 40 kilome-o the northeast of Toquepala (de Silva and Francis, 1991).

Local Geology

Cretaceous-Paleogene Stratigraphic Relationships. A sequence of several thousand meters of volcanic rocks assigned by Bellido and Landa (1965) and Bellido (1979) to the Paralaque and Quellaveco Volcanics of the middle and upper sections of the Toquepala Group is exposed in the Toquepala District (fig. 3; stratigraphic relationships in the area of the mine are summarized in the legend to fig. 5). The Paralaque Volcanics (Bellido and Landa, 1965) constitute the oldest local member of the Toquepala Group and crop out only to the south of the Incapuquio Fault (fig. 3), where the section is composed of andesite, dacite, and rhyolite flows with minor volcaniclastic and conglomeratic lenses. Exposed to the north of the fault are lavas and ash-flows of the Quellaveco Volcanics (Bellido, 1979). These correspond to the Quellaveco Formation of Richard and Courtright (1958a), who divided this sequence into the Quellaveco Quartz Porphyry (oldest), the Toquepala Series, the Alta Series, and the thin Yarito and Tinajones Rhyolites (youngest). The Quellaveco Quartz Porphyry comprises a number of rhyolite flows, whereas the overlying Toquepala Series consists of a succession of two andesitic to rhyolitic cycles approximately 420 meters thick. This succession is exposed only in the immediate vicinity of the Toquepala Mine and may represent vestiges of eruptive edifices broadly related to the Toquepala Dacitic Intrusive Center. Flows of the Toquepala Series overlie the Quellaveco Quartz Porphyry unconformably and are separated from one another by less pronounced unconformities; all units strike northwest and dip gently but variably to the southwest.

Andesite to rhyolite lavas, breccia flows, agglomerates, and volcaniclastic rocks of the Alta Series (Richard and Courtright, 1958a) overlie units of both the Quellaveco Quartz Porphyry and Toquepala Series on ridge crests and pampas above the Toquepala Mine. Two rhyolite flow-domes define the rounded hills of Cerros Yarito and Cruz Laca 8 kilometers west-northwest and 15 kilometers northwest of the mine respectively (Bellido and Landa, 1965). Bellido (1979) assigned these domes to the Yarito Rhyolite and regarded them as the youngest members of the Quellaveco Volcanics. Thin quartz porphyry flows exposed in the Quellaveco and Cuajone Mine areas are petrographically similar to the Quellaveco Quartz Porphyry and are tentatively interpreted as being directly related to the intrusive centers of those porphyry copper deposits.

Intrusive rocks. Phaneritic granitoid plutons are exposed extensively in the region, and evidence from extensive exposures in railway tunnels connecting the Cuajone and Toquepala Mine areas suggests such intrusions underlie much of the district at shallow depth. These plutons have been assigned to the Toquepala Segment of the Peruvian Coastal Batholith by Pitcher and others (1985). They intrude all members of the Paralaque and Quellaveco Volcanics up to and including the Alta Series in the Toquepala District (fig. 3) and are cut by the porphyry stocks of the mine area. Mid-Tertiary uplift and erosion exposed these plutonic rocks, which were subsequently covered by ash-flow sheets of the Huaylillas Formation.

With the exception of minor monzonite and granite bodies, the bulk of plutonic rocks in the area have been mapped by Bellido and Landa (1965) as diorite-granodiorite (fig. 3). Stevenson and Damiani (1968) and Damiani (1969) distinguish two varieties of

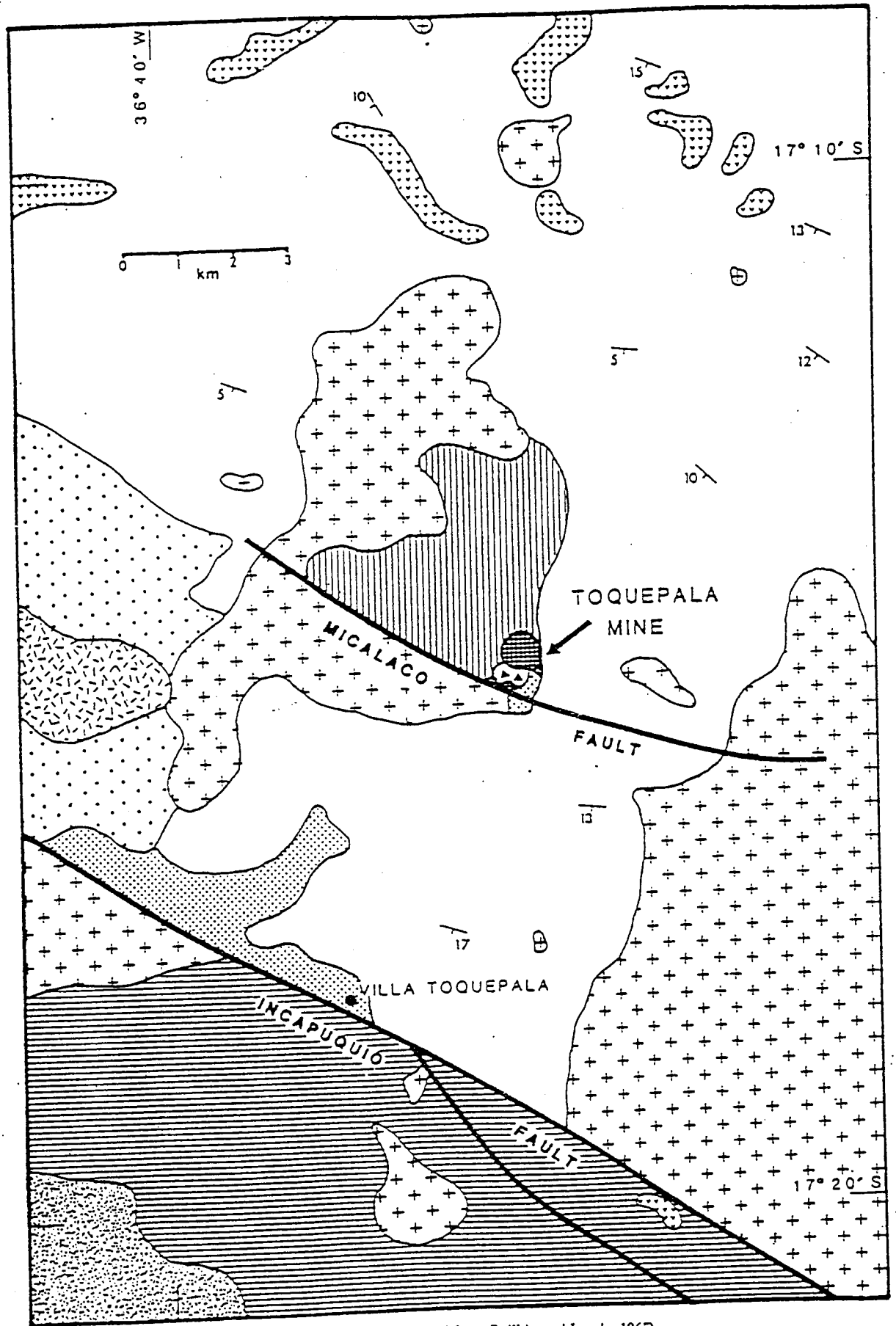

Figure 3. Map showing simplified geology of the Toquepala District (modified from Bellido and Landa, 1965).

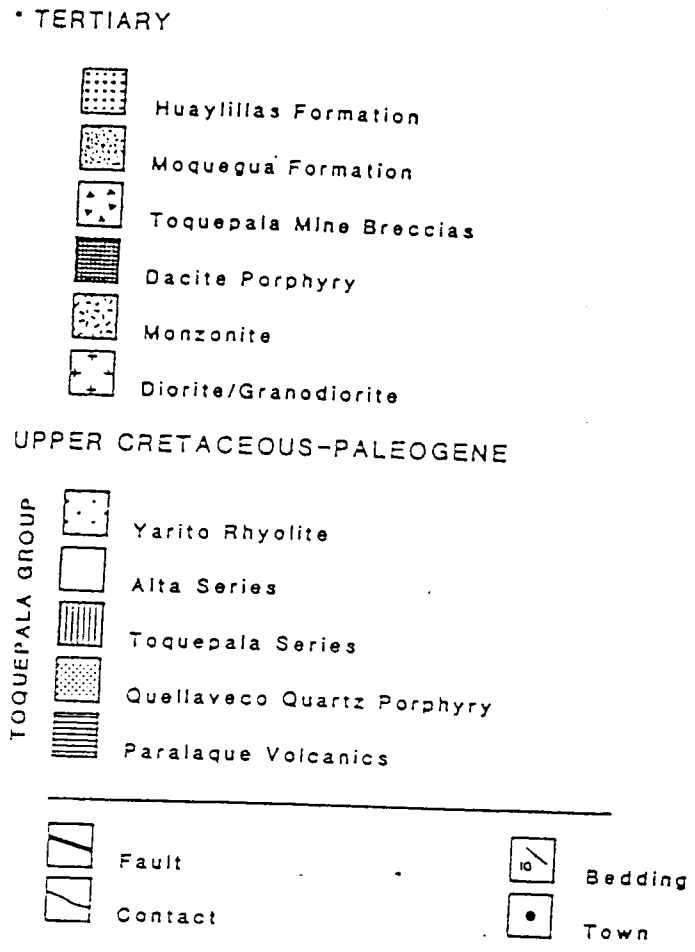

diorite-granodiorite in the Toquepala Mine area: a granodiorite body at the western edge of the deposit and a diorite mass several kilometers to the east. These have been assigned by Pitcher and others (1985) to the Toquepala and Norvill Plutons respectively (but see Clark and others, 1990a). Petrographic studies of rocks from numerous outcrops in the area (A.H.C., unpublished data) indicate that the granitoids define a spectrum from (pyroxene-hornblende) gabbro through diorite, (quartz-)monzodiorite, monzonite, quartz-bearing monzonite, and monzogranite to alkali feldspar granite (nomenclature of Streckeisen, 1976). Linear compositional trends on Harker diagrams and macroscopic features including melanocratic microgranular enclaves with scalloped borders indicate that several intermediate members of the suite originated through commingling of silicic (probably monzogranitic) and basic (gabbroic) magmas. Quartz-rich monzodioritic facies predominate.

The intrusive facies exposed in the southwestern quadrant of the Toquepala Open Pit (figs. 3 to 5) comprise a mesocratic equigranular biotite- and hornblende-bearing rock of quartz monzodiorite to quartz-bearing monzonite composition, but the term "diorite" traditionally employed by mine personnel is retained for this rock in this paper. Electron microprobe analyses integrated with reflected-light Nomarski interference contrast imaging of plagioclase growth history confirm that magma mixing played an important role in the crystallization of this pluton and reveal up to two calcic spikes within individual plagioclase grains indicative of significant temperature increases (A.H.C., unpublished studies).

Many members of the granitoid suite are markedly potassic with $K_2O - Na_2O$ ratios greater than 1, and analogies may be drawn with the shoshonitic clan, the calc-alkaline-monzonitic (high-potassium) trend of Lemeyre and Bowden (1982), and to some extent with the Linga (-Ica) Super Unit of more northwesterly segments of the Coastal Batholith (Agar and Le Bel, 1985). Assignment to the Yarabamba Super Unit (for example, Pitcher, 1985), the type area of which lies in the Arequipa Segment, is not convincing on petrographic grounds.

The subvolcanic dacitic and latitic stocks and dikes of the mine area and associated large-scale breccia bodies are here named the "Toquepala Intrusive Center." These rocks intrude both the diorite pluton and the youngest units of the Quellaveco Volcanics.

Age relationships. Although the age of the Toquepala Group is inadequately defined, there is no reason to question the general validity of the published Late Cretaceous (70 Ma rubidium-strontium isochron, James and others, 1974) date assigned to the Paralaque Volcanics. Argon isotope incremental-heating age data for a rhyolite of the Toquepala Formation (the basal unit of the group) are interpreted as evidence that arc construction began at approximately 75 Ma (Clark and others, in press). The late Oligocene potassium-argon age (36.5 Ma) reported for a rhyolite of the Alta Series by Laharie (1973) is considered improbable because this unit has been intruded by Paleocene granitoids.

Although Beckinsale and others (1985) have presented an imprecise (mean squared weighted deviation = 2.6) rubidium-strontium whole-rock isochron age of 61 ± 4 Ma for 16 granitoid samples of the Yarabamba Super Unit in the Toquepala District, potassium-argon and argon isotope incremental-heating geochronological studies of the plutonic rocks of the mine area (Clark and others, 1990a and in press; R.J. Langridge, unpublished data) demonstrate that the intrusions surrounding the Toquepala Deposit were emplaced from 68 Ma (Maastrichtian) to early Paleocene time. The youngest quartz-monzodioritic stock (the "Toquepala Pluton," 58.44 ± 0.36 (2σ) Ma) lies immediately west and northwest of the deposit. Argon isotope age data for the Toquepala Intrusive Center and the mineralization are ambiguous but have been interpreted (Clark, 1993; Clark and others, in press) as evidence that hypogene hydrothermal activity and copper-molybdenum ore deposition took place predominantly at 56.0 ± 1 Ma, that is, in latest Paleocene or early Eocene time, and that post-ore intrusion of latite dikes, hydrolytic alteration, and essentially barren pyritic late stage mineralization may have persisted to 52 Ma.

Structure. The major structural features in the district are faults (figs. 3 and 4) of the regionally extensive Incapuquio System (Barúa, 1961). Most prominent is the Incapuquio Fault proper (fig. 3), which has been traced for over 140 kilometers from the Chilean border to the outskirts of the town of Moquegua (Barúa, 1961; Wilson and García, 1962). It is generally vertical and strikes N50 to 70°W parallel to the regional trend of the Cordillera. The amount and sense of displacement are problematic: sinistral/transcurrent, normal (southwest side down), and dextral/reverse movements have been advocated by Wilson and García (1962), Stevenson and Damiani (1968), and

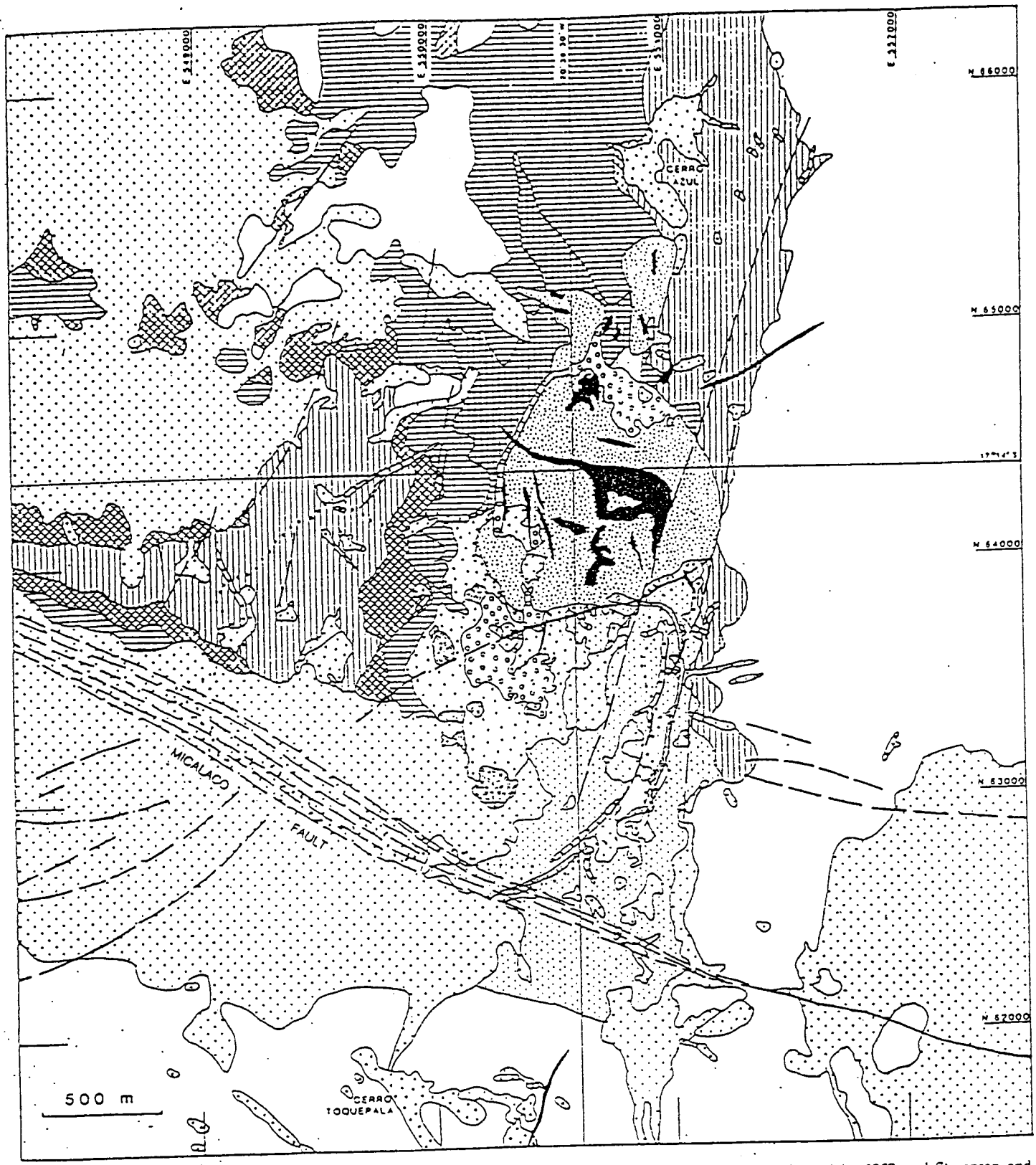

Figure 4. Geologic map of the Toquepala Porphyry Copper-Molybdenum Deposit (modified after Richard and Courtright, 1958, and Stevenson and Damiani, 1968).

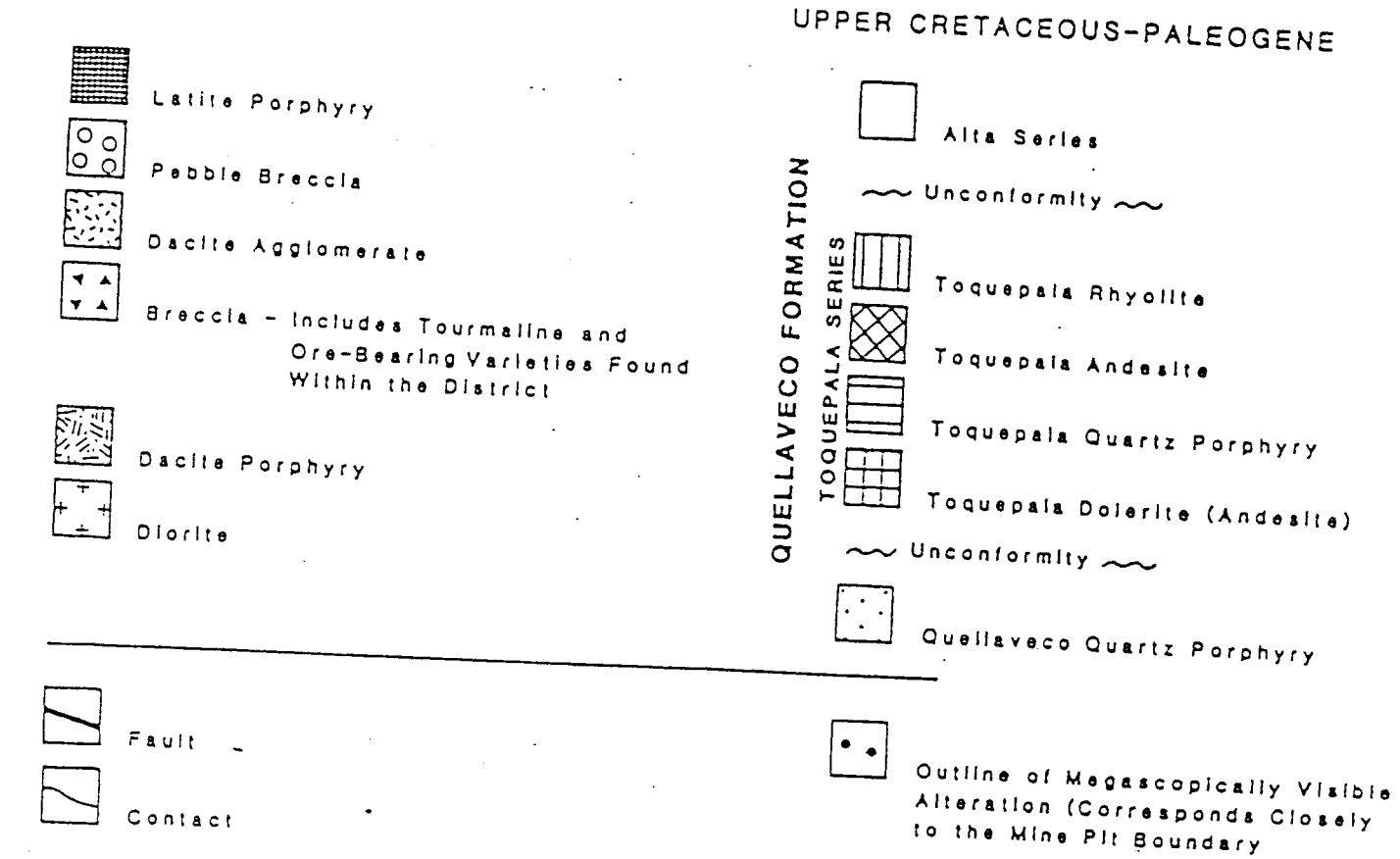

Marocco and Noblet (1990) respectively. The fault probably experienced a complex history, but minor structures in Quebrada Micalaco (A.H.C., unpublished data) indicate that the latest movements were normal and down to the southwest. The other major structure in the district is the Micalaco Fault (fig. 4), which Stevenson and Damiani (1968) considered to be related to the Incapuquio System. It also trends northwestward, dips steeply, and has been traced for over 20 kilometers. The fault zone is narrow throughout much of its course, but in the vicinity of the mine it broadens to several hundred meters. Stevenson and Damiani (1968) have proposed that the Micalaco Fault may have guided the emplacement of the Toquepala Intrusive Center.

Wilson and García (1962) and Tosdal and others (1981) have delimited the main period of movement on these faults as postdating granitoid emplacement but predating Huaylillas Formation eruption and development of the Altos de Camilaca erosion surface during latest Oligocene time (Tosdal and others, 1984). Marocco and Noblet (1990) interpret the Incapuquio fault as having been active during late-Moquegua Formation sedimentation and defining the continentward boundary of the Moquegua Fore-Arc Basin. In contrast, post-ore pebble and latite dikes intrude and cut the Micalaco Fault and show it to have been active before or during the waning stages of the evolution of the Toquepala Intrusive/Hydrothermal System about 52 to 53 Ma.

A minor set of faults mapped only in the immediate mine area (Stevenson and Damiani, 1968) is defined by a consistent north-northeast trend (fig. 4). Several of these faults, which cut every lithological unit in the mine area, are filled by pebble breccia bodies. Stevenson and Damiani (1968) proposed the name "Toquepala Lineament" for a N15 to 20°E array of three porphyry stocks, two breccia columns, numerous pebble and latite dikes, and the nearby Cerro Toquepala and Cerro Azul Breccia Pipes (fig. 4); this alignment may have been determined in part by the north-northeast-trending faults.

Cretaceous and Tertiary volcanic strata in the mine area dip consistently at a low angle to the southwest (fig. 4). This tilting postdates the extrusion of the regionally extensive ash-flow tuffs of the post-ore Huaylillas Formation (Tosdal and others, 1981, 1984), and it is therefore inferred that the Toquepala hydrothermal system has itself been tilted 5 to 20° to the southwest.

ROCKS OF THE TOQUEPALA INTRUSIVE CENTER

Five groups of rocks comprise the sub-volcanic Toquepala Intrusive Center: dacite porphyries, hydrothermal breccias, dacite agglomerate, latite porphyry, and pebble breccia (figs. 4 and 5). All have been affected by hydrothermal alteration.

Dacite Porphyries

Stocks and dikes of dacite porphyry intrude the volcanic flows and diorite within the Toquepala hydrothermal alteration

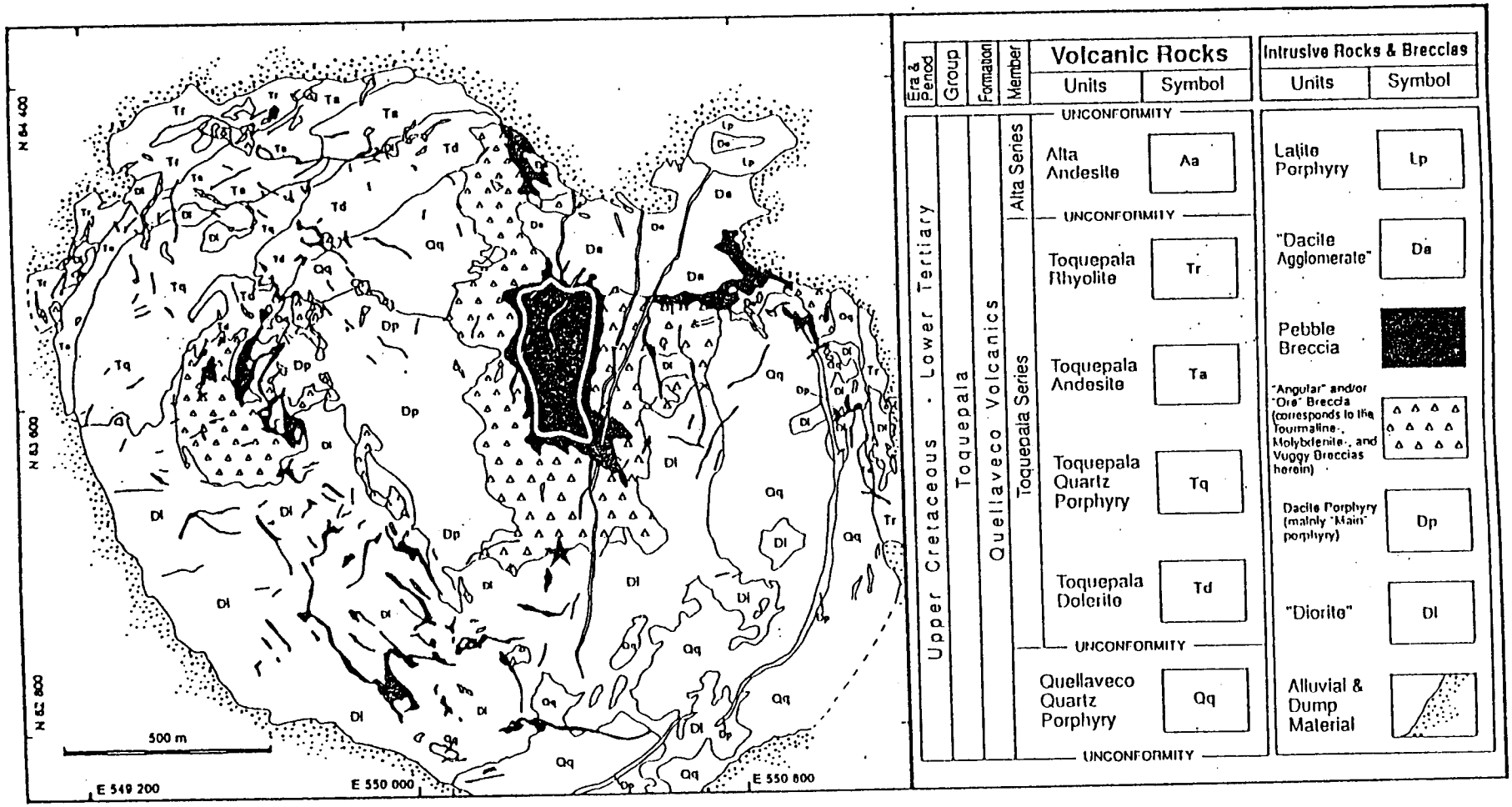

Figure 5. Geological sketch map of the Toquepala Deposit emphasizing the distribution of hydrothermal breccias. Simplified after Southern Peru Copper Corporation open-pit map, January, 1981, prepared by A. Plazolles V. and J. Maurique C. The stippled outer line approximately delimits the open pit and lies at about 3,325-3,560 m.a.s.l. The center of the lowest level at 3,085 m.a.s.l. is indicated by a star. The continuous white line within the pebble pipe approximately separates the core and border facies of that phreatomagmatic breccia body (P.L. Zweng, unpubl. data).

Table 1. Petrographic features of the dacitic intrusive rocks, Toquepala, Peru.

Unit	Distinguishing Features	Phenocrysts	Groundmass
T Porphyry	Abundant feldspar, but generally minor quartz phenocrysts; abundant groundmass; pervasive biotitization	P (0.2-3.5 mm, seriate distribution, mode centered about 2 mm; 42-47 vol. %), euhedral; oscillatory zoning; locally replaced by alkali feldspar along fractures Q (0.3-3.0 mm, average 1-2 mm, 2-6 vol. %); generally subhedral; resorbed edges; wormy alkali feldspar inclusions B (0.3-3.5 mm; 3-5 vol. %); scattered books; relatively fresh H (0.7-3.5 mm; <2 vol. %); inferred from altered phenocryst outline; replaced by shreddy biotite, anhydrite, calcite, apatite, alkali feldspar, chalcopyrite, pyrite and rutile	(0.01-0.03 mm; 44-49 vol. %); aplitic-sugary granular mixture of quartz, alkali feldspar, and biotite; accessory apatite and zircon; ubiquitous fine-grained shreddy biotite scattered throughout matrix; disseminated secondary chalcopyrite, pyrite, anhydrite; trace amounts of sericite and chlorite
Main Porphyry	Ubiquitous quartz eyes and feldspar phenocrysts; abundant groundmass	P (0.2-4.0 mm, seriate distribution, mode centered about 2 mm; 41-46 vol. %); euhedral; oscillatory zoning; clay and sericite dusting even in freshest samples Q (0.3-3.1 mm, average: 1-2 mm; 6-8 vol. %); generally subhedral, but bipyramidal habit common; resorbed edges; wormy alkali feldspar inclusions B (0.3-3.5 mm; average 1 mm; 4-6 vol. %); scattered books; locally replaced by chlorite, sericite, pyrite, chalcopyrite, and rutile H (1.0-3.5 mm; <1 vol. %); inferred from altered phenocryst outline; completely replaced by sericite, chlorite, anhydrite, calcite, alkali feldspar, chalcopyrite, pyrite and rutile	(0.01-0.03 mm; 42-47 vol. %); aplitic-as T Porphyry; disseminated anhydrite, calcite, sericite, chlorite, pyrite, and chalcopyrite; groundmass appears aphanitic in hand-specimen
L/M Porphyry	Absence of quartz phenocrysts; crowded porphyritic texture, relatively coarse-grained groundmass	P (0.4-3.0 mm, majority between 1.0-1.5 mm; 61-66 vol. %); subhedral with ragged outline; An content unknown due to alteration to clay- and sericite-bearing assemblages B (0.5-1.5 mm; 1-3 vol. %); inferred from altered phenocryst outline; completely obliterated to sericite, clay, anhydrite, pyrite, chalcopyrite, and rutile	(0.03-0.12 mm; 39 vol. %); aplitic, but relatively coarse grained; quartz > alkali feldspar; alteration masks identity of mafic and accessory phases; individual matrix grains are readily discernible in hand-specimen

B = biotite; H = hornblende; P = plagioclase (An_{33-42}); Q = quartz; vol. % = volume percent

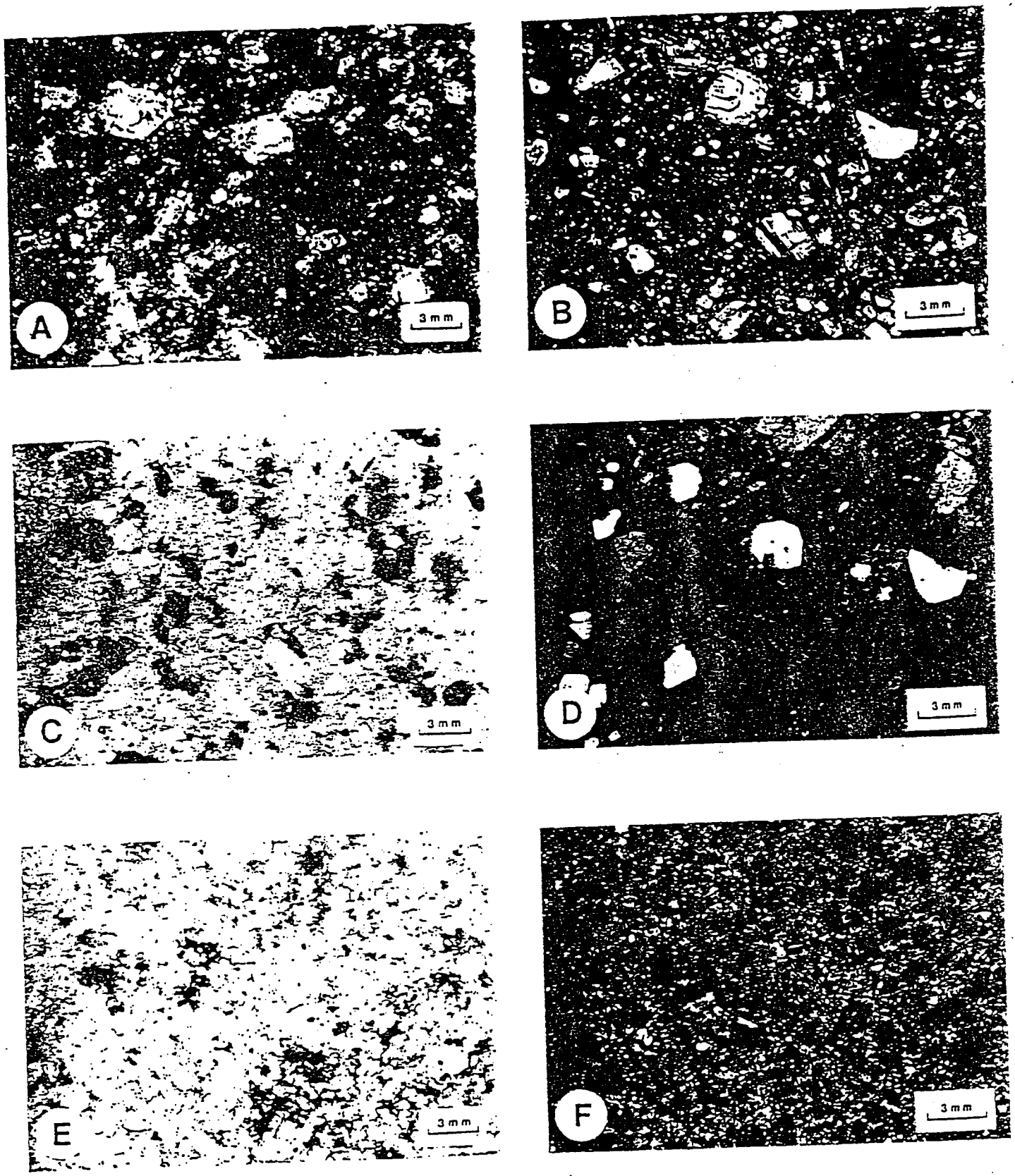

Figure 6. Petrographic features of the T. Main, and L/M Dacite Porphyries, Toquepala.

A. Macrophotograph of T Porphyry showing porphyritic texture, abundant plagioclase phenocrysts, scarce quartz phenocrysts, and pervasive biotitization of the groundmass. The milky white coloration of the plagioclase is the result of alteration to alkali feldspar along cleavage and fractures. Groundmass appears aphanitic in hand-specimen (SPZ-C-258: DDH T20-662m).

B. Photomicrograph of T Porphyry showing abundant fine-grained aplitic groundmass, seriate size distribution of plagioclase phenocrysts, and low modal percent of quartz phenocrysts. Most plagioclase crystals are isolated and are not in contact with other phenocrysts. Cross-polarized transmitted light (SPZ-C-258: DDH T20-662m).

C. Macrophotograph of Main Porphyry showing porphyritic texture, ubiquitous quartz eyes, and plagioclase and biotite phenocrysts. Fine-grained sulfide (pyrite>chalcopyrite) is disseminated in the rock and is localized in mafic phenocryst sites. Weak sericitic alteration of silicates is widespread. Groundmass appears aphanitic in hand specimen (SPTOQ83-2: open pit; 3070m level-NW).

D. Photomicrograph of Main Porphyry showing porphyritic texture and mineral assemblage very similar to that of the T Porphyry except for higher quartz phenocryst content. Feldspar phenocrysts appear cloudy due to dusting by sericite. Many mafic minerals are sulfidized to pyrite and chalcopyrite. Cross-polarized transmitted light (SPTOQ83-2: open pit: 3070m level-NW).

E. Macrophotograph of L/M Porphyry showing crowded porphyritic texture and lack of quartz and mafic phenocrysts due to alteration. Disseminated pyrite is present throughout the specimen. Supergene alteration has converted plagioclase to a kaolinite-rich assemblage. Although small, individual groundmass grains are clearly discernible (SPZ-C-199: DDH L/M18–452m).

F. Photomicrograph of L/M Porphyry showing crowded porphyritic texture consisting of abundant even-sized plagioclase phenocrysts and interstitial aplitic groundmass. Plagioclase is typically ragged in outline and in point or edge contact with phenocrysts. Groundmass is coarse relative to that of the T and Main Porphyries. Plagioclase is dark due to alteration to supergene clays. Cross-polarized transmitted light (SPZ-C-199: DDH L/M18–452m).

N.B. Hand specimen numbers (e.g., SPZ—) refer to Zweng (1984).

zone (figs. 4 and 5). The stocks are irregular to circular in plan, and most are less than 150 meters in diameter. Two narrow dikes form a ring approximately 1,500 meters long around the southeast quarter of the breccia complex (fig. 5). Exposures of the dacite porphyry in the open pit reveal a steep-walled mass approximately 400 meters across in sharp contact with the enclosing wallrocks. In the past the porphyritic rocks exposed in the mine were assigned to a single intrusive unit despite Richard and Courtright (1958a) and Hart (1958) having inferred that several intrusions might be represented. Observations made in this study indicate that the dacitic rocks do indeed constitute a single hypabyssal intrusive complex, and the intrusions are tentatively divided into the Main, L/M, T, and Late Porphyries based on mineralogical and textural fractures and crosscutting relationships. Petrographic descriptions for the Main, L/M, and T Porphyries are presented in table 1.

T Porphyry. The T Porphyry has been definitely encountered only near the bottom of drill-hole T-20, the deepest at Toquepala as of 1982, where the apparent apical portion of a porphyry stock has been intersected at an elevation of approximately 2,550 meters above sea level. The rock is characterized by a variable but generally low quartz phenocryst content and an abundant aplitic groundmass (figs. 6A and B).

The T Porphyry is situated directly beneath the apparent root zone of the hydrothermal breccia complex. No breccia xenoliths occur within the T Porphyry, but it is not known if fragments of this intrusion are incorporated in the breccias. Pervasive shreddy biotite alteration of the T Porphyry locally imparts a brown color to the rock, but potassic alteration has not converted the extremely fine-grained groundmass to a coarser, more ragged matrix as has been documented in the intensely potassically altered stocks at El Salvador (Gustafson and Hunt, 1975). Early quartz veins, some with feldspathic alteration envelopes, cut the biotitized porphyry. Later vein types (including some quartz-pyrite veins with sericitic halos) are also hosted by the porphyry even at this deep level within the system.

The T Porphyry is inferred to be the earliest of the dacitic intrusions and to be temporally and perhaps genetically linked to the initial stages of alteration and mineralization at Toquepala.

Main Porphyry. The Main Porphyry is so named because it forms the bulk of the dacite exposed in the open pit. The stock persists downward at least to 2,770 meters above sea level and is characterized by ubiquitous quartz phenocrysts and an abundant aplitic groundmass (figs. 6C and D). Numerous clasts of the Main Porphyry are contained in the tourmaline breccias, and many such clasts have been cut by pre-breccia quartz veins associated with the earliest hydrothermal episodes. There is no evidence of potassic alteration in this rock, but pervasive albite-sericite alteration occurs at elevations of approximately 2,700 to 2,810 meters above sea level (drill holes O-18 and Q-21) in what appears to be Main Porphyry. A few early stage veins with albitic envelopes are also present in drill core from this level but are not directly associated with pervasive alteration. The Main Porphyry Stock is relatively barren and may have been emplaced after the early stage of alteration and mineralization of the T Porphyry had commenced but before the initiation of major brecciation. Because of the shallow position of much of the Main Porphyry Stock, it is heavily overprinted by supergene argillic and hypogene sericitic alteration and mineralization. An argon isotope age spectrum for slightly chloritized phenocrystic biotite from this intrusion (sample 3160m-NW(1983)) records significant disturbance, but a four-step plateau for fractions with low calcium-potassium ratios yields a latest Paleocene age of 56.71 ± 0.40 (2σ) Ma (Clark and others, in press). This date is preferred to the 57.1 ± 0.6 conventional potassium-argon date previously recorded (Zweng, 1984; Clark and others, 1990a).

L/M Porphyry. The L/M Porphyry, named after the drill-hole (L/M-18) in which it was first observed, is the most distinctive dacitic intrusion at Toquepala. A crowded porphyritic texture and the absence of quartz phenocrysts (figs. 6E and F) have caused it to be confused with diorite in drill-core records. The L/M Porphyry intrudes the southern part of the Main Porphyry, but the contact is obscured by an approximately 55-meter-wide zone of breccia in the latter rock. No xenoliths have been observed in the L/M Porphyry. The apparent apex of the stock is located immediately below the 3,085-meter level, and drill-hole intersections persist downward to at least 2,665 meters above sea level.

The L/M Porphyry clearly postdates the Main Porphyry. However, the occurrence of early stage vein types in the L/M Porphyry indicates that it was also emplaced prior to the termi-

A

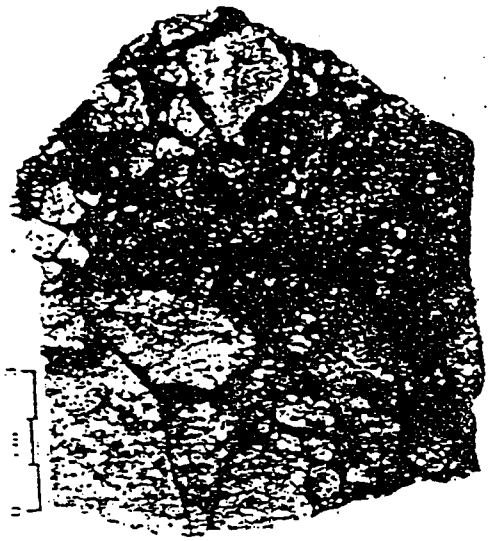

B

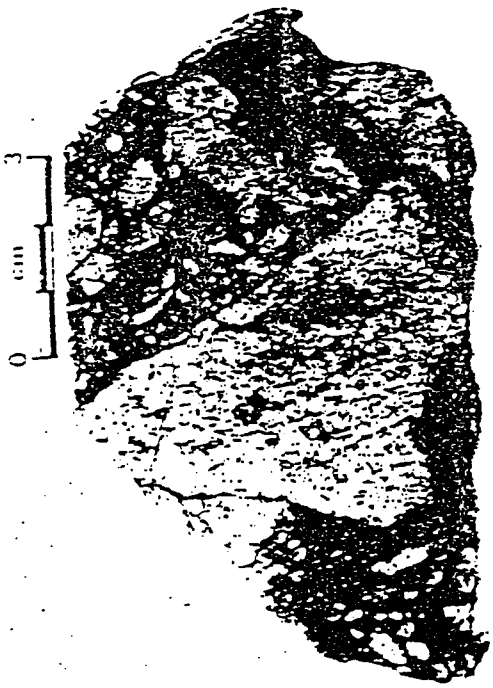

C

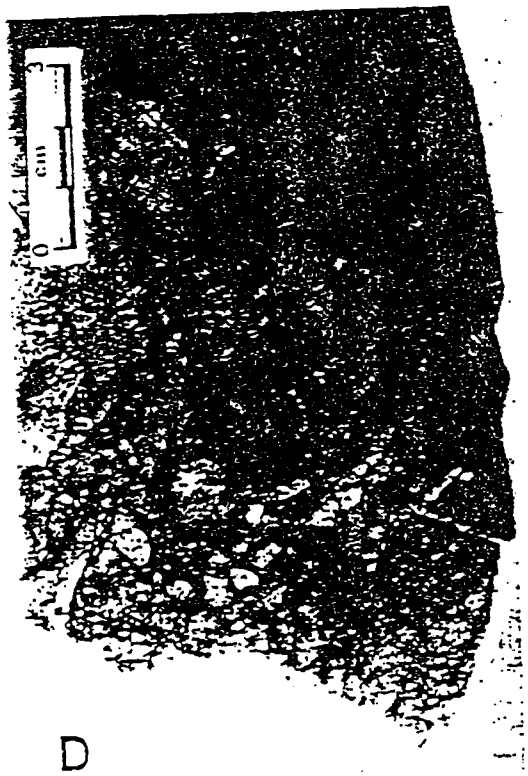

D

Figure 7. Hydrothermal breccias at Toquepala.

A. Hand specimen of pristine tourmaline breccia. Angular clasts are converted to a quartz-sericite assemblage. Matrix consists of tourmaline needles and minute wholly silicified rock fragments with little primary void space. Traces of chalcopyrite-pyrite-anhydrite mineralization overprint the sample. Supergene gypsum veinlets cut the base of the sample (SPZ-C-138: DDH 021 1/2-180m).

B. Hand specimen of tourmaline breccia overprinted by late-stage alteration and mineralization. Quartz-sericite-pyrite alteration is locally intense within clasts, and sericite is coarse-grained relative to that in pristine tourmaline clasts. Tourmaline in contact with sulfide is depleted in iron (see Fig. 10C) (SPZ-40: open pit: 3085m level-SE).

C. Hand specimen of molybdenite breccia. Tourmaline breccia and silicified fragments are enclosed in fine-grained molybdenite matrix (medium-gray material interstitial to clasts). Late-stage quartz-sericite-pyrite-bornite mineralization cuts the breccia and fills voids (SPTOQ83-1A: open pit: 3160m level-SW).

D. Hand specimen of vuggy breccia. Void space, sericitically altered fragments, and abundant pyrite characterize this breccia. Matrix is predominantly pre-existing tourmaline that has undergone significant iron depletion and bleaching (SPZ-28: open pit: 3130m level-NE).

nation of that stage of alteration and mineralization. Other major vein types cut L/M Porphyry, but it is not clear whether any alteration and mineralization were genetically associated with the porphyry itself. The low density of early veins and lack of pervasive shreddy biotite alteration suggest that the L/M Porphyry, like the Main porphyry, either did not contribute much copper or molybdenum to the system or was not a conduit for early hydrothermal fluids. Pervasive supergene alteration has converted groundmass and phenocrystic feldspars of the L/M Porphyry to argillic mineral assemblages.

Late dacite porphyries. Exposures in the open pit and in drill core indicate that the above tripartite subdivision of the dacite porphyries is an oversimplification. At one location (3145m-N(1975)) a porphyritic dacite body at the western margin of the main tourmaline breccia pipe contains fragments of that breccia and is cut by quartz-chalcopyrite-pyrite veinlets. This dacite exhibits numerous spheroidal cavities 2 to 8 millimeters in diameter, the walls of which are encrusted by euhedral quartz, pyrite, and chalcopyrite. Similarly, a contact between two texturally similar dacite porphyry bodies exposed elsewhere in the pit (3205m-NW(1975)), indicates that multiple intrusive units exist at this level: One porphyry contains many pyrite veins that are truncated at the contact, while the other porphyry hosts veins that are continuous across the contact. Only the latter porphyry contains abundant xenoliths of tourmaline breccia and volcanic rocks. It is not clear whether the earlier of these intrusions represents the Main Porphyry.

These observations confirm that intrusion of dacitic porphyries persisted after emplacement of the tourmaline breccias. The body exposed on the 3,145-meter level may have been broadly contemporaneous with the main stage of copper-molybdenum mineralization, whereas the younger of the two porphyries outcropping on the 3,205-meter level appears to have been introduced during late stage, pyrite-dominated mineralization and may therefore have post-dated emplacement of the dacite agglomerate.

Hydrothermal Breccias

The most remarkable feature of the Toquepala Deposit (Richard and Courtright, 1958a) is an unusually large hydrothermal breccia complex emplaced along the vertical axis of its intrusive center. Major volumes of breccia are contained within a steep-walled, upward-flaring body with a crudely pipe-like form. The configuration of the complex in plan is an irregular oval approximately 700 by 1,200 meters (fig. 5); inclusion of the nebulous breccia would extend the main breccia body some 250 meters to the south-southwest, emphasizing the north-northeast "Toquepala Lineament" (Stevenson and Damiani, 1968). Drilling confirms the persistence of hydrothermal (tourmaline) breccia down to the 2,550-meter level and establishes a vertical continuity of over 950 meters from the pre-mining surface. Large-scale features such as well-defined sheeted contacts between breccia bodies and the enclosing wall rocks and zones of either vertically or horizontally oriented slab-like fragments (described by Sillitoe and Sawkins (1971) as typical of the much smaller tourmaline breccia pipes of north and central Chile) are absent or rare at Toquepala.

Satellite breccia bodies are scattered throughout the district. The two largest (both approximately 600 meters in diameter and broadly commensurate with the axial tourmaline breccia) are the Cerro Azul and Cerro Toquepala Tourmaline Breccia Pipes (fig. 4) located approximately 2.6 and 1.6 kilometers from the center of the deposit respectively. These are barren of base-metals, but barite-rich veinstone float is abundant on the upper slopes of Cerro Toquepala where it is considered to be locally derived (Plazolles, personal communication, 1975).

The main Toquepala Breccia Complex is composite in nature and consists of several mappable units each of which corresponds to a specific stage of the evolving hydrothermal system. The composite nature and relative ages of the breccias are clearly demonstrated by truncation and by the incorporation of older breccias into successively younger breccias. We define five breccia types: tourmaline breccia, nebulous breccia, molybdenite breccia, vuggy breccia, and pebble breccia. The so-called slump breccias (Richard, Courtright and others, 1951) are documented elsewhere (Clark, 1990); these texturally unusual stockwork-breccia associations are interpreted as marginal or root facies of the pebble breccias.

Tourmaline breccia. Tourmaline breccia (figs. 7A and B) corresponds to the ore breccia of Richard and Courtright (1958a) and the angular breccia of mine personnel (fig. 5) and is the most widespread type of breccia at Toquepala. It spans the entire vertical exposure of the deposit and attained a maximum mean diameter of 800 to 900 meters at the pre-mine surface. Much of what was originally tourmaline breccia is not preserved due to removal by mining, modification to other hydrothermal breccia types, and attrition to form pebble breccia. The best remaining exposures are on the lower levels of the pit, adjacent to the dacite porphyry, and away from the pebble pipe. Most exposures of the tourmaline breccia pipe exhibit irregular but crudely parallelepipoidal domains ("chambers") of breccia which are commonly 40 to 80 centimeters wide and connected by narrow (less than 10 centimeter) sheets or pipes of breccia.

Tourmaline breccia consists of quartz-sericite altered fragments in a tourmaline-quartz matrix. The extent to which the

fragments are altered increases with depth. Clasts are angular, poorly to moderately sorted, and commonly 2 to 3 centimeters in size, but blocks tens of centimeters across are not rare. A consistent parallel to subparallel orientation of the clasts is developed locally. The matrix is generally aphanitic in hand-specimen and almost free of primary void space. In many exposures it is evident that tourmaline brecciation was a polyphase event and that the matrix tourmaline became coarser with time. Fine tourmaline needles form massive aggregates surrounding breccia fragments or outward-projecting rosettes nucleated on clasts. Quartz in the matrix is coarse-sand size or smaller and consists of completely silicified fragments of shattered vein material. Sulfides, anhydrite, and lesser amounts of sericite and clay minerals occur independently or together as disseminations, along fractures, or within secondary voids in the matrix. Where exposed to strong late stage sericitic alteration, clasts are replaced by relatively coarse-grained sericite and impregnated with pyrite, but the matrix is not visibly altered.

A salient feature of the tourmaline breccias is that they are barren of inherent copper and molybdenum: our field and microscopic observations over a decade show that pristine breccia contains very low amounts of total sulfide, generally much less than 0.5 volume percent. Ore-grade tourmaline breccia was generated by later events.

Nebulous breccia. Field observations in 1975 and 1976 by A.H.C. and T. Freemark (1977) revealed that extensive areas mapped as diorite in the southwestern quadrant of the pit (3,160- to 3,205-meter levels) are in fact hydrothermal breccia. Fragments and matrix of this breccia are generally readily distinguishable only in shade or close to sunset due to superimposed alteration and stockwork development, hence the name "nebulous breccia." This breccia is similar to the tourmaline breccia in that tourmaline is a major constituent of the matrix. Ragged fragments of diorite with quartz-sericite altered cores and intensely silicified margins are enclosed in an essentially aphanitic matrix which is only slightly darker gray. The areal extent of this rock-type is unclear, but it is probable that it represents an outer or southwestern facies of the main column of tourmaline breccia.

Molybdenite breccia. Molybdenite breccia is present in zones of intense molybdenum mineralization which have been superimposed on earlier breccia bodies within the complex. These zones form narrow, irregularly cylindrical shoots which are generally restricted to the lower parts of the ore-body below the 3,100 meter level. Molybdenite is present in the matrix as massive to disseminated aggregates which engulf fine fragmental and re-brecciated material (fig. 7C). Clasts (some rounded; Clark, 1990) are typically tourmaline breccia. Late drusy quartz and pyrite fill voids and fractures and are associated with late stage sericitic alteration.

Vuggy breccia. Zones of strongly sericitized and mineralized vuggy breccia are developed within the upper and middle portions of the hydrothermal breccia complex. Their contacts with the tourmaline breccia and the pebble pipe are not sharply defined. The vuggy breccia is distinguished by an abundance of cavity and fracture space, bleached angular clasts, and coarse-grained sulfide clots (fig. 7D). The breccia typically contains 3 to 15 volume percent total sulfide, much of which is present in cavities or as impregnations in sericitized clasts. Pyrite is the most common sulfide, but pyrite-chalcopyrite and rare pyrite-bornite assemblages also occur. Relatively coarse-grained sericite and quartz line cavities and are intergrown with the sulfides. Clasts are generally angular fragments of tourmaline breccia. Intense sericitic replacement of fragments imparts a bleached appearance to the vuggy breccia which contrasts with the salt and pepper coloration of the tourmaline breccia. No consistent orientation of fragments has been noted. Vuggy breccia bodies in the upper part of the deposit were especially susceptible to supergene enrichment because of their permeability and high sulfide content.

Dacite Agglomerate

A large, steep-walled, crudely cylindrical felsic porphyry stock intrudes the northern margin of the breccia complex (fig. 5) and is accompanied by another and apparently similar stock immediately to the north. Only the pebble breccia and latite porphyry cut these bodies. Similarities in composition and texture to the dacite porphyry and the presence of abundant small xenoliths led Richard and Courtright (1958a) to classify this rock as an agglomerate, but this term is inappropriate because the rock is not pyroclastic. The concentration of inclusions decreases significantly with depth, and by the 3,225-meter level there are no inclusions. Exposures on the 3,280-meter level reveal subsequent intrusion by two lithologies: an early aphanitic dacite traversed by veinlets of porphyritic dacite.

Figure 8. Pebble breccias and latite porphyry, Toquepala. ▶

A. Hand specimen of the core facies of the pebble pipe. The pebble breccia is characterized by small, well-sorted, and indurated fragments enclosed in rock-flour matrix (SPZ-7: open pit; 3145m level-N).

B. Hand specimen of border facies of the pebble pipe. Compared to the core facies, this breccia contains larger, less-rounded, and less-sorted fragments enclosed in comminuted hydrothermal matrix (SPZ-15: open pit; 3145m level-NE).

C. Photomicrograph of core facies pebble breccia groundmass. Groundmass consists of finely comminuted material converted to a clay assemblage. Arrows point to minute fragments of tourmaline. Note the high degree of rounding of sulfide grains (black) within matrix. Plane-polarized transmitted light (SPZ-7: open pit; 3145m level-NE).

D. Photomicrograph of border facies pebble breccia groundmass composed of tourmaline needles finely comminuted to stubby and equant grains. Plane-polarized transmitted light (SPZ-4: open pit; 3145m level-NE).

E. Hand specimen of latite porphyry dikelet autobrecciated and injected into pebble pipe breccia (SPZ-C-56: DDH T22-59m).

F. Hand specimen of latite porphyry dike in pebble pipe breccia. The margin of the latite is intensely altered to a sericite+pyrophyllite assemblage. Pyrite has been deposited locally in plagioclase sites. Alteration intensity lessens and feldspar sites are discernible away from the margin and towards the center of the dike. (SPZ-C-53: DDH T22-45m).

G. Hand specimen of pebble breccia clasts in pebble pipe breccia. This sample is unusual in that clasts are of core rather than border facies pebble breccia (SPZ-2: open pit; 3145m level-N).

H. Hand specimen of a pebble dike. The large well-rounded fragment contains a quartz-sericite-pyrite vein, demonstrating that pebble dike formation postdated initiation of the late stage environment. The Peruvian coin is about 3 centimeters in diameter (open pit; 3190m level-S).

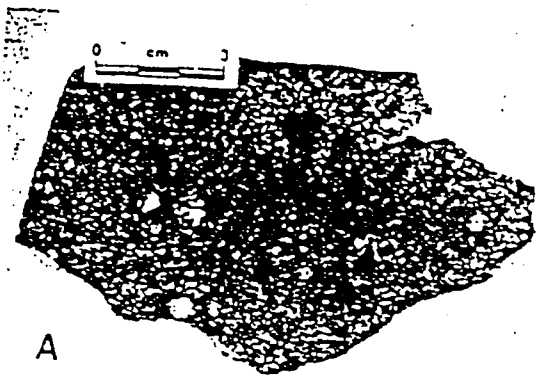

A

B

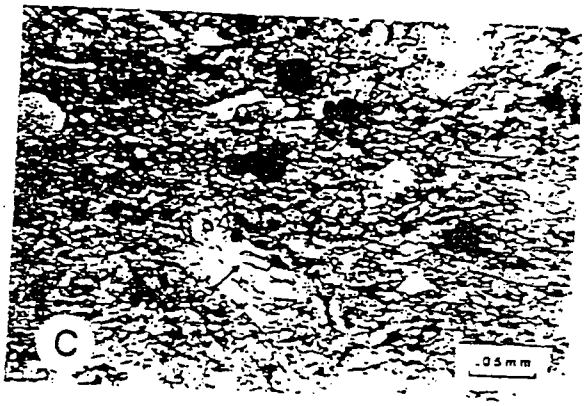

C

D

E

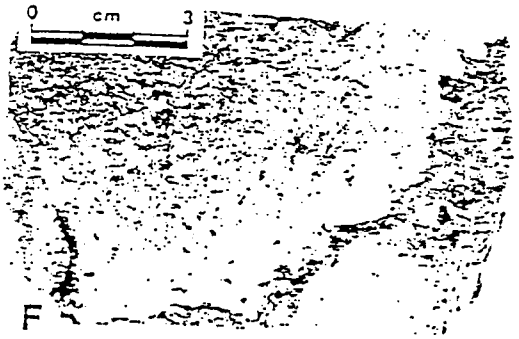

F

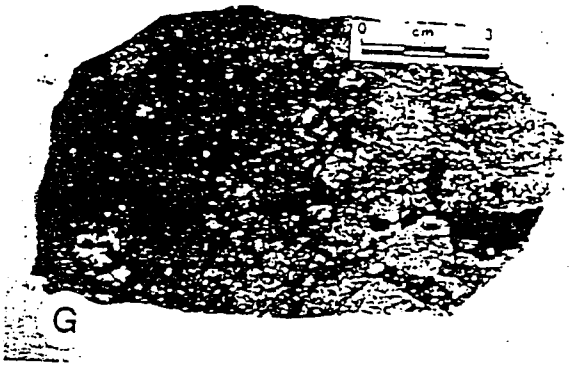

G

H

The dacite agglomerate represents a barren composite dacite stock which contains a xenolith swarm in its upper portion and was emplaced relatively late in the evolution of the hydrothermal system. This stock is cut by abundant late-stage veinlets and constitutes a crudely semi-circular waste-rock projection into the north-northeastern sector of the open pit.

Latite Porphyry

The youngest intrusions are a plagioclase- and biotite-phyric stock and a series of petrographically similar dikes (fig. 5). All previously described lithologies of the intrusive center are cut by this so-called latite porphyry. The rocks are typically greenish and have been altered to argillic mineral assemblages. Several varieties of latite dikes are present, some with and some without quartz phenocrysts, and no attempt has been made to delimit the different phases. Whether these rocks are indeed latitic in composition cannot be established because of the lack of whole-rock compositional data: the presence of quartz phenocrysts in some of the dikes and the absence of potassium feldspar and augite phenocrysts in all specimens examined are not indicative of hypabyssal latitic rocks.

Pebble Breccia

Pebble breccia occurs in two contexts at Toquepala: as an exceptionally large pebble pipe and in numerous dike-like bodies exposed throughout the open pit (fig. 5). Both are near-surface features. The pebble pipe terminates abruptly at about the 2,980-meter level, and the number of pebble dikes diminishes markedly a few tens of meters lower. Pebble breccia formation was strictly post-ore and overall contemporaneous with the emplacement of latite porphyry, the waning stages of sericitic alteration, and the development of advanced argillic alteration.

Pebble pipe. The major body of pebble breccia at Toquepala is a steeply dipping pipe which is approximately 300 meters wide and irregular in plan (fig. 5). Contacts between this pebble pipe and the earlier tourmaline breccias are gradational, but the northern edge of the pipe is in sharp contact with the dacite agglomerate. The pipe is intruded by numerous latite bodies, but no stock is present beneath its root-zone.

Two end-member types of pebble breccia make up the pipe: an inner core facies and an outer border facies (figs. 5; 8A, B). The former is characterized by small well-rounded pebbles in a finely comminuted rock-flour matrix (fig. 8C), while the latter contains less rounded fragments in a coarser comminuted hydrothermal mineral matrix (fig. 8D). No abrupt contact separates the two facies, and either may be present anywhere in the pipe. Although development of the two facies was broadly synchronous, emplacement of the border facies predated that of the core facies at any given point. Petrographic data for the pebble breccias presented in table 2 suggest that the pebble breccias formed predominantly from milled and comminuted hydrothermal breccia. The central portion of the pipe displays well-developed pebble breccia features and may have undergone a greater degree of attrition than did the periphery. Pebble breccia characteristics are less developed in the border facies, where vestiges of the hydrothermal breccia protolith are more clearly seen. This may explain the variation in copper grades between the two pipe facies (table 2), with the low copper content of the core facies reflecting the limited amount of sulfide minerals retained during pebble breccia formation.

Pebble dikes. These dikes are tabular bodies filled with breccia very similar in lithology to that of the central portion of the pebble pipe. Specimens of pebble breccia from the dikes are indistinguishable from specimens from the pipe except for the larger mean size of the pebbles in the dikes and the greater degree of sorting of fragments in the pipe. The pebble dikes at Toquepala are identical in almost every respect to those at El Salvador, Chile, studied by Langerfeldt (1964) and summarized by Gustafson and Hunt (1975), and several episodes of dike emplacement are represented.

Pebble dikes cut all rock types exposed in the pit (fig. 5), and their formation coincided with latite porphyry emplacement. Pebble and latite dikes commonly occupy the same structures (figs. 8E and F) and are parallel to one another. Pebbles from the pebble dikes are commonly included in massive latite, and unrounded autobrecciated latite fragments have commonly been incorporated into pebble dikes. On the upper mine levels both rock types have been altered to intermediate or advanced argillic assemblages; such alteration has obscured their identities, especially where pebbles are contained within the latite. The intensity of alteration decreases away from the pebble breccia-latite contacts and towards the interiors of the latite dikes so that feldspar sites may be distinguished in the interiors of the dikes.

The pebble dikes exposed in the open pit (fig. 5) define a concentric pattern with only a few oriented radially. It is not known whether this pattern changes with depth or if the concentric and radial sets are of different ages. The widths of the dikes are typically one to two meters, and their continuity along strike ranges from a few to more than 450 meters. Vertical continuity is not well established, but Juan Torres (personal communication, 1983) considers that it may exceed 500 meters. The abundance of pebble dikes decreases markedly with depth, and few are known to exist below the 2,900-meter level.

Transport distances for the pebbles were probably not great. Most clasts in dikes cutting the diorite are of that lithology. No entirely exotic lithotypes have been observed, but rounded fragments of tourmaline breccia are locally present in pebble dikes several tens of meters from the nearest exposure of tourmaline breccia. Preliminary studies by Freemark (1977) of one concentric pebble dike in the western quadrant of the pit indicate that both mean clast diameter and degree of rounding decrease upwards (3,160- to 3,220-meter levels), suggesting that fragmentation during transport was dominated by essentially planar fracture development in the clasts. Indeed, the local occurrence of curviplanar fractures in unmineralized stockworks adjacent to and beneath some pebble breccia dikes has led one of us (Clark, 1990) to propose that the rounded forms of clasts in these and in other pebble breccias may have resulted in part from initial Hertzian fragmentation under conditions broadly analogous to those of shock metamorphism rather than inter-clast attrition during transport.

Pebble dikes truncate pyrite-quartz veins with sericitic envelopes in the enclosing wallrock, but many such dikes also bear pebbles cut by that vein type and a few such veins cut the dikes. Pyritic veins commonly cut pebble dikes.

Table 2. Features of the pebble pipe rocks, Toquepala, Peru.

Parameters	Core Facies	Border Facies
Position	Generally restricted to the central part of the pebble pipe	Forms the outer fringe of the pebble pipe
Relative timing of facies	Later at any point in space	Earlier at any point in space
Breccia clasts:		
lithology	Indurated material within the hydrothermal breccias (e.g., silicified and rhyolite fragments, tourmaline breccia), quartz vein material, earlier pebble breccia	As Central Facies, but with the addition of sulfide fragments; lack of pebble breccia as clasts
size (diameter)	<1/4 to 5 cm; most < 1 cm	<1/4 to >5 cm; most >1 cm
degree of rounding	Subrounded to well-rounded	Angular to subrounded
sorting	Moderate to good	Poor to moderate
Breccia matrix:		
composition	Rock flour; very fine-grained clastic material produced from milled hydrothermal breccia clasts and matrix	Comminuted hydrothermal breccia matrix (e.g., tourmaline, quartz, sulfides); relatively low clay content
structure	Generally massive; flow banding uncommon except adjacent to latite porphyry dikes	Massive, nowhere flow-banded
void space	Nil	Variable, 0-5%
Sulfide textures	Cataclastic pyrite and chalcopyrite grains disseminated and clustered within the matrix (syn-pebble breccia formation)	As in Central Facies, but only minor cataclastic sulfide; euhedral pyrite infills voids (post-pebble formation)
Clast: matrix ratio	Typically 1:5; matrix supported	Generally 2:5 to 3:5; clast supported
Hypogene alteration and mineralization	Cut by late pyritic veins and a few quartz-sericite-pyrite veins: nowhere cut by early quartz veins; pervasively altered to advance argillic assemblages near fault zones and lithological contacts; copper derived from that contained in pre-pebble brecciated rocks (i.e., hydrothermal breccias)	
Copper grade	0.1 to 0.5%; typically 0.2 to 0.3%	0.4 to >2%
Supergene mineralization	Nearly absent	Minor; chalcocite coats and replaces sulfide within voids and along fractures

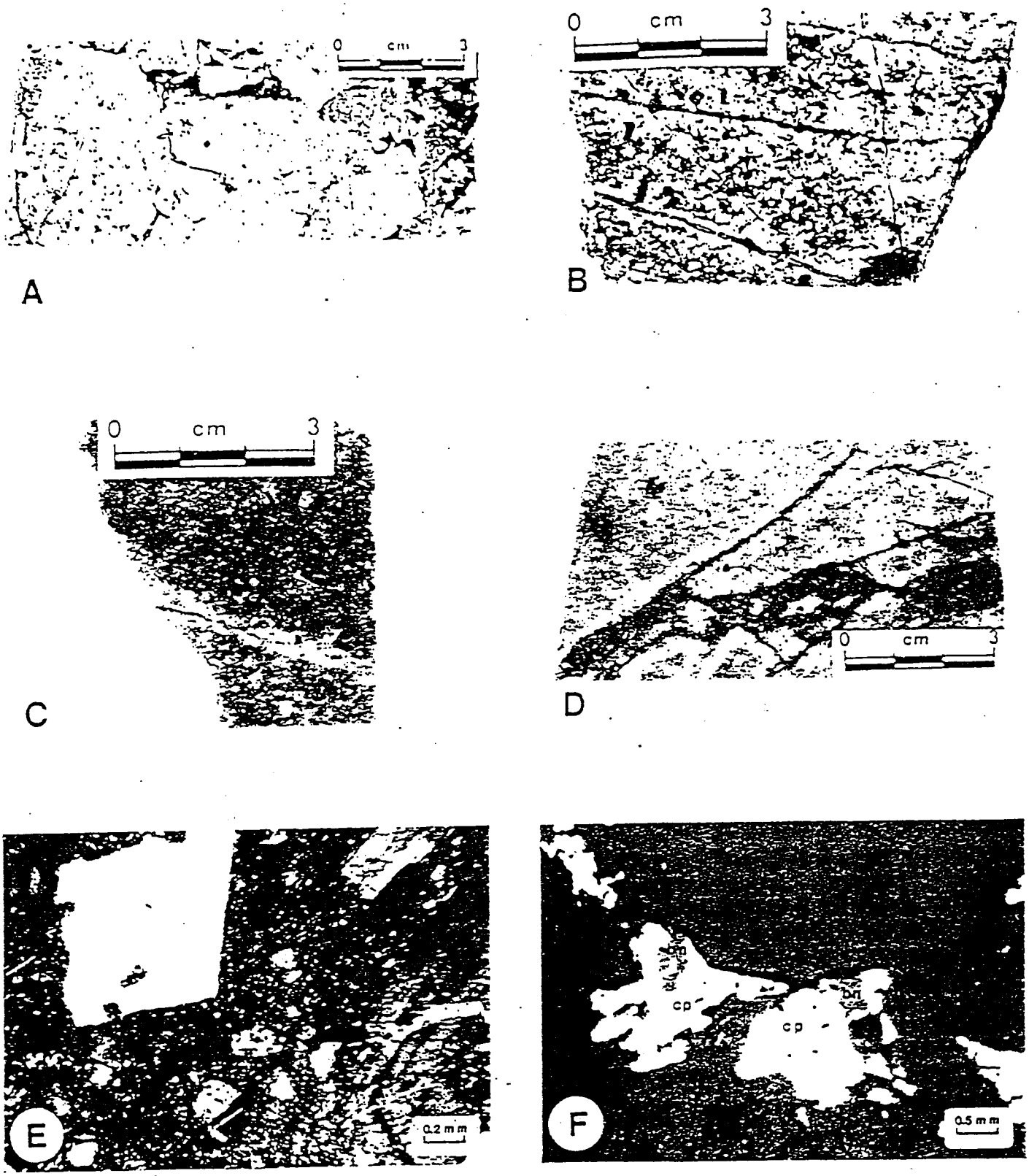

Figure 9. Features of early-stage alteration and mineralization, Toquepala.

◀ A. Hand specimen of tourmaline breccia containing clasts of Quellaveco Quartz Porphyry cut by early-stage type 1 veins. The quartz veins are contained solely within fragments and do not cut the tourmaline matrix, thereby indicating a pre-tourmaline-stage age (SPZ-C-244: DDH T20-568m).

B. Hand specimen of a type 2 early-stage vein cutting Main Porphyry. These through-going sheeted quartz veins have thin and discontinuous albite alteration haloes and are poor in sulfide. A type 1 early-stage vein is cut by the type 2 veins (SPZ-C-30: DDH P19-218m).

C. Hand specimen of a type 3 early-stage vein cutting biotitized T Porphyry. These veins are characteristically narrow, irregular, and discontinuous along strike, contain chalcopyrite-pyrite mineralization, and are enclosed by thin albite alteration haloes (SPZ-C-259: DDH T20-665m).

D. Hand specimen of a type 6 early-stage vein cutting biotitized T Porphyry. Such veins typically anastomose, contain quartz, biotite, and anhydrite, and display diffuse albite alteration haloes (SPZ-C-260: DDH T20-666m).

E. Photomicrograph of a type 5 early-stage vein cutting T Porphyry. The vein contains quartz where it cuts groundmass and albite where it cuts andesine phenocrysts. Cross-polarized transmitted light (SPZ-C-257: DDH T20-662m).

F. Photomicrograph of chalcopyrite+bornite mineralization in type 5 early-stage vein. This low-sulfur assemblage is observed only in these early-stage veins. Plane-polarized reflected light (SPZ-C-257: DDH T20-662m).

ALTERATION AND MINERALIZATION

The Toquepala Intrusive Center was the focus of multiple alteration and mineralization events. On the basis of observed mineralogical features and crosscutting relationships, four major stages of alteration and mineralization are defined: early, tourmaline, main, and late. Each stage corresponds to a specific period in the evolution of the hydrothermal system and represents a distinct physicochemical environment.

Much of the information presented here is derived from observations recorded during core-logging of the intermediate and deep portions of the porphyry system (Zweng, 1984). Coverage did not permit full definition of the spatial relationships of mineral assemblages, and alteration zones cannot be portrayed in either plan or cross-section. The study was successful in defining the relative ages of the mineral assemblages in the deeper part of the porphyry system, but the hypogene features of the upper part of the system are less reliably documented. Except with regard to the tourmaline breccias, the use of the term assemblage and the names applied to the different types of alteration are in accordance with Meyer and Hemley (1967).

Early Stage

Early stage alteration and mineralization at Toquepala have not been previously recorded. They are best developed within the T Porphyry exposed in the deepest levels of the deposit (below 2,550 meters above sea level) and in clasts contained in the overlying hydrothermal breccia complex. Minor early stage alteration and mineralization have also occurred at slightly shallower levels in probable Main Porphyry. This stage preceded the initiation of widespread brecciation and is characterized by veins containing potassium and sodium feldspar assemblages and local pervasive biotitization of T Porphyry. Molybdenite has not been observed in veins of this stage.

Early stage veins. Early stage veins are diverse (fig. 9) with respect to vein and alteration envelope mineralogy, structural style, and intensity of copper mineralization. Most common are through-going and sheeted veins which contain major amounts of quartz with little if any sulfide and lack alteration haloes (vein type 1; fig. 9A). A series of structurally similar veins have albite ($An_{<5}$) alteration envelopes but are also copper-poor (vein type 2; fig. 9B). Further veins with albite ($An_{<5}$) haloes are lensey, discontinuous, and randomly oriented but contain significant chalcopyrite-pyrite mineralization (vein type 3; fig. 9C). Other broadly similar sulfide-bearing veins lack well-defined alteration halos but have converted wallrock andesine phenocrysts to either potassium feldspar (vein type 4) or albite (vein type 5; fig. 9E). The only documented occurrences of the assemblage chalcopyrite-bornite are contained in type 5 veins (fig. 9F). Cobaltite and cobalt-rich mackinawite have been confirmed as minor constituents in a single clast of vein material (possibly of type 5) in tourmaline breccia. Other veins are biotite-rich, display well-developed albite ($An_{<5}$) selvages, and are sulfide-poor (vein type 6; fig. 9D). Despite their diversity, all of these veins developed early in the formation of the ore deposit and are the products of an early potassium-sodium metasomatic environment. Only trace amounts of sericite and chlorite occur in the veins, where they are directly associated with sulfide grains. Clay minerals are absent.

Descriptive data for the early stage veins are presented in table 3. It should be noted that the numerical designation applied to these bodies reflects their apparent relative abundances (type 1 is more common than type 2) rather than their temporal sequence, thus planar types 1 and 2 are probably younger than sinuous types 3 to 6. Early veins are largely restricted to the T Porphyry, but both the Main and L/M Porphyries are locally cut by quartz-rich, sulfide-poor vein types 1 and 2, and discontinuous chalcopyrite-pyrite(-anhydrite) veins with albitic envelopes (probably of type 3) occur in probable Main Porphyry at the 2,750-meter elevation, well above the inferred apex of the T Porphyry. Vein type 1 is contained in clasts throughout the tourmaline breccia complex. Vein type 2 may also be present in this setting but is difficult to distinguish from vein type 1 because of obliteration of the feldspathic alteration envelopes by subsequent hydrothermal events. Such early stage veins exposed in the intermediate and upper parts of the deposit (above approximately 2,750 meters) are thought to represent the distal and in part later equivalents of those veins which are present only or largely in the T Porphyry.

Pervasive potassium-silicate alteration of T Porphyry. A striking early stage feature is the development of fine-grained shreddy biotite in the groundmass of the T Porphyry. Biotitization has only been observed in this rock type, and because of the very fine-grained nature of the groundmass it is not certain whether matrix plagioclase was converted to a more albitic plagioclase or transformed into potassium feldspar. Details of the pervasive potassium-silicate alteration of the T Porphyry are provided in table 4.

Propylitic alteration. A propylitic zone is not well developed on the fringes of the Toquepala Deposit, at least at the exposed shallower levels of the hydrothermal system. The area of megascopically visible wallrock alteration (fig. 4) delimited by surface mapping by Richard and Courtright (1958a) is essen-

Table 3. Early stage veins at Toquepala, Peru.

	Mineral Assemblage and Texture	Alteration Halo	Structural Style	Comments
Vein-type 1 Barren quartz veins	Quartz+anhydrite+(carbonate)+ apatite±(chalcopyrite)>(pyrite); all minerals are fine-grained and equigranular	Absent	Open-space veins; sheeted; 0.1-0.5 mm vein widths; continuous, but split into fine wispy structures	Most common early vein-type in the upper portions of the deposit; cut dacite porphyry clasts contained in the breccias
Vein-type 2 Barren quartz veins with albite halos	As Vein-type 1	Na-feldspar+(carbonate); narrow width (<0.5-3 mm); irregular and discontinuous; texture destructive; very fine-grained; carbonate as very fine-grained platelets disseminated throughout the halo; sulfides absents	Open-space veins; sheeted; vein widths are typically 1 mm	Vein-type 2
Vein-type 3 Sulfide veins with albite halos	As Vein-types 1 and 2, but with greater proportions of sulfide, and lesser amounts of quartz	Albite; 2-5 mm width; irregular geometry; texture destructive; very fine-grained	Replacement veins; very narrow width (0.1-0.3 mm); discontinuous; irregular and often segmented	Vein-type occurs only in T Porphyry
Vein-type 4 Sulfide veins with K-feldspar halos	As Vein-type 3	K-feldspar; very thin and inconspicuous	As Vein-type 3	Vein-type occurs only in T Porphyry
Vein-type 5 Chalcopyrite+ bornite veins	Quartz+albite+anhydrite+ chalcopyrite+bornite; all the minerals, except albite,	Albite seams form where the vein cuts andesine phenocrysts	Replacement veins: very narrow widths (0.5-<1mm); continuous, not segmented or wispy	Uncommon vein-type; only known occurrence of chalcopyrite+bornite mineralization; occurs only in T Porphyry; most similar to El Salvador A veins
Vein-type 6 Biotite-quartz veins with albite halos	Biotite+quartz+anhydrite+ (apatite)±(chalcopyrite+ rutile); biotite occurs as a felted, fine-grained mass; quartz and apatite are equigranular and fine-grained; anhydrite and sulfides form clots	Albite; as Vein-type 3	Replacement veins; up to 8 mm in width; wispy	Rare vein-type; occurs only in T Porphyry

( ) = minor amounts of the mineral phase;
± = not always present in the assemblage

Table 4. Pervasive potassium silicate alteration of the T Porphyry, Toquepala, Peru.

Alteration Site	Alteration-Mineralization Assemblage	Texture	Comments
Plagioclase	Alkali feldspar+(anhydrite)+(biotite)	Alkali feldspar replaces andesine along fractures and cleavage planes; anhydrite occurs as fine clots; very fine-grained biotite platelets are present along fractures or as disseminations	The plagioclase is only incipiently altered; complete conversion to alkali feldspar is not observed
Biotite	Biotite±anhydrite±apatite±carbonate ±chalcopyrite>pyrite+rutile	The overall texture of the biotite is preserved; edges of the phenocrysts are embayed; included magmatic rutile needles are destroyed; anhydrite, apatite, and carbonate	A low-Fe composition for these biotites is inferred from the loss of pleochroism
Hornblende	Aggregate of shreddy biotite+ anhydrite+apatite±alkali feldspar(?) ±chalcopyrite>pyrite+rutile	Texture destroyed; biotite occurs as a shreddy mass; anhydrite and alkali feldspar(?) are equigranular; apatite occurs as hexagonal euhedra	Presence of amphibole inferred from rhombic to pseudohexagonal cross-sectional outline
Groundmass	Shreddy biotite+alkali feldspar(?) +quartz+anhydrite+apatite+ carbonate+chalcopyrite>pyrite+ rutile	Preserved; the relatively coarse-grained perthitic groundmass, typical of the strongly potassically-altered feldspar porphyries at El Salvador, Chile, is not developed	The development of fine-grained biotite within the groundmass, i.e., pervasive biotitization produces a striking brown coloration of T porphyry in hand-specimen

( ) = minor amounts of the mineral phase;
± = not always present in the assemblage

tially coextensive with the ore deposit. Locally intense chloritic (± actinolite) alteration occurs in the roof zones of several of the granitoid plutons exposed at surface and in railway tunnels in the Toquepala District but is thought to have resulted from sulfide-free deuteric activity which preceded development of the Toquepala Intrusive Center and porphyry copper mineralization.

The timing of propylitic alteration at Toquepala is unknown. Such alteration at El Salvador, Chile (Gustafson and Hunt, 1975), and Bingham, Utah (Bowman and others, 1987), is inferred to be contemporaneous with early potassium-silicate alteration and mineralization. It is noteworthy that two porphyry systems located a few tens of kilometers to the north-northwest of Toquepala (fig. 1) exhibit well-developed propylitic zones and large volumes of either potassium-silicate alteration and mineralization (Quellaveco: Estrada, 1975) or sericite-clay-chlorite alteration which probably record retrograde degradation of potassic assemblages (Cuajone: Manrique and Plazolles, 1975; A.H.C., unpublished data), while the Toquepala Deposit displays little of either of these alteration facies.

Summary. Early stage alteration and mineralization at Toquepala is similar to that recorded in many porphyry copper (-molybdenum) deposits in the Central Andes and elsewhere. As compared to many well-documented porphyry systems, however, early events at Toquepala were both weak and areally restricted. Although some veinlet types contain abundant chalcopyrite, the best-developed early stage veins (types 1 and 2) are essentially sulfide-free, and little copper and no molybdenum were introduced in this stage. It is inferred that the early stage vein system exhibited a decrease in copper sulfide content both upward and with time.

The abundance of hydrothermal albite in early vein types 3 and 6 should be emphasized. The presence of chalcopyrite and the apparent absence of more calcic plagioclase and hydrothermal amphibole discourage analogies with early and barren sodium-calcium alteration such as has been documented at Yerington, Nevada, by Carten (1986), and there is no evidence for the development of magnetite-plagioclase-amphibole alteration such as dominated the earliest alteration at Park Premier, Utah (John, 1989), and Island Copper, British Columbia (Arancibia and Clark, 1990 and in press).

Tourmaline Stage

Widespread brecciation, minor stockwork development, and deposition of abundant tourmaline characterize this second stage. The breccias consist of quartz-sericite enriched clasts in a tourmaline-quartz matrix. Features of this period were superimposed upon those of the early stage and define an inherently sulfide-poor, copper- and molybdenum-barren stage.

Tourmaline breccia. Two alteration assemblages are developed in tourmaline breccia: quartz-sericite and tourmaline-quartz. The quartz-sericite assemblage is restricted to the larger fragments (generally greater than 1 centimeter in diameter) in the breccia. Feldspar sites in dacite porphyry and diorite clasts are replaced by sericite and quartz, while the groundmass of the porphyry is converted to a granoblastic quartz-sericite-rutile assemblage. Quartz is present as equant polygonal grains with equilibrium triple junctions, and sericite is present as dispersed platelets (fig. 10C). Rare tourmaline rosettes are present in feldspar sites. Normative calculations based upon whole-rock analyses and specific gravity measurements of altered diorite clasts define a composition of 67 to 72 volume percent quartz and 27 to 33 volume percent sericite. The alteration front against unaltered fragment cores is sharp in clasts which were large enough to buffer the hydrothermal fluid, and no background alteration is present other than sericite dusting of feldspar. The quartz-sericite ratio increases slightly towards the margins of clasts until fragments are completely converted to fine-grained aggregates of quartz at their rims (fig. 10A). Original wallrock textures are obliterated in areas of intense quartz replacement, but even the most altered clasts are not embayed, altered in outline, or rendered significantly more porous in the main tourmaline breccias. Quartz-sericite replacement appears to have been a constant-volume process, and no pyrite or other sulfide accompanies the alteration.

Minerals indicative of either intermediate (illite and smectite) or advanced argillic (alunite, diaspore, dickite, dumortierite, kaolinite, and pyrophyllite) alteration are not present in the clasts or matrix of pristine tourmaline breccias at Toquepala. Small amounts of sericite relative to quartz, lack of pyrite, and removal of significant alumina from clasts are characteristic of alteration of the tourmaline breccias at Toquepala and of the copper-bearing tourmaline breccia pipes of north and central Chile (Sillitoe and Sawkins, 1971) and at El Salvador, Chile (Heatwole, 1973); Copper Creek, Arizona (Walker, 1979); Shaft Creek, British Columbia (Fox and others, 1976); and Wheal Remfry, Cornwall (Allman-Ward and others, 1982). It is suggested that this unusual type of alteration be termed "quartz-sericite," thereby distinguished it from normal sericitic (quartz-sericite-pyrite) alteration.

A. Photomicrograph of tourmaline breccia showing interface between tourmaline matrix (right) and quartz-sericite altered clast (left). The abundance of sericite decreases towards rims of clasts. Quartz is present in the clast as equant polygonal grains with equilibrium triple-junctions, whereas sericite is present in dispersed platelets. Cross-polarized transmitted light (SPTF: DDH Q21–464m). ▶

B. Photomicrograph of tourmaline breccia showing tourmaline+quartz assemblage in breccia matrix. Small matrix-size clasts have been recrystallized and metasomatized to quartz and are enclosed by tourmaline needles. Note lack of sulfide in Figs. 10A and 10B. Plane-polarized transmitted light (SPZ-C-28: DDH P19-214m).

C. Photomicrograph showing iron depletion in tourmaline rosette partially engulfed by sulfide. Tourmaline needles are oriented to display maximum possible absorption. Arrows point to tourmaline crystals which were presumably comminuted during a mineralizing and fracturing event related to sulfide deposition. Plane-polarized transmitted light (SP-93: open pit; location unknown).

D. Hand specimen of tourmaline breccia cut by main-stage quartz-molybdenite-chalcopyrite veins. Cross-cutting relationship demonstrates older age of tourmaline breccia (SPZ-C-145: DDH 021 - 214m).

E. Hand specimen of tourmaline breccia cut by main-stage chalcopyrite-pyrite mineralization. Note sulfide veinlet which trends from the lower left-hand to upper right-hand side of sample (SPZ-C-37: DDH P19-236m).

F. Hand specimen of late-stage pyrite vein cutting tourmaline breccia. Tourmaline needles within the alteration halo are altered to pyrophyllite (SPTF: DDH Q21–465m).

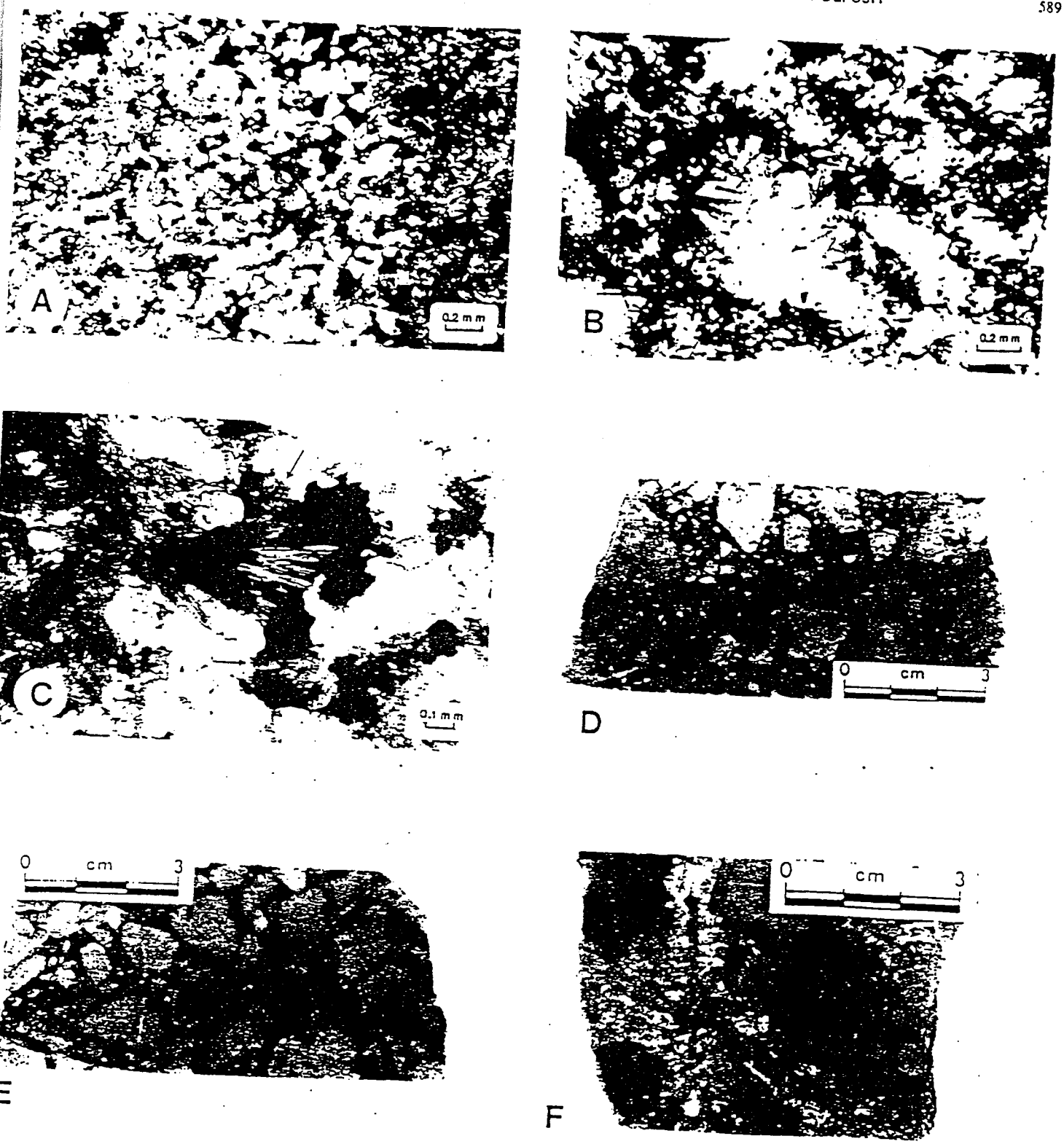

Figure 10. Features of tourmaline-stage alteration and mineralization, Toquepala.

A simple tourmaline-quartz assemblage comprises the breccia matrix. Fine tourmaline needles are present either as a mass intergrown with fine-grained quartz-replaced matrix material or as rosettes nucleated on the edges of breccia clasts (fig. 10B). Quartz is present solely as a replacement of finer clastic material; no "free" quartz has been precipitated. Only traces of sericite and no primary sulfides are present in the matrix. Tourmaline is altered to pyrophyllite where cut by late stage pyrite veins (fig. 10F). Whether tourmaline formed predominantly as an open-space filling or as a matrix replacement is not clear: Lack of abundant primary void space, crustification, comb structure, symmetrical banding, and cockade structure in the matrix all point away from extensive open-space deposition (consider the San Francisco de los Andes Tourmaline Breccia Pipe, Argentina: Llambías and Malvicini, 1969, and the Ilkwang Tourmaline Breccia Pipe, Korea: Fletcher, 1977), and the fine-grained nature of the tourmaline further supports a replacement origin.

Sulfides occur in the tourmaline breccia only in pre-breccia early stage quartz veins, disseminations in clasts and crosscutting veins, and disseminations related to subsequent mineralizing stages. Quartz veins are preserved even in the most intensely quartz-sericite altered clasts, but any alteration envelopes that may have been associated with such veins have been destroyed and the amount of copper present in such veins is negligible. Almost all sulfide in the breccias post-dates breccia emplacement and is described in the section on main stage alteration and mineralization.

Because tourmaline is represented in a wide variety of alteration facies such as the sodium-calcium alteration at Yerington, Nevada (Carten, 1986), potassium-silicate alteration at Ann-Mason, Nevada (Dilles and Einaudi, 1992) and Los Pelambres, Chile (Sillitoe, 1973), sericitic alteration at Yerington (M.T. Einaudi, personal communication, 1984), and in many porphyry copper deposits of the Cascade Range, Washington (Hollister, 1979), tourmaline-bearing assemblages must be carefully specified. Tourmaline appears to be absent in advanced argillic assemblages, where it is either proxied for or replaced by dumortierite (Island Copper, British Columbia: Cargill and others, 1976; Arancibia, unpubl. data) or destroyed (Toquepala, this study; Wedekind and Peavine District, Nevada: Hudson, 1977).

Tourmaline-quartz veinlets. Poorly developed stockworks and sheeted arrays of tourmaline veinlets with narrow tourmaline-quartz alteration selvages have been observed in numerous exposures of the diorite and in pebbles contained within the pebble pipe. These veinlets are up to 1 millimeter wide and consist of radiating tourmaline needles that extend into and replace wallrock. Minor quartz intergrown with tourmaline needles replaces wallrock adjacent to the veinlets. The tourmaline veinlets are barren of sulfides but are cut and reopened by chalcopyrite-pyrite (-molybdenite) veinlets of the main stage and by late stage pyrite-quartz veins with sericitic envelopes. No direct relationship between the tourmaline-quartz veinlets and the tourmaline breccias has been observed, but the former are confidently assigned to the tourmaline stage based on their mineralogy and age relationships.

Main Stage

The main stage is so named because it represents the major period of both copper and molybdenum mineralization at Toquepala. Numerous cross-cutting relationships (figs. 10D and E) confirm that this was a distinct event that followed the essentially barren tourmaline stage. Main stage alteration and mineralization terminated prior to emplacement of the dacite agglomerate and before the hydrothermal system evolved to the strongly hydrolytic state characteristic of the late stage. Copper- and molybdenum-mineralized quartz veins without alteration haloes, molybdenite breccia, and rare magnetite veinlets developed during the main stage.

Quartz-molybdenite-chalcopyrite veins. Quartz-rich veins which contain important amounts of molybdenite and chalcopyrite are a common and distinctive feature of the main stage. These veins lack well-defined alteration envelopes, occupy continuous fractures, and are typically about 3 millimeters wide. All rock types with the exceptions of the dacite agglomerate, vuggy breccia, latite porphyry, and pebble breccia are cut by these veins (fig. 11A). Unambiguous cross-cutting relationships with early stage veins, tourmaline breccia, and pyrite-quartz veins of the late stage demonstrate that the quartz-molybdenite-chalcopyrite veins postdate the early and tourmaline stages but predate the late stage (fig. 11B). The veins are analogous to the B veins of El Salvador, Chile (Gustafson and Hunt, 1975), and are remarkably homogeneous in texture and mineralogy. Abundant quartz and minor anhydrite comprise 90 to 95 percent of the veins, and molybdenite commonly exceeds chalcopyrite in abundance. Pyrite is generally rare, and bornite and sulfosalts have not been observed.

Where these veins cut porphyritic rocks, molybdenite occurs as bladed aggregates nucleated on vein walls (fig. 11C). Deposi-

A. Hand specimen of quartz-molybdenite-chalcopyrite vein cutting type 1 early-stage sheeted veins in Main Porphyry. Superimposed late-stage alteration has converted much of sample to quartz-sericite-chlorite-pyrite assemblage (SPZ-C-246: DDH T20-603m). ▶

B. Hand specimen showing quartz-molybdenite-chalcopyrite vein cut and offset by later quartz-sericite-pyrite vein in L/M Porphyry. Supergene alteration has converted plagioclase to kaolinite (SPZ-C-197: DDH L/M-18-420m).

C. Photomicrograph of molybdenite depositional site within a quartz-molybdenite-chalcopyrite vein. Molybdenite blades (black) are nucleated on feldspar phenocryst in wall-rock. Feldspar is converted to fine-grained sericite aggregate, whereas relatively coarse-grained sericite blades are intergrown with molybdenite. Plane-polarized transmitted light (SPZ-C-263: DDH T20-673m).

D. Hand specimen showing magnetite vein cutting molybdenite breccia. Silicified fragments were originally contained in tourmaline breccia. Overprinting by late-stage alteration partially sulfidized magnetite to pyrite and minor chalcopyrite and transformed previously unaltered cores of silicified fragments to quartz-sericite-pyrite assemblage (SPZ-C-221: DDH V20-390m).

E. Hand specimen of main-stage breccia displaying multiple fracturing and mineralizing events. Type 1 early-stage veins cut Main Porphyry wall-rock to record the first event. Incorporation of Main Porphyry as fragments in tourmaline breccia followed. Rebrecciation and infilling of tourmaline breccia by main-stage chalcopyrite-pyrite mineralization record the final event. Note that only those portions of breccia clasts that were originally in contact with tourmaline matrix have been silicified (SPZ-C-09: DDH P19-82m).

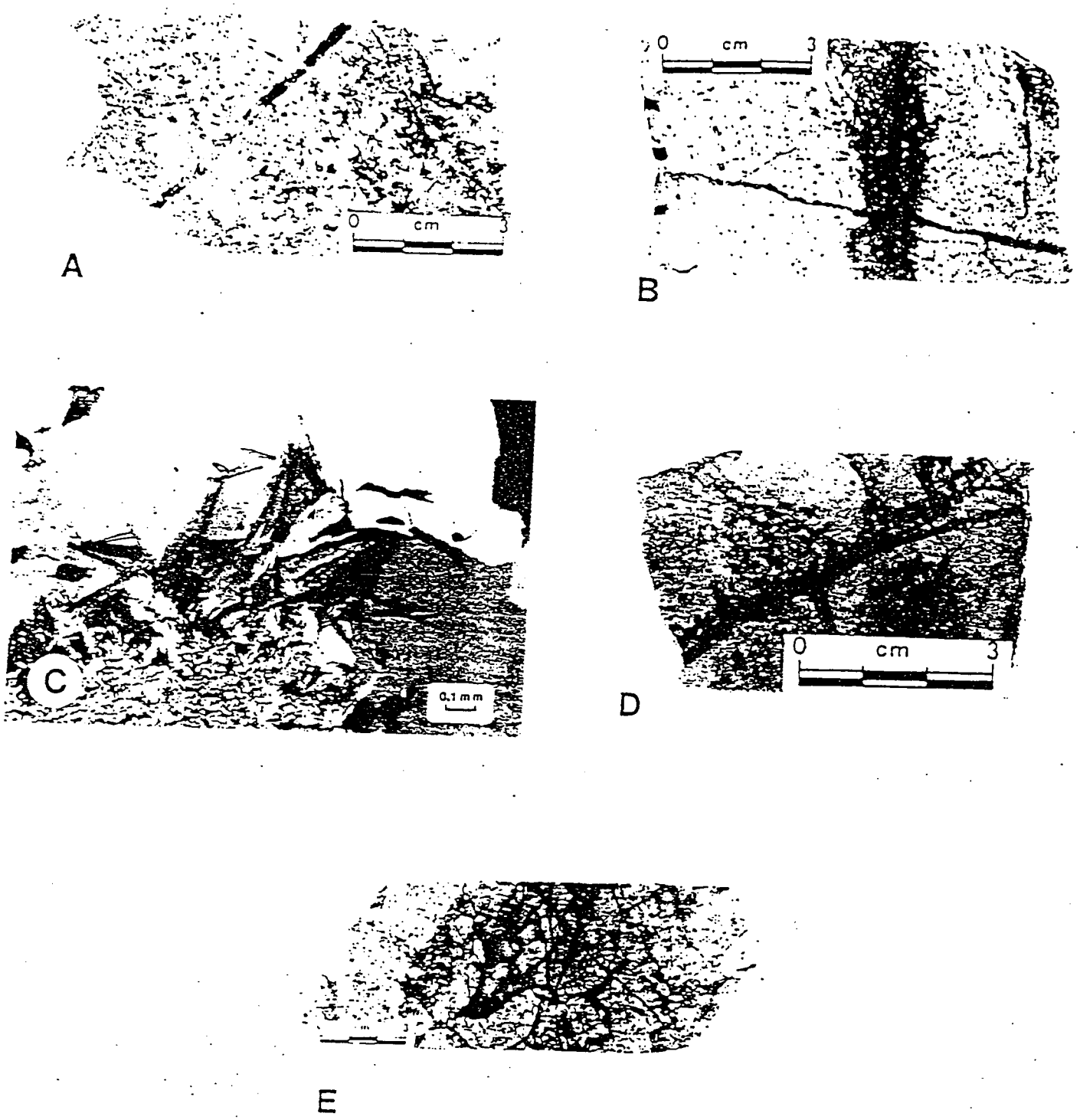

Figure 11. Features of main-stage alteration and mineralization, Toquepala.

tion of molybdenite and of other sulfides was site-specific and strongly controlled by feldspar phenocrysts. Feldspar has been converted to a fine-grained assemblage of sericite-calcite-anhydrite-apatite, and microscopic platelets of sericite are typically intergrown with molybdenite blades. Feldspar grains which have been cut by the veins but not utilized as deposition sites remain unaltered. The veins typically contain lesser amounts of quartz and clasts where they cut tourmaline breccia, and portions of the breccia matrix containing a high density of fine fragmental material proxy for feldspar as sulfide depositional sites. Similar observations regarding the role of wallrock feldspar in the deposition of molybdenite have been recorded from the Henderson Deposit, Colorado (Carten, Geraghty, and others, 1988).

Chalcopyrite-pyrite mineralization. Abundant chalcopyrite-pyrite veins and seams cut and mineralize tourmaline breccia (fig. 11E), and much of the copper-iron sulfide within the tourmaline breccia was deposited in association with these main stage veins. Chalcopyrite and lesser pyrite are present as narrow veinlets and fracture-controlled disseminations. The volume percent of total sulfide is low, ranging from 0.5 to 2. However, broken wallrock is cemented by massive chalcopyrite to form a copper analog to the molybdenite-rich breccia in strongly mineralized areas; copper grades attain several percent in these breccias. Pinkish-purple anhydrite is conspicuous as disseminations and coarse-grained patches in the breccias. Little if any quartz was precipitated with copper-iron sulfide, and no megascopically visible wallrock alteration attended copper-iron sulfide deposition.

Overview of molybdenum mineralization. The distribution of molybdenum mineralization at Toquepala corresponds essentially to the occurrence of quartz-molybdenite-chalcopyrite veins, molybdenite breccia, and molybdenite paint or smears along fractures and joints. All are main stage features. Molybdenite in the last form is unaccompanied by other sulfide or gangue phases or by wallrock alteration. Quartz-molybdenite-chalcopyrite veins contributed the greatest proportion of molybdenum.

Much of the molybdenite in the deposit is confined to irregular vertical shoots within the hydrothermal breccia complex (Stevenson, 1981). Only minor amounts occur in the dacite porphyry and diorite, and no molybdenite ore shell has been defined over the apices of dacite stocks. Geologic reserves and grades of molybdenum delineated from the 1973 to 1980 deep drill program are high relative to those in most Andean porphyry copper(-molybdenum) deposits. Grades range from less than a fraction of a percent to over 2 percent MoS_2, and intervals over 150 meters in width with more than 0.5 percent MoS_2 are known. A downward increase in molybdenum grades in the orebody implies that the abundance of quartz-molybdenite-chalcopyrite veins increases relative to that of chalcopyrite-pyrite veins with depth.

Magnetite veins. Magnetite veins are rare at Toquepala where they are known to exist only in the deeper zones (2,920 to 2,815 meters) of the central part of the hydrothermal breccia complex. Magnetite is the only mineral in this sulfide-free assemblage. These mineralogically simple veins are narrow (2 to 3 millimeters), through-going features that lack alteration haloes.

The relative ages of the magnetite veins and breccias are not well documented, but from a single observation of a magnetite vein cutting molybdenite breccia (fig. 12D) it is inferred that the formation of the magnetite was later than the deposition of molybdenite-bearing assemblages. As at Island Copper, B.C. (Arancibia and Clark, 1990), magnetite is apparently absent in early stage veins. Magnetite veins have commonly been reopened; quartz and anhydrite fill the fractured veins, but more significant is the sulfidation of magnetite to pyrite and minor chalcopyrite in the fractured veins. Chlorite rims fractured magnetite grains and lines vein walls. Sericitic alteration is pervasive where the veins have been reopened and may be associated with pyrite, therefore deposition of magnetite is inferred to have predated late stage mineralization.

Late Stage

Widespread hydrolytic alteration and abundant pyrite introduction took place during late stage alteration and mineralization, which formed copper-poor pyrite-quartz veins with sericitic alteration envelopes, pyritic veins, and pyrite-rich vuggy breccia which locally contains minor amounts of chalcopyrite and bornite-pyrite associated with sericitic, intense sericitic (sericite-andalusite), or advanced argillic alteration. An unusual feature is the local development of albite-sericite alteration.

Pervasive albite-sericite alteration. Albitic alteration has affected significant volumes (drill core intersections of 20 to 80 centimeters) of probable Main Porphyry at the 2,780- to 2,810-meter level overlying the T Porphyry Stock. The cream-colored altered rocks are extremely fine-grained and appear porcelaneous and aphanitic in hand specimen. Lath-like albite (An_{1-7}; Or_{0-1}) is intimately intergrown with sericite (5 to 15 volume percent), which is inferred to have formed contemporaneously. Only minor quartz survives in the albitized zones of the original mineral assemblage. Albite and sericite also replace quartz and anhydrite in main stage quartz-molybdenite-chalcopyrite veins in these zones.

A. Hand specimen showing quartz-sericite-pyrite vein cutting latite porphyry (SPZ-C-288: DDH Q21-186m). ▶

B. Hand specimen of bornite+pyrite mineralization (immediately left of center) filling void within vuggy breccia (SPZ-35: open pit: 3085m level-W).

C. Hand specimen of late-stage bornite+pyrite vein cutting pervasively sericitized dacite porphyry. Creamy plagioclase phenocrysts adjacent to vein are altered to pyrophyllite (SPZ-C-309: DDH Q21-455m).

D. Photomicrograph of altered plagioclase phenocrysts in porphyry clast in pebble pipe breccia. Phenocryst is intensely altered to pyrophyllite and unknown almost opaque mineral. Cross-polarized transmitted light (SPZ-81: open pit: 3205m level-NE).

E. Photomicrograph of andalusite rosette in quartz-sericite-andalusite-pyrite assemblage. Plane-polarized transmitted light (SPCC-6: open pit; 3160m level-SW).

F. Photomicrograph of andalusite aggregate altered to fine-grained pyrophyllite in alteration halo of late stage pyrite vein. Plane-polarized transmitted light (SPCC-6: open pit; 3160 level-SW).

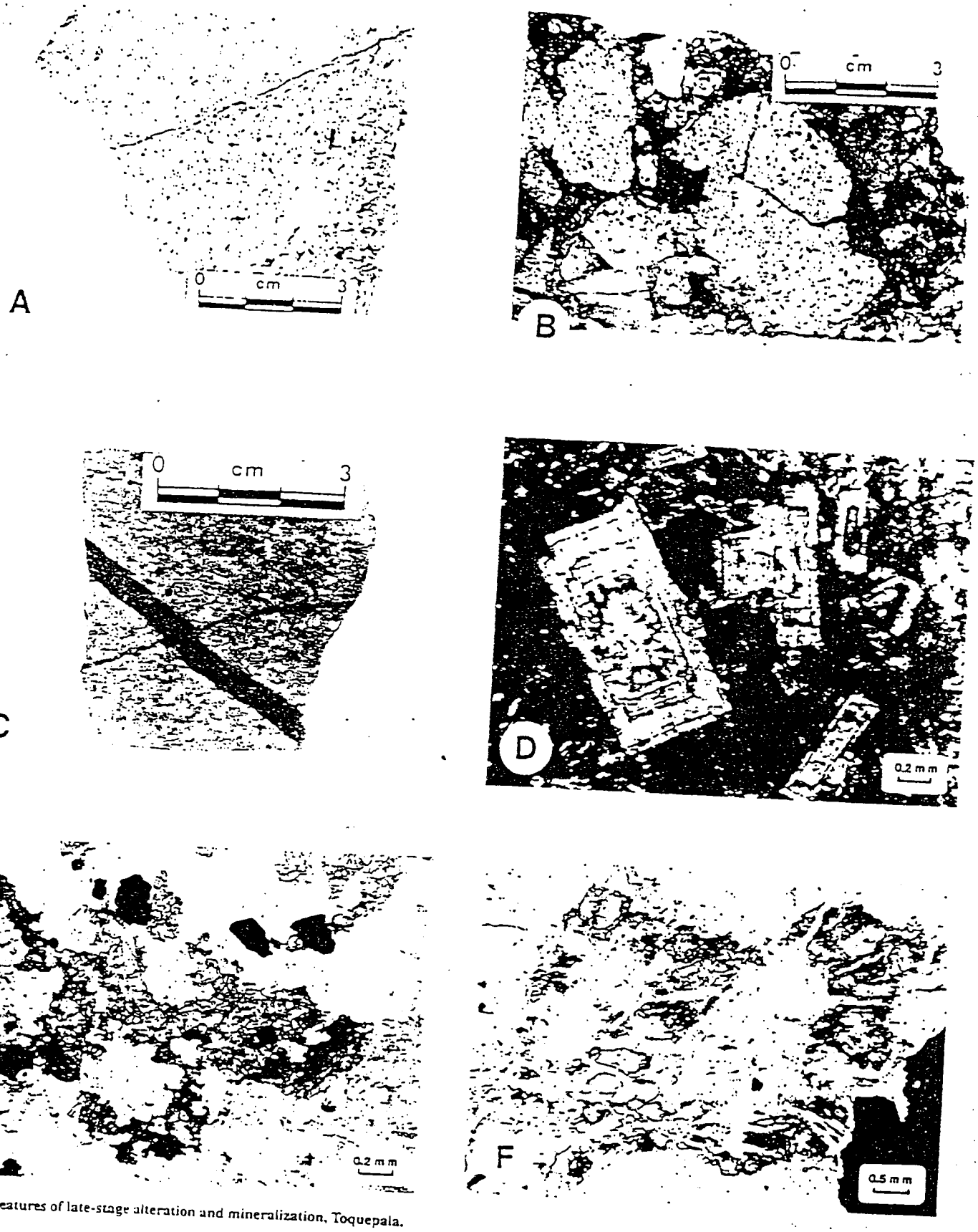

Figure 12. Features of late-stage alteration and mineralization, Toquepala.

Quartz-sericite-pyrite alteration and associated pyrite-quartz veins. These veins are characterized by sericitic alteration halos and lack andalusite. The veins cut every rock type and all early, tourmaline, and main stage features (fig. 12A). Overall they probably represent the most abundant and widespread vein type at Toquepala, particularly in the pit. Pyrite-quartz veins tend to occur in greatest abundance high in the system but are observed even in its lowest exposed portions. These veins are through-going structures, and some are continuous over several meters.The assemblage is pyrite-quartz-anhydrite. Quartz-rich variants are rare higher in the system, where veins tend to be more pyrite-rich. Dissolution of anhydrite in veins located above the hypogene sulfate zone generates voids and imparts a vuggy appearance. Vein widths are typically 1 to 2 millimeters. Alteration selvages of the assemblage quartz-sericite-anhydrite-carbonate-apatite-pyrite-rutile typically extend 3 to 10 millimeters into the wallrock and terminate abruptly. As with the main stage veins of Butte, Montana (Meyer and others, 1968), no outer kaolinite or montmorillonite alteration zones have been observed. Chlorite is locally present in the haloes of veins in the deeper levels. Original rock textures are obliterated within the alteration envelopes.

Pyrite is the dominant sulfide in the pyrite-quartz veins. Molybdenite is not present, and chalcopyrite is generally not common. The assemblage tennantite (2 to 4 weight percent silver)-chalcopyrite has been observed in only two veins in the deeper parts of two drill-holes at the 2,903- and 3,036-meter levels (see also Mendoza, 1980). The high-sulfur bornite-pyrite assemblage present at these depths partially to completely replaces chalcopyrite but appears to be in equilibrium with tennantite, with which anhydrite and quartz are closely associated. Minor enargite, sphalerite, and galena have been reported from copper concentrates by Mendoza (1980) and are probably derived from pyrite-quartz veins cutting tourmaline breccia. Cobaltite and cobaltian pyrite have been observed in three polished sections of two separate late stage pyrite-quartz vein samples. The average copper content of these widespread veins is estimated not to exceed 15 percent, and their contribution overall to the ores has been minor.

Quartz-sericite-andalusite-pyrite alteration and associated pyrite veins. An intensely feldspar-destructive alteration type characterized by the assemblage quartz-sericite-andalusite-pyrite-rutile is widespread within the supergene sulfide enrichment blanket in the upper levels of the open pit. The term "intense sericitic" is applied here to such alteration to distinguish it from sericitic alteration that lacks andalusite. Veins directly associated with this alteration occupy through-going fractures similar to those of the pyrite-quartz veins. These veins are filled with granular pyrite with only minor quartz. Anhydrite has not been observed, but this may be a function of the location of the veins above and outside of the present-day sulfate zone. Alteration haloes are similar in geometry and size to those surrounding pyrite-quartz veins, and quartz is the most common constituent of these haloes. Sericite is not as abundant as in the quartz-sericite-pyrite vein haloes but does replace all rock-forming silicates other than quartz. Andalusite is abundant (25 to 40 volume percent) as coarse, radiating rosettes or equant grains (fig. 12E) generally surrounded by and intergrown with sericite. Andalusite appears as pseudomorphs after plagioclase phenocrysts in dacite porphyry, but the destruction of primary host-rock textures in the alteration envelopes has rendered the original mineralogic sites difficult to distinguish. Considerable pyrite (5 to 10 volume percent) is disseminated in the wallrock. The abundance of quartz and andalusite in alteration haloes is evidence that aluminum was mobile on at least a local scale. The quartz-sericite-andalusite-pyrite assemblage at Toquepala is very similar to the upper-level sericite-andalusite assemblage (as opposed to the deep-level potassium feldspar-andalusite-quartz-sericite assemblage) at El Salvador (Gustafson and Hunt 1975), the andalusite-quartz-sericite assemblage in the Elkhorn District, Montana (Steefel and Atkinson, 1984), and the andalusite-sericite-quartz assemblage at La Granja, Peru (Schwartz, 1982). In all these localities the andalusite-bearing assemblage is high in the porphyry system and appears to represent an intense facies of sericitic alteration. At La Granja this has been described as advanced argillic alteration despite pyrophyllite having replaced andalusite (Schwartz, 1982, p. 485).

Pyrite veins. A further group of pyrite-dominated veins occurs in the upper sericitically altered portions of the deposit. These veins have limited vertical continuity compared to the pyrite-quartz veins with sericitic envelopes and are relatively scarce in the deepest levels of the deposit. They clearly post-date the sericite-associated veins and cut every lithology in the mine. Pyrite is usually the only mineral in the veins, but minor bornite is present locally (fig. 12C); the pyrite-bornite assemblage is concentrated in voids of contiguous bodies of vuggy breccia (fig. 12B). Although pyrophyllite is disseminated in rocks cut by this class of pyritic vein, alteration halos are not discernible around many of these veins because of earlier pervasive sericitic alteration of wallrocks. The structural habit of these veins is one of their most distinctive features: Whereas the pyrite-quartz veins typically infill narrow structures, the pyrite veins are generally over 5 millimeters in width. The association of these veins with advanced argillic alteration and their younger age relative to the pyrite-quartz(-sericite) veins warrant their classification as a distinct group.

Figure 13. Types of fluid inclusions at Toquepala.

A. Photomicrograph of a type 1 fluid inclusion in quartz. Low vapor-to-liquid ratio and absence of salt daughter minerals characterize these weakly to moderately saline inclusions. Plane-polarized transmitted light (SPZ-89: open pit; 3205m level-NE).

B. Photomicrograph of a type 2 fluid inclusion in quartz. High vapor-to-liquid ratio is diagnostic of these fluid inclusions. Small opaque mineral, presumably hematite, is widely present in these inclusions. Plane-polarized transmitted light (SPZ-C-30: DDH P19-218m).

C. Photomicrograph of type 3 inclusions in quartz. Halite daughter mineral and low vapor-to-liquid ratio typify this inclusion type. The large type 3 inclusion shown here contains two additional daughter products: a small opaque, presumably hematite, and a small colorless unknown mineral. Plane-polarized transmitted light (SPZ-C-30: DDH P19-218m).

D. Photomicrograph showing coexistence of vapor-rich type 2 inclusions and saturated type 3 inclusions in quartz from main-stage quartz-molybdenite-chalcopyrite vein. Plane-polarized transmitted light (SPZ-C-30: DDH P19-218m).

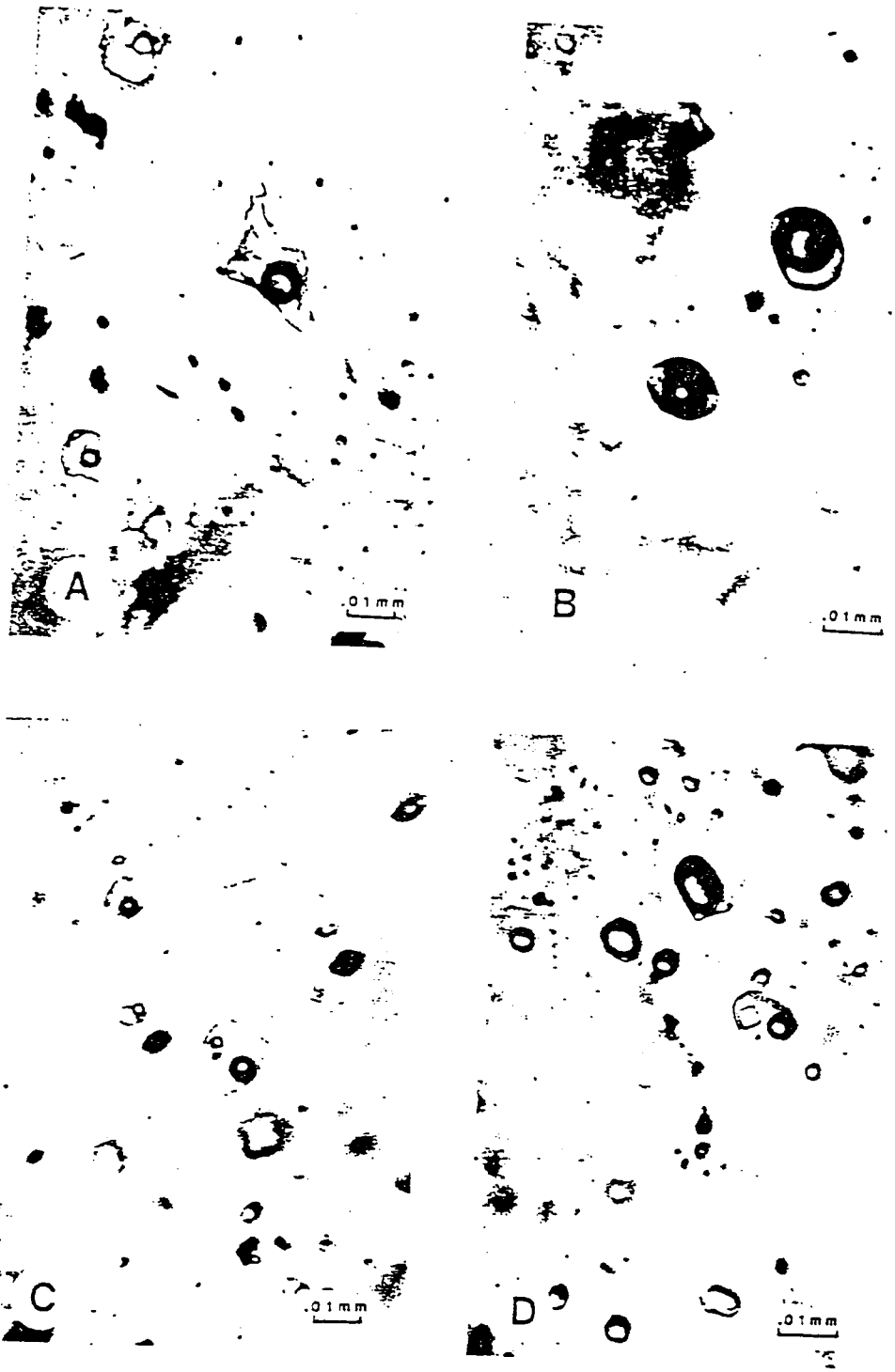
A
.01 mm
B
.01 mm
C
.01 mm
D
.01 mm

Advanced argillic alteration. Advanced argillic alteration assemblages were not examined in detail during this study. The only advanced argillic index mineral identified is pyrophyllite, which is associated with both pyrite veins and pebble breccia. Where associated with pyrite veins, pyrophyllite is located both in the veins and (more commonly) in irregular patches immediately adjacent to the veins. It is unclear whether sericite is stable with the pyrophyllite. Where andalusite was once present in the wallrock, pyrophyllite has replaced it: these minerals probably do not constitute a stable assemblage (fig. 12F). Pyrophyllite has destroyed tourmaline in the alteration haloes of late stage pyrite veins in tourmaline breccia.

Clasts in the pebble breccias are intensely altered to pyrophyllite and sericite. This may represent either incorporation of previously altered wallrock or later replacement of the breccias. Pyrophyllite and sericite are intergrown in highly corroded feldspar sites in pebbles (fig. 12D), and pyrophyllite is present in irregular patches and is commonly accompanied by sericite in matrix. Freemark (1977) has observed that montmorillonite is abundant in some pebble dikes and is locally associated with sericite and chlorite, indicating that at least some of the alteration associated with brecciation was of intermediate argillic type (the sericite-clay-chlorite association of Sillitoe and Gappe (1984)).

FLUID INCLUSION RELATIONSHIPS

A reconnaissance fluid inclusion study was undertaken to document changes in temperature, salinity, and pressure of hydrothermal fluids involved in the evolution of the Toquepala Deposit. Microthermometric data were collected from 187 inclusions in quartz crystals from seven hand specimens considered to be representative of the four stages of alteration and mineralization. Details of the analytical techniques and fluid inclusion apparatus have been recorded in Zweng (1984). The only previous study of fluid inclusions in the deposit is that of Shanks (1977), who examined mainly late stage veinlet quartz from locations in the pit.

Types of Fluid Inclusions

Fluid inclusions are abundant in all samples with the exception of those from a quartz-sericite-pyrite vein. Most are small (less than 15 microns), but those utilized in the freezing and heating experiments generally measured between 25 and 60 microns.

Three types of inclusion have been recognized:

Type 1: Two-phase (liquid+vapor) liquid-rich inclusions. These inclusions contain 5 to 35 volume percent vapor at room temperature, homogenize to a liquid when heated, are of low to moderate salinity, and are the most common type in all veins (fig. 13A).

Type 2: Two-phase (liquid+vapor) vapor-rich inclusions. These inclusions contain approximately 40 volume percent vapor at room temperature, homogenize to a vapor when heated, and are generally low in salinity. A small opaque phase, presumably hematite, is commonly present (fig. 13B).

Type 3: Polyphase liquid-rich (35 volume percent vapor) inclusions. These highly saline inclusions contain one or more daughter minerals and homogenize to a liquid when heated (fig. 13C).

Fluid inclusions with characteristics intermediate between types 1 and 2 were classified depending on whether they homogenized to a liquid or to a vapor. No CO_2-bearing inclusions were observed. Halite is abundant in type 3 inclusions; other daughter minerals identified by scanning electron microscopic studies of opened inclusions include sylvite, anhydrite, hematite, antarcticite, and chalcopyrite. Vapor-rich (type 2) inclusions coexist with either liquid-rich (type 1) or highly-saline (type 3) inclusions in many samples (fig. 13D).

In nearly all samples there is an abundance of secondary inclusions, and care was therefore exercised in choosing inclusions for study. The distinction between primary and secondary inclusions is critical to the correct assignment of fluid compositions and trapping temperatures to specific vein-forming events. Roedder's (1979) criteria for the origin of fluid inclusions were helpful in this regard, but ambiguities remained in many instances. To distinguish primary from secondary inclusions, the following approach adopted from Shaver (1984) was employed: Inclusions which were spatially isolated, randomly oriented, and significantly larger than those grouped along fracture planes were designated as apparently primary. Homogenization temperatures of clearly secondary inclusions present as planar groups along fractures which transect mineral grain boundaries were utilized in each sample as a basis for comparison with those of the apparently primary inclusions, and only if the filling temperatures of the latter inclusions defined a population distinct from and at a higher temperature than the secondary or control population were they inferred to be primary. Roedder (1971) suggested that samples with numerous secondary inclusions should not be used for microthermometric study, but as pointed out by Shaver (1984) "for many porphyry deposits with multiple fracturing and mineralization events. . .secondary inclusions are ubiquitous features which cannot be avoided even by careful sample selection, and the above method of separating secondary and primary inclusions may be the only means available."

Early Stage

Twenty-six apparently primary and 21 secondary inclusions 25 to 80 microns in diameter were studied in eight doubly polished quartz slabs prepared from a type 2 vein (fig. 14). The sample was taken from diamond drill hole P19 at an elevation of 2,940 meters above sea level and was only weakly overprinted by main stage chalcopyrite-pyrite mineralization. Other early stage vein types were found to be unsuitable for study either because they lacked inclusion-bearing minerals (vein type 4) or were composed of quartz crystals too small to host sizable inclusions (vein type 1). Secondary inclusions are more abundant in quartz in early stage veins than in younger veins and homogenize between 305 and 405°C. These inclusions are of types 1, 2, and 3, and their fluids are inferred to have undergone boiling.

Some inclusions of each of the three types are apparently primary. A chalcopyrite daughter mineral was observed in only one type 3 apparently primary inclusion. Anhydrite is not un-

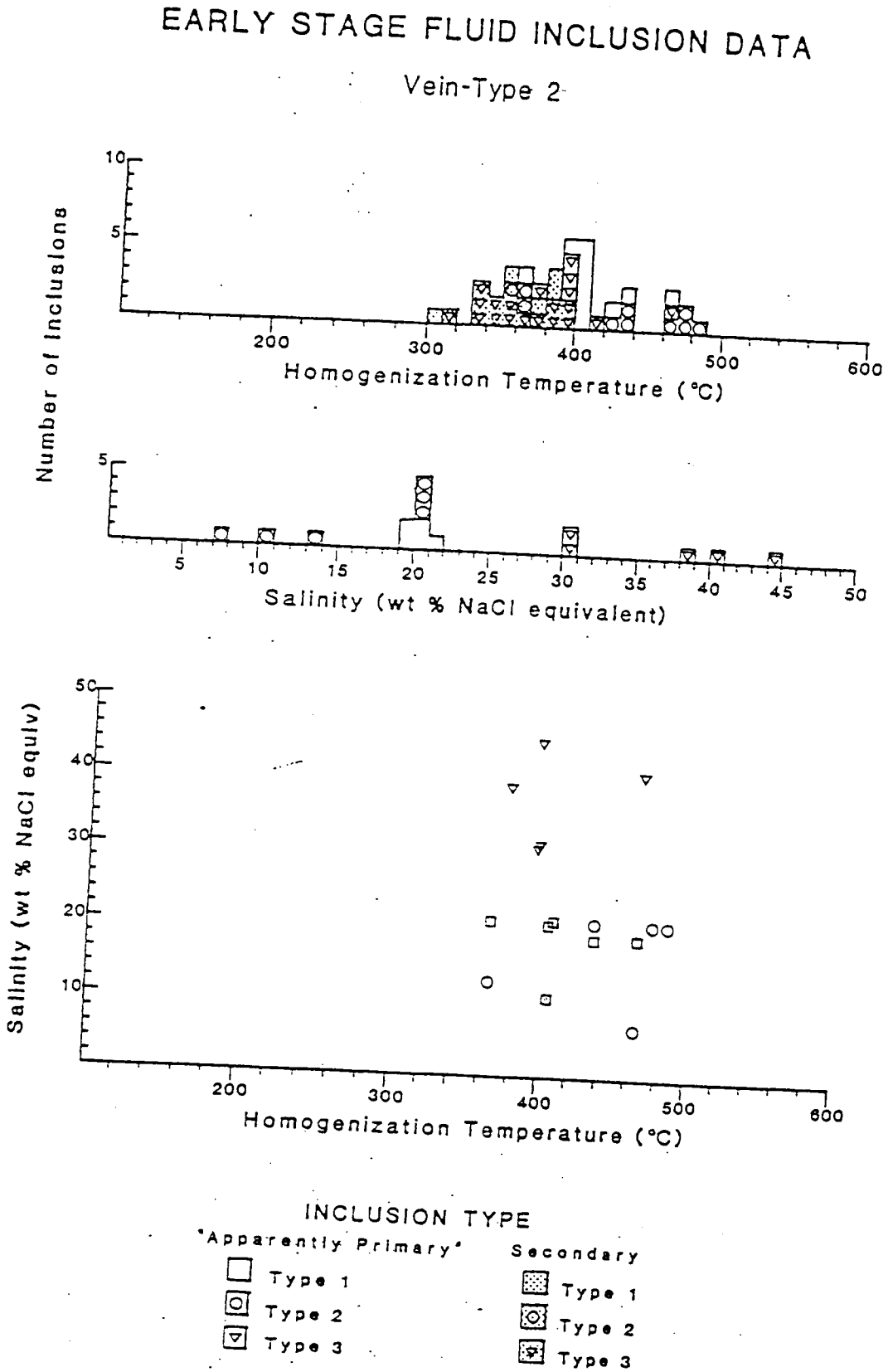

gure 14. Histograms of fluid inclusion homogenization temperatures and salinities for quartz in early-stage alteration and mineralization.

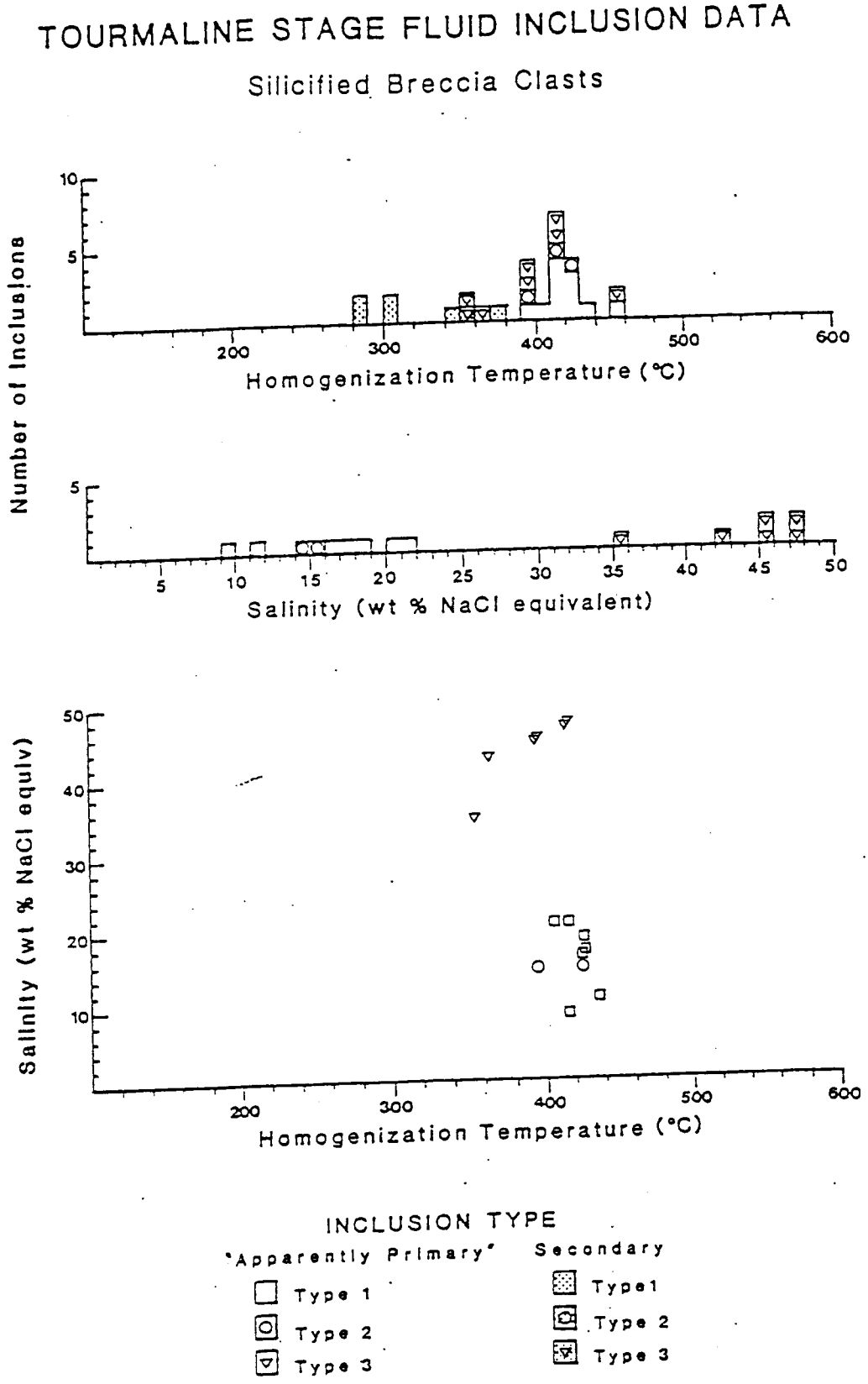

Figure 15. Histograms of fluid inclusion homogenization temperatures and salinities for quartz in tourmaline-stage alteration and mineralization.

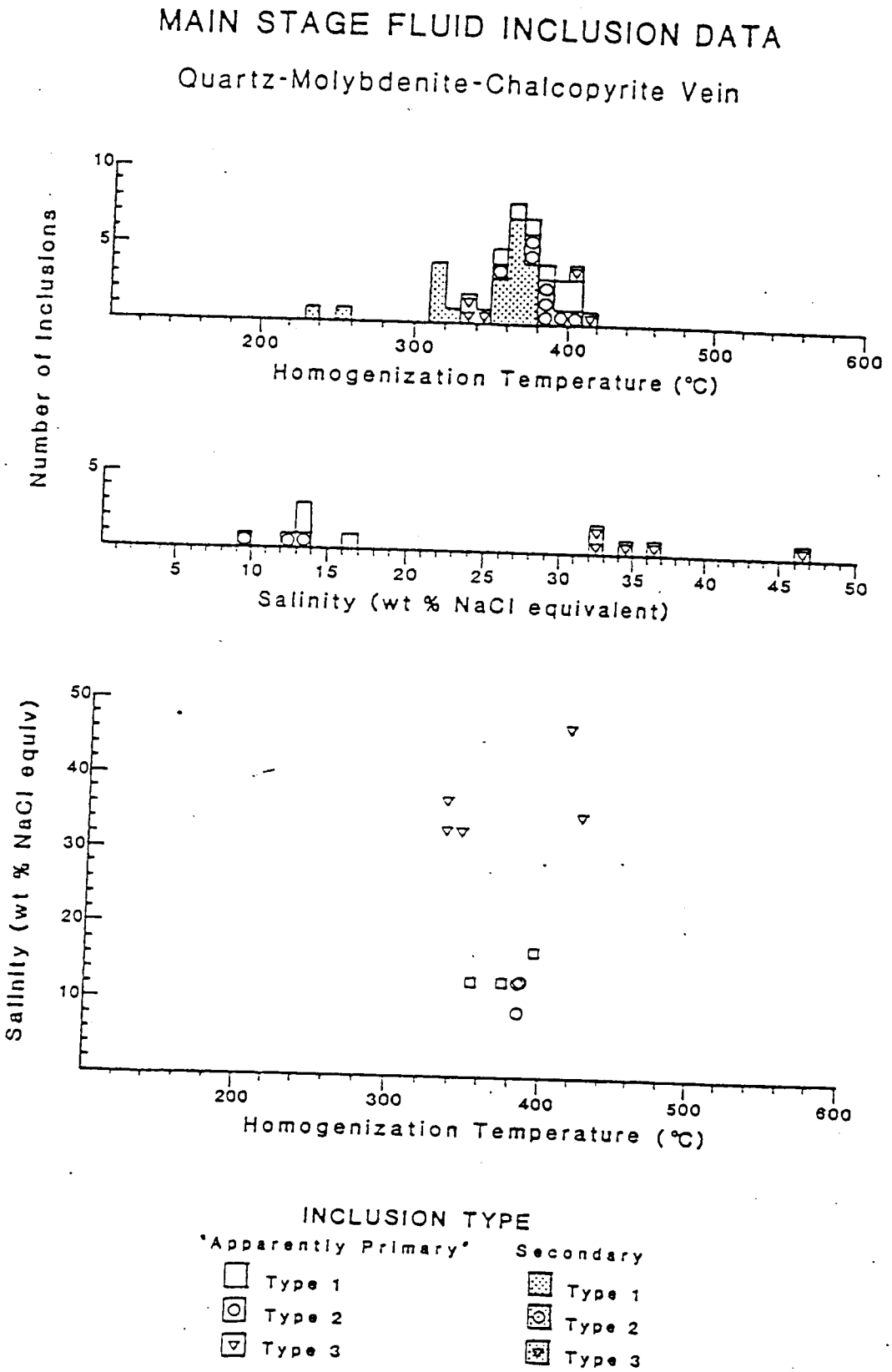

Figure 16. Histograms of fluid inclusion homogenization temperatures and salinities for quartz in main-stage quartz-molybdenite-chalcopyrite vein.

common in these inclusions, but sylvite is rare and no accurate sylvite dissolution temperatures were recorded. Apparently primary inclusions homogenize between 364 and 480°C, and homogenization temperatures fall into three groups: 364 to 414°C (similar to those of the secondary inclusions), 422 to 436°C, and 460 to 480°C (fig. 14). The latter two temperature groups consist predominantly of undersaturated inclusions, but with only 11 data points it is difficult to assess whether this is significant. The three different inclusion types homogenize within a narrow temperature range and indicate that the fluids were boiling when trapped.

Salinities for the apparently primary inclusions are crudely bimodal in distribution: Types 1 and 2 contain 7.7 to 20.7 equivalent weight percent NaCl, and type 3 contains 30.2 to 44.4 weight percent NaCl. The bimodal salinity distribution is consistent with boiling conditions at the time of entrapment.

Tourmaline Stage

Twenty-eight inclusions (21 apparently primary and 7 secondary) in three silicified breccia clasts were measured in a drill core sample (DDH P19; elevation 2,922 meters above sea level) of tourmaline breccia (fig. 15). The sample site is relatively deep in the deposit and is essentially unaffected by later mineralization. In an effort to avoid inclusions trapped in earlier pre-tourmaline stage events, inclusions were selected from equant, polygonal quartz grains with equilibrium triple-junctions located in the outer silicified rims of large breccia clasts.

Inclusions of all three types have been identified as apparently primary. Such inclusions range from 25 to 75 microns in size. All but one type 3 inclusion were oversaturated as indicated by vapor disappearance prior to halite dissolution on heating. Other smaller, colorless daughter minerals (including possibly sylvite) were usually present, but accurate observations could not be made during heating experiments. Measured homogenization temperatures of the apparently primary inclusions define two distinct populations (fig. 15): The first includes two inclusions which homogenized between 358 and 361°C, while the second (which includes the majority of the apparently primary inclusions) homogenized between 390 and 456°C. Homogenization temperatures of the first group are similar to those of measured secondary inclusions. Apparently primary inclusion salinities are again bimodal in distribution, with 9.8 to 21.3 equivalent weight percent NaCl for types 1 and 2 and 35.6 to 47.3 weight percent NaCl for type 3. It is inferred that these fluids were boiling when trapped.

Clearly secondary inclusions are small (5 to 15 microns) and homogenized at temperatures (280 to 374°C) which overlap only with the lower temperature mode of the apparently primary fluid inclusions. Type 2 inclusions are absent, thus there is no evidence that these fluids boiled.

Main Stage

Fluid inclusion data representative of main stage alteration and mineralization were collected from a quartz-molybdenite-chalcopyrite vein and from a vug-filling quartz crystal associated with chalcopyrite-pyrite mineralization in refractured tourmaline breccia. These will be considered separately.

Quartz-molybdenite-chalcopyrite vein. Twenty-one apparently primary and 21 secondary inclusions were examined from a single molybdenite-rich vein from DDH P19 at 3,145 meters above sea level (fig. 16). This vein offsets an early stage type 1 vein and has been overprinted by weak sericitic alteration. Studied apparently primary inclusions range in size from 20 to 70 microns; secondary inclusions are generally smaller. Most apparently primary inclusions are type 1 or 2. The only minerals other than halite observed in type 3 inclusions were anhydrite, hematite, antarcticite, and an unidentified birefringent phase. Hematite is common in type 2 inclusions. Type 1 inclusions are relatively vapor-rich, are similar to those contained in the early stage quartz veins, and can be distinguished from associated type 2 inclusions only by their homogenization behavior. Homogenization temperatures of apparently primary inclusions fall within a continuous but broad range (334 to 419°C) centered around 380°C. Homogenization of the three inclusion types at similar temperatures suggests that the fluids were boiling when trapped. Only apparently primary inclusions belonging to the high temperature range homogenize at temperatures exceeding those of obvious secondary inclusions.

Salinities of apparently primary inclusions reflect physical separation of a solution into low-density (type 1 and 2) and high-density (type 3) fluids by boiling. Inclusion types 1 and 2 contain 9.9 to 16.4 equivalent weight percent NaCl, and type 3 inclusions contain 32.9 to 46.2 weight percent NaCl.

All of the 21 measured secondary inclusions were of type 1. Their homogenization temperatures group into three ranges: 233 to 258°C, 311 to 324°C, and 355 to 377°C. The first two temperature ranges are below the homogenization temperatures recorded for the apparently primary inclusions, but the third range overlaps the lower-temperature half of the homogenization temperature range for associated apparently primary inclusions.

Chalcopyrite-pyrite mineralization. Seventeen inclusions contained in three euhedral quartz crystals in fractures and vugs in tourmaline breccia were studied (fig. 17). These samples were taken from the northeastern part of the 3,205-meter bench of the open pit.

Chalcopyrite-pyrite mineralization is spatially associated with these crystals and is thought to be coeval. All observed inclusions in these crystals are coplanar and inferred to be pseudosecondary; in keeping with convention, they are referred to as "apparently pseudosecondary;" the occurrence of coplanar inclusions in a vug-filling euhedral crystal is not proof of a pseudosecondary origin (Roedder, 1967).

The coplanar inclusions are 24 to 80 microns in size and consist solely of type 2 and 3 inclusions; most data are from the latter because the type 2 inclusions in these crystals are extremely vapor-rich and therefore difficult to study. Homogenization temperatures form a single but broad range from 357 to 432°C. The coexistence of type 2 and 3 inclusions (which homogenize over a similar temperature range) suggests that these fluids were boiling when trapped. Salinities are bimodal: Vapor-rich inclusions contain 12.6 to 15.9 equivalent weight percent NaCl, and vapor-poor inclusions contain 32.5 to 37.6 weight percent NaCl.

Late Stage

Twenty-one apparently primary inclusions (including inferred pseudosecondary inclusions) from five samples taken from two quartz-sericite-pyrite veins provide the data for this

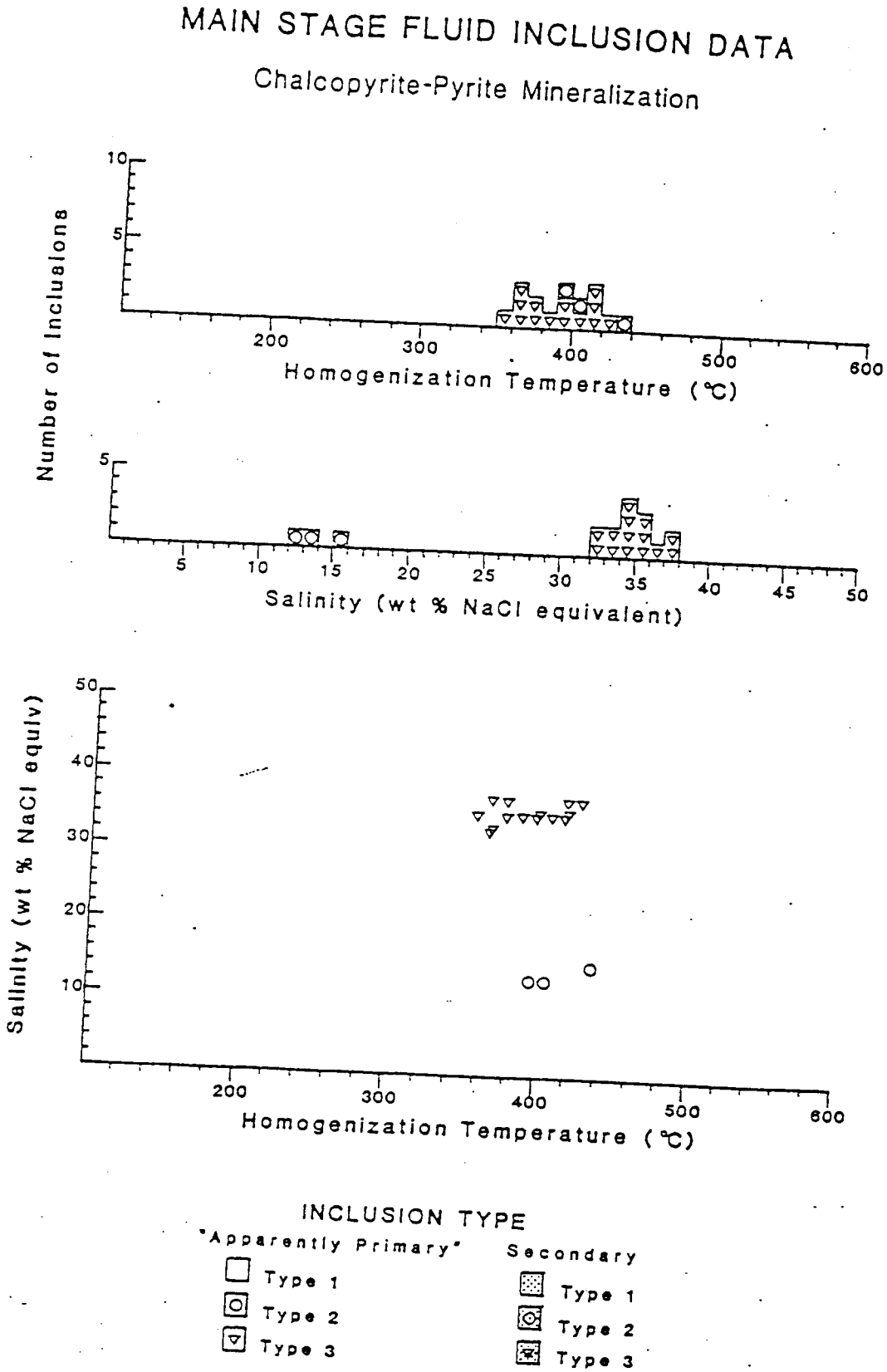

Figure 17. Histograms of fluid inclusion homogenization temperatures and salinities for quartz in main-stage chalcopyrite-pyrite mineralization.

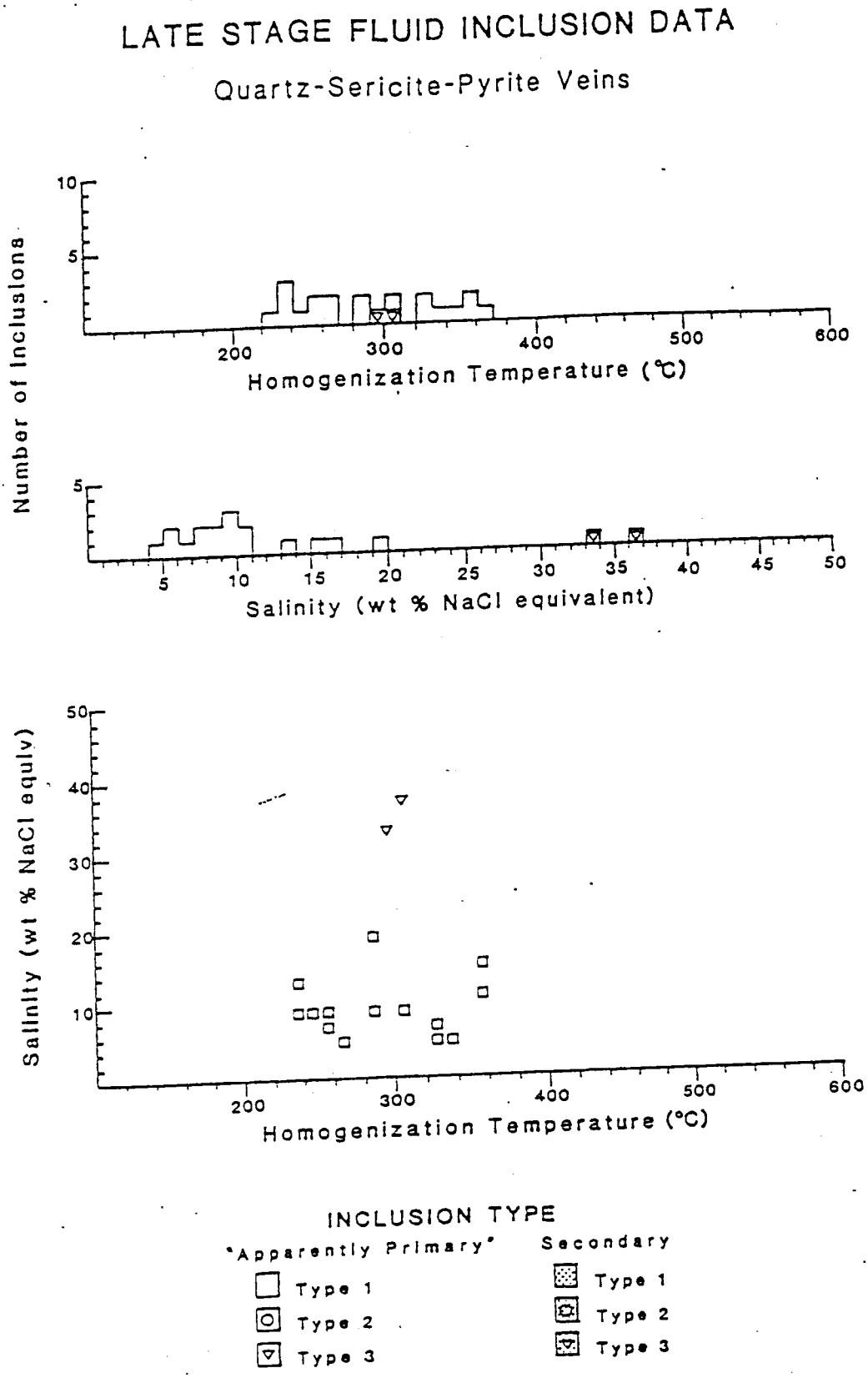

Figure 18. Histograms of fluid inclusion homogenization temperatures and salinities for quartz in late-stage alteration and mineralization.

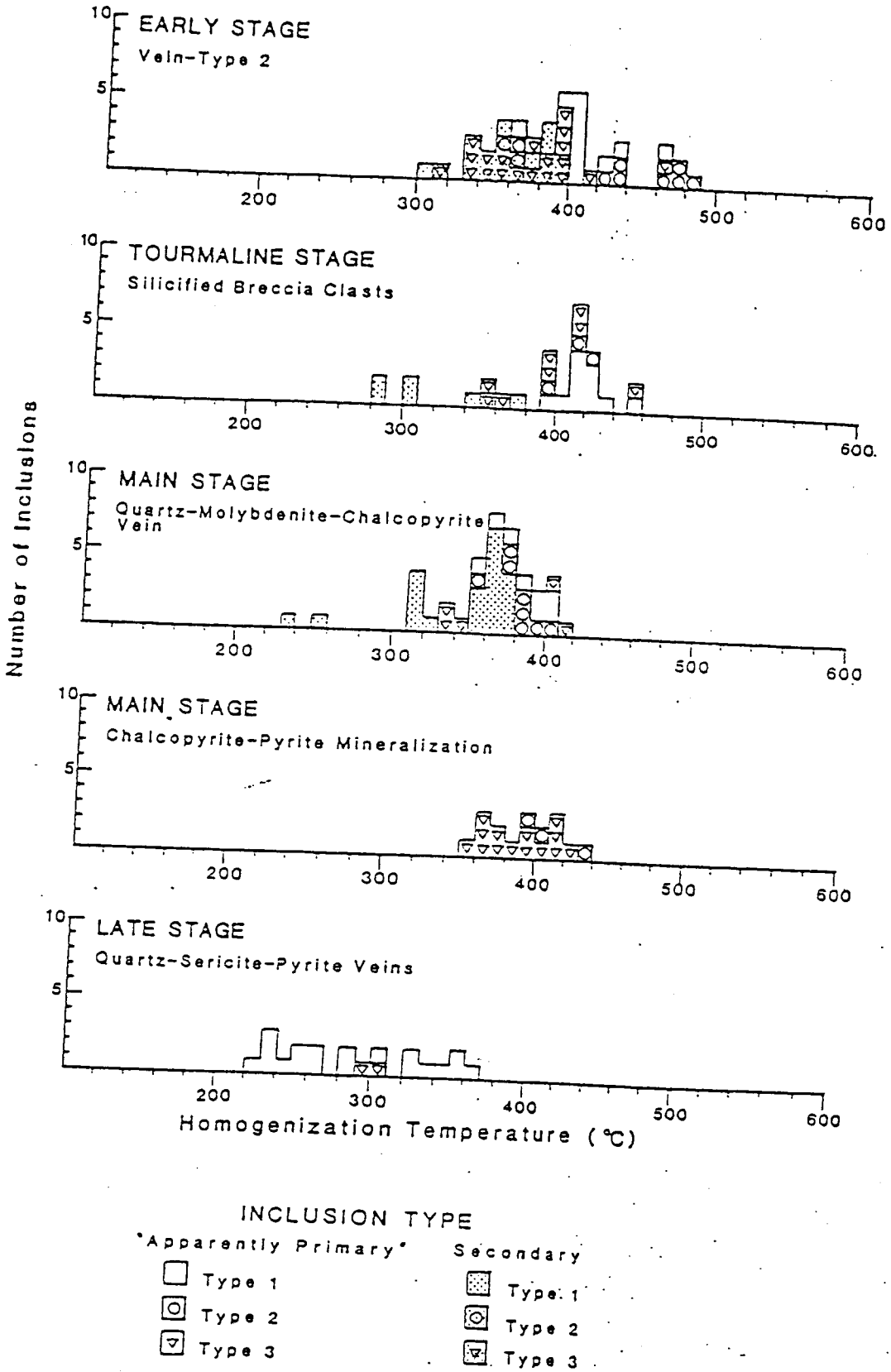

Figure 19. Histograms of fluid inclusion homogenization temperatures for all Toquepala alteration and mineralization stages.

alteration and mineralization stage (fig. 18). The samples were obtained from the northeastern part of the 3,205-meter bench of the open pit and from an elevation of 2,895 meters above sea level in DDH L/M18. The size of the inclusions ranges from 15 to 50 microns. With the exception of two type 3 inclusions contained in a single sample, only type 1 inclusions were analyzed. Quartz-sericite-pyrite veins contain the lowest concentration of fluid inclusions among the Toquepala vein types, probably a reflection of the few fracturing and alteration events which occurred after these veins were emplaced. As a consequence, no secondary inclusions were studied from these veins. The estimated amount of vapor in type 1 inclusions ranges between 5 and 15 volume percent, the lowest vapor-to-liquid ratios in type 1 inclusions observed in the deposit. No daughter minerals are present in these undersaturated inclusions.

Many of the type 1 inclusions in sites coplanar with the two observed type 3 inclusions failed to homogenize upon heating. This together with the rarity of type 3 inclusions suggests that saturated inclusions are the result of necking down or leakage of originally undersaturated inclusions and are therefore unreliable as sources of data. Homogenization temperatures of the inclusions ranged between 229 and 369°C; Shanks (1977) obtained a range of 312 to 400°C for similar inclusions. Salinities range from 4.5 to 19.4 equivalent weight percent NaCl in the undersaturated inclusions, but most of the values cluster around 7 to 8 weight percent NaCl.

Pressure and Temperature Conditions of Mineralization

Homogenization temperatures. Fluid inclusions were selected for study on the basis of their being either apparently primary or clearly secondary in origin. The purpose of the study was to determine whether the measured homogenization temperatures summarized in figure 19 reflected primary trapping conditions or subsequent reopening events. In all of the alteration and mineralization assemblages studied at Toquepala the apparently primary inclusions show either a broad quasi-continuous range or several distinct concentrations of homogenization temperature. Homogenization temperatures for the corresponding secondary inclusions generally overlap with all but the highest temperature ranges of the apparently primary inclusions. This suggests that only the highest temperature range in the data reflects the conditions of the alteration and mineralization stage and that lower temperature ranges record later fracturing and mineralizing events. That many of the lower temperature populations associated with earlier veins are similar in temperature ranges to later vein types suggests a common origin.

Early stage quartz veins yielded the highest homogenization temperatures documented for apparently primary inclusions at Toquepala. The two highest-temperature modes (422 to 436°C and 460 to 480°C) are above the homogenization temperatures recorded for all secondary inclusions and are therefore interpreted to represent the temperature range of true primary inclusions associated with such veins. The significance of the hiatus between these two groups is unclear: It is possible that the 422 to 436°C range is not representative of truly primary inclusions; a 422 to 480°C range for these fluids is low when compared to homogenization temperature data published for early alteration and mineralization assemblages documented in numerous other porphyry copper deposits (see, for example, Nash, 1976). However, the inferred temperature is consistent with field relationships which suggest that this specific high level vein type (vein type 2) is temporally equivalent to the presumably higher temperature early stage veins (vein types 3 to 6) located at lower levels in the T Porphyry, a possible source for these fluids. The 422 to 480°C temperature range is therefore considered to be minimal for the fluids responsible for the major concentration of early stage alteration and mineralization at depth. The secondary inclusions measured in early stage veins may be related to the apparently primary main stage fluids. Both include types 1, 2, and 3 inclusions which homogenize over a similar temperature range and appear to have been boiling when trapped.

The high temperature range (390 to 446°C) defined by 19 of the 21 measured apparently primary inclusions in the tourmaline breccia clasts exceeds the homogenization temperatures of all secondary inclusions recorded at Toquepala and is considered to represent the temperature range of fluids associated with this stage of alteration and mineralization. That the only type 3 inclusion in the apparently primary population which did not homogenize by halite dissolution belongs to the lower end of this temperature range lends support to the classification of such inclusions as secondary. Because the inferred primary inclusions are thought to have been trapped while boiling, the temperature range corresponds to their conditions of trapping. Fluid inclusion homogenization temperatures and field relationships suggest that the clearly secondary inclusions in the tourmaline breccias may correspond to the apparently primary inclusions in the quartz-molybdenite-chalcopyrite vein: Both populations comprise types 1, 2, and 3 inclusions, homogenize in the range 390 to 420°C, and were boiling when trapped. The studied tourmaline breccia sample is overprinted by minor disseminated molybdenite mineralization, thus supporting the above interpretation. The two type 1 secondary inclusions which homogenized around 300°C are inferred to have been associated with late stage fluids.

Interpretation of the apparently primary inclusions observed in the main stage quartz-molybdenite-chalcopyrite vein is more complicated than for the early or tourmaline stages. The high temperature range of secondary inclusions roughly corresponds to the median temperature of the single broad homogenization range of the apparently primary inclusions. This overlap may indicate (1) that the two populations are actually one and are related to the same fluid, (2) that only those apparently primary inclusions which homogenized at temperatures greater than those of the secondary inclusion are primary, or (3) that all of the apparently primary inclusions are primary regardless of whether their homogenization temperatures exceed those of the clearly secondary inclusions. The first two interpretations imply that the lower temperature apparently primary inclusions belong to the same group as the obvious secondary inclusions, but the contrast between these two populations (the apparently primary inclusions consist of types 1, 2, and 3 inclusions and were boiling at entrapment, whereas the secondary inclusions consist solely of type 1 inclusions and provide no indication of boiling) does not support a consanguineous relationship between them. The striking similarity in type and homogenization temperature between these main stage secondary inclusions and the late stage inclusions suggests that the last interpretation is the most probable. Field evidence also supports this model: The studied

main stage sample was located relatively high in the system in an area with many quartz-sericite-pyrite veins. It is therefore likely that late stage fluids would be present to form secondary inclusions as implied only by the last interpretation. It is suggested that the fluids associated with this main stage vein were trapped at temperatures between 340 and 420°C, were moderately saline, and were boiling.

The pseudosecondary inclusions in the three vug-filling quartz crystals associated with main stage chalcopyrite-pyrite mineralization give no indication of a secondary origin. Although no clearly secondary inclusions were examined in these samples, homogenization temperatures occupy a relatively narrow range and most are in excess of all but the highest homogenization temperatures measured in the younger late stage veins. The main and late stage inclusions which overlap in homogenization temperature have no common inclusion types, therefore none of the studied main stage inclusions are interpreted to be secondary.

Apparently primary late stage fluid inclusions are also not associated with clearly secondary inclusions which would provide a basis for comparison. Although the origin of the inclusions cannot be rigorously tested, the late emplacement of these veins confirmed by cross-cutting relationships observed in cores suggests that the inclusions are plausibly ascribed to the late stage. The inferred temperature range for their formation (which is not significantly affected by pressure correction; see Potter, 1977) is 230 to 370°C.

Pressure considerations. Measured homogenization temperatures and salinities for boiling fluids can be utilized to estimate pressure at the time of their trapping and to provide constraints on their depth of formation. Evidence for contemporaneous trapping of vapor-rich (type 2) and liquid-rich (types 1 and 3) inclusions is widespread for all but the late stage veins, but boiling in each of the three earlier stages appears to have occurred over a wide temperature range. Because individual inclusions within a group thought to have boiled usually trap an arbitrary mixture of two phases (liquid and gas) rather than a single homogeneous phase, homogenization temperatures are higher for inclusions that have trapped only liquid or vapor (Roedder and Bodnar, 1980). The minimum homogenization temperature for a group of inclusions therefore provides the best estimate of the true trapping temperature.

On the basis of the data of Chou (1987) for the NaCl-H_2O system, the following approximate pressures may be defined for each of the hydrothermal stages attended by boiling fluids:

Mineralization Stage	Estimated Trapping Temperature and Mean Salinity of Polyphase Inclusions	Estimated Pressure
Early stage	422°C 35 weight percent NaCl equivalent	300 bars
Tourmaline stage	390°C NaCl saturation	170 bars
Main stage (qtz-mo-cp veins)	334°C 35 weight percent NaCl equivalent	< 100 bars
Main stage (cp-py min)	357°C 35 weight percent NaCl equivalent	100 bars

Oversaturated fluid inclusions representative of tourmaline stage hydrothermal solutions would provide erroneously high pressures if a low salinity estimate were used, but in the other cases the error in pressure resulting from an erroneous salinity assumption is not significant. For example, the difference between pressure estimates for the main stage chalcopyrite-pyrite mineralization as calculated from the NaCl saturation curve and from the 10 weight percent NaCl equivalent L+V curve is less than 40 bars.

Pressure estimates from fluid inclusion data can be used to approximate the depths of vein and breccia formation. Fluid pressures may be equivalent to hydrostatic pressure, lithostatic pressure, or some value between the two (Roedder and Bodnar, 1980). It seems likely that estimated pressures for the hydrothermal breccias developed during tourmaline and main stage events represent predominantly hydrostatic conditions. Assuming a 100 bars per kilometer hydrostatic pressure gradient, these pressures (170 and 100 bars respectively) yield depths of formation of 1.7 and 1 kilometers respectively. The field relationships of the main stage quartz-molybdenite-chalcopyrite veins indicate they are open-space structures and therefore suggest they formed under hydrostatic pressure conditions. Fluid pressures estimated for the inclusions in these veins (less than 100 bars) imply a maximum depth of emplacement of approximately 1 kilometer. In contrast, many of the earlier early stage veins (types 3 to 6) are characterized by irregular and discontinuous structures suggestive of fracturing in a plastic rather than brittle rock under or approaching lithostatic pressure. Early stage type 1 and 2 veins display structures intermediate between those of the earliest early veins (types 3 to 6) and those of the main and late stage veins, suggesting that the type 1 and 2 veins formed as the hydrothermal system underwent a transition from early lithostatic pressure conditions to a later hydrostatic pressure regime. The estimated fluid pressure (300 bars) for these veins implies a 1.1- to 1.2-kilometer minimum depth for their development based on a 265 bars per kilometer lithostatic pressure gradient. Under hydrostatic conditions, the fluid pressure would correspond to a considerably greater (3 kilometers) depth of emplacement. Utilizing an average 10 weight percent NaCl equivalent salinity and a 280°C homogenization temperature, minimum pressures for the late stage fluids are estimated to have been about 60 bars (Haas, 1976). Assuming hydrostatic pressure conditions at the time of their formation, depths of about 1 kilometer are indicated.

Fluid salinities. The estimated salinities of the fluid inclusions in each of the hydrothermal stages at Toquepala reveal (1) a bimodal distribution with a higher mode centered around 35 equivalent weight percent NaCl and a lower mode at about 10 to 15 equivalent weight percent NaCl and (2) a broad population that spans the range 5 to 20 equivalent weight percent NaCl. The first pattern is representative of fluids in the first three hydrothermal stages (early, tourmaline, and main). The involvement of these fluids in the early hydrothermal stages and the high salinities recorded for many of these inclusions suggest a magmatic source, and the associated low-density fluid component is inferred to have been formed by boiling of these fluids. The second pattern is observed in inclusions in late stage quartz-sericite-pyrite veins. These low-density fluids cannot be the result of the physical separation of vapor from higher density fluids because

there is no evidence that boiling occurred at this stage. The many oxygen and hydrogen isotope studies conducted on ores from porphyry copper deposits (see, for example, Sheppard and Gustafson, 1976; Sheppard and others, 1969, 1971; Taylor, 1974) demonstrate that late stages are characterized by the influx of meteoric waters into hydrothermal systems. The low-salinity fluids contained in the late stage veins at Toquepala may thus represent dilution of magmatic fluids by meteoric water, and the broad salinity range measured in these fluid inclusions may reflect incomplete or inhomogeneous mixing between such fluids.

The measured salinities of inclusions from tourmaline stage breccias deserve special comment. These inclusions are oversaturated and contain multiple crystalline salts for which only halite dissolution temperatures were recorded. Sylvite is also present and indicates salinities of the order of 50 to 65 equivalent weight percent NaCl. Similar high-temperature, oversaturated, and polyphase inclusions have been reported by Walker (1979) from a tourmaline breccia pipe in the Copper Creek Mining District in Arizona, and Grant and others (1977) also documented such inclusions in the tourmaline breccia pipes associated with Bolivian porphyry tin deposits.

Fluid composition. First melting temperatures have been confidently measured for only a few inclusions in each hydrothermal stage (Zweng, 1984). In no instance did melting begin in the range -20.8 to -22.9°C for inclusions in which first melting temperature could be determined. These data indicate a more complex fluid composition than the NaCl-H_2O or even NaCl-KCl-H_2O systems. Recorded first melting temperatures clustered in the temperature ranges -60 to -56°C, -53 to -50°C, and -37 to -30°C, suggesting the presence of $CaCl_2$ and $MgCl_2$ in the fluids (Crawford, 1981). The presence of the former is confirmed by the identification of antarcticite in several inclusions, but no clear correlation between daughter mineral type and first melting temperature was evident. Carbon dioxide was not observed as an immiscible phase but may be present in small quantities as in other porphyry deposits (for example, El Salvador, Chile; Gustafson and Hunt, 1975). First melting temperatures of -60 to -56°C, though suggestive of first melting of CO_2, are interpreted to reflect eutectic melting in the system NaCl-$CaCl_2$-$MgCl_2$-H_2O (Crawford and others, 1979).

DISCUSSION

The present study has been based on traditional mapping, core logging, and petrographic techniques, and considering the wealth of information potentially available must be considered a reconnaissance. In several important respects, however, our observations clearly necessitate significant revision to the description provided by Richard and Courtright (1958a and b). Although our core logging was not comprehensive and could not define alteration and mineralization zonation of the deposit as a whole, it did define the temporal evolution of the hydrothermal system. Perhaps the most important departures from the Richard and Courtright depiction include (1) establishment of the existence of an early stage of alteration and mineralization, (2) recognition that the gigantic tourmaline-cemented "ore breccia" was almost inherently barren, and (3) demonstration that the great bulk of copper and molybdenum was deposited after tourmaline breccia emplacement but prior to late stage alteration and mineralization.

Hypogene Evolution of the Toquepala Deposit

Interrelationships with magmatic activity. Hydrothermal activity commenced within the Toquepala Intrusive Center by 56.7 ± 0.4 Ma, approximately 2 to 3 m.y. after crystallization of the contiguous quartz-monzodioritic Toquepala Pluton (Clark and others, in press). The Center constitutes the local terminal stage in the development of the Toquepala Segment of the Peruvian Coastal Batholith, which, together with the thick volcanic succession of the Toquepala Group, constitutes a potassium-rich and in part shoshonitic subaerial arc. Most rock types in this assemblage record processes of magma commingling and mixing, and it is not unreasonable to suggest that the dacitic hypabyssal bodies of the Center were also ejected from felsic magma chambers undergoing periodic incursions of more mafic melts. Lead isotope data for the latest Cretaceous to Paleocene granitoid rocks of the area (Barreiro and Clark, 1984) reveal that the magmas were only minimally contaminated by Precambrian to Paleozoic continental crust, and one of us (Clark, 1993) has suggested that the primitive nature of the parental magmatism is reflected in the great size and high cobalt content of the deposit.

Petrographic relationships confirm that several dacite porphyry plugs are temporally and spatially associated with mineralization. At least three separate subvolcanic intrusions, the T, Main, and L/M Porphyries, were emplaced during the initial stages of hydrothermal activity. These intrusions predate the great bulk of economic copper mineralization and all molybdenite deposition, but we infer that less well-defined and apparently smaller dacite porphyry bodies are temporally associated with the major periods of copper and molybdenum deposition. The Dacite Agglomerate of Richard and Courtright (1958a), reinterpreted here as another dacite porphyry stock with its upper part highly charged with xenoliths, was intruded during the late main stage and after formation of the hypogene orebody, thus the entire history of sulfide deposition was accompanied by the rise of dacitic melt from an underlying magma chamber. The assignment of the latest intrusions of the Center to the latite clan is not entirely convincing, but such potassium-rich felsic rocks are not out of place in a broadly shoshonitic (K_2O > Na_2O) igneous complex. It cannot be assumed, however, that the terminal stage in the development of the Toquepala Intrusive Center saw a radical change in magmatic chemistry.

As in other porphyry deposits and in contrast to Climax-type molybdenum stockworks (Carten, Walker, and others, 1988), the genetic correlation between individual hypabyssal dacitic stocks and episodes of mineralization is not well-established at Toquepala. Even the early T Porphyry with its aplitic groundmass and locally pervasive biotitization displays no direct evidence of retrograde boiling processes such as unidirectional solidification textures in its roof zone: The entire copper-molybdenum stockwork is effectively epigenetic with respect to the spatially associated porphyry stocks, and both may be regarded as products of the evolution of a magma chamber at depth. We tentatively favor a model in which subvolcanic intrusive and hydrothermal events reflect perturbations of the chamber caused perhaps by mafic melt incursion (see Keith and others, 1986).

History of mineralization. For the first time paragenetic relationships have been defined for the Toquepala Deposit. The early, tourmaline, main, and late stages distinguished by us at

Toquepala broadly correspond to the early, transitional, and late stages defined by Gustafson and Hunt (1975) at El Salvador, demonstrating that this breccia-pipe deposit represents a "variation on the porphyry copper theme" (Gustafson and Hunt, 1975; Gustafson, 1978). The adherence of many porphyry copper (-molybdenum) deposits worldwide to the El Salvador evolutionary pattern, albeit with many economically critical variations (Clark, 1993), is prima facie evidence that relatively consistent magma-fluid equilibria exert an overriding control on porphyry evolution.

The major locus of early stage alteration and mineralization was deep in the hydrothermal system below approximately 2,550 meters above sea level. The most copper-rich of the early veins (types 3 to 5) are concentrated in the T Porphyry, while the copper-poor vein types (types 1 and 2) were emplaced at higher levels where their original distribution has been disguised by later events. The deeper veins were predominantly earlier than the shallower and display more sinuous and discontinuous forms, implying that hydrothermal activity expanded upwards from higher to lower P-T environments in its initial stages. The fluids associated with the shallower veins were boiling, approximately 420 to 480°C in temperature, and saturated with respect to NaCl. These veins are inferred to have formed at depths of 0.9 to 2.5 kilometers.

The deeper early veins compare closely to the A veins at El Salvador (Gustafson and Hunt, 1975) in their form and mineralogy. However, our incomplete coverage suggests that only minor amounts of copper were deposited during the early stage at Toquepala, while three-quarters of the total copper budget at El Salvador is related to A veins. Another important difference between these deposits is the predominance of albite (overall, $An_{<1}$) over potassium feldspar in the alteration haloes associated with deeper early veins at Toquepala, while albite-bearing alteration envelopes are known from below the Inca adit level at El Salvador (Gustafson, personal communication, 1993). Biotite is present in veins and alteration envelopes cutting the T Porphyry, but sodium enrichment was at least as important as potassium metasomatism in the early environment. Albite-bearing alteration assemblages have been recorded from few porphyry copper deposits (Clark, 1993; Dilles and Einaudi, 1992). The absence of more calcic hydrothermal plagioclase, actinolite, and chlorite and the presence of sulfide distinguish this alteration from the sodic-calcic alteration documented at Yerington by Carten (1986) and at Ann-Mason by Dilles and Einaudi (1992). A relatively high sodium-potassium ratio would be in permissive agreement with the low temperatures (400 to 450°C) we estimate for the early stage fluids (see Whitney and others, 1985), and it may be assumed that the composition of such fluids contributed to the alteration of potassium feldspar to albite (Dilles and Einaudi, 1992).

An enormous upward-flaring tourmaline breccia column of the tourmaline stage defines the vertical axis of the Toquepala Deposit (fig. 5) and distinguishes it from the great majority of other porphyry copper deposits. In essence this body and its associated tourmaline-quartz veinlets are comparable to the less voluminous tourmaline-veinlets and breccia of the transitional stage at El Salvador (Gustafson and Hunt, 1975). A significant difference is the rarity of rounded fragments in the Toquepala tourmaline breccias. Where rounding has occurred (Clark, 1990), it may be the product of hypogene foliation as advocated by Sillitoe (1985).

Fluid inclusion data for a sample from 2,922 meters above sea level suggest that the root of the tourmaline breccia pipe, which is located immediately above the apex of the T Porphyry stock, lay at a maximum depth of about 2 kilometers and that brecciation was attended by boiling highly saline fluids. Although no stable isotope data are available, it is improbable that brecciation at this stage resulted from interaction of cool ground waters with an intruded stock as we do not see advanced argillic assemblages, high-sulfur assemblages, or other features common to base-metal lode deposits or other hydrothermal systems with early histories of groundwater incursion (see Einaudi, 1982). The widespread concentration of tourmaline in pipes, lodes, and veins of breccia in a great variety of magmatic-hydrothermal ore deposits may indicate that boron enrichment during retrograde boiling in epizonal felsic magma chambers results almost invariably in intense and even catastrophic mechanical energy release. Pichavant (1981, 1987) has demonstrated that the concentration of boron in water-saturated haplogranitic melts at 1 kilobar significantly depresses both liquidus and solidus and increases water solubility in the melt. Strong enrichment of boron in magma during extraction of aqueous fluids in the initial stages of second boiling (Candela, 1989a and b) may even interrupt that process so that when vapor exsolution resumes an unusually large volume of fluid will be generated and result in extreme and rapid expansion of the apical portion of the magma chamber and intense brecciation. Since such models apply equally to the generation of stockwork fracturing (see Burnham, 1967, 1979; Burnham and Ohmoto, 1980; and Phillips, 1973), the writers consider the focusing of both hydrothermal fluids and mechanical energy to be critical to the formation of major breccia-pipe-like structures. It remains uncertain whether boron in an hydrothermal system promotes the formation of breccia (Allman-Ward and others, 1982) or if the breccia environment is structurally or chemically favorable to the precipitation of tourmaline; the deposition of tourmaline (an aluminum-rich cyclosilicate) may be promoted by the relatively high fluid-to-wallrock environment of a breccia in which leaching of aluminum from wallrocks to the fluid is facilitated.

Although itself barren, the tourmaline breccia pipe at Toquepala served as a permeable conduit for evolved metal-rich fluids. Main stage fluids with compositions precluding either significant alkali metasomatism or hydrolytic alteration were responsible for the vast bulk of hypogene copper mineralization and all of the molybdenum mineralization. Like the B veins at El Salvador (Gustafson and Hunt, 1975) and comparable veins emplaced in the intermediate stage of evolution of most porphyry copper deposits (Clark, 1993), the main stage veins display copper-molybdenum ratios lower than those characteristic of the A veins; indeed, the low overall copper-molybdenum ratio at Toquepala is thought to reflect the predominance of B-type mineralization. Quantitative data are lacking, but our petrographic studies and limited core logging indicate that the main stage vein complex exhibits an upward enrichment in copper relative to molybdenum as is reflected in the higher proportion of chalcopyrite-pyrite relative to quartz-molybdenite-chalcopyrite mineralization in the upper preserved 500 meters of the deposit.

Our field studies show that tourmaline and molybdenite deposition were closely related in time, with molybdenite precipitation just after the formation of tourmaline breccia and veinlets. The close geochemical affiliation of boron and molybdenum, neither of which was transported by chloride complexes, suggests the broad contemporaneity of their extraction from the magma (Candela, 1989a and b). Why, then, are tourmaline and molybdenite mutually exclusive in their depositional sites? Petrographic examination of molybdenite- and tourmaline-bearing hydrothermal features suggests that the deposition of molybdenite occurred where quartz-molybdenite-chalcopyrite veins cut feldspar phenocrysts in the wallrock. The intergrowth of microscopic blades of sericite with molybdenite and other sulfides suggests that molybdenite deposition was controlled by a neutralization reaction triggered at feldspar sites. Breccia fragments were converted to a quartz-sericite assemblage during tourmaline precipitation, however, thereby destroying the nucleation sites required for molybdenite deposition. These observations may also explain why iron and copper-iron sulfide deposition did not attend the tourmaline formation in the breccias.

Late stage alteration and mineralization at Toquepala shares many features with the El Salvador late stage environment (Gustafson and Hunt, 1975). These include moderate to strong hydrolytic alteration, deposition of high-sulfur and arsenic-rich (bornite- or tennantite-pyrite) assemblages, and through-going vein fabrics. Although no stable isotope data are available and the role of meteoric water cannot be delimited, detailed lead isotope analysis of sulfide minerals by Barreiro and Clark (unpublished data) reveals (1) no major differences between early, main, and late stage assemblages and (2) marked similarities to the lead isotope compositions of the precursor granitoid rocks (Barreiro and Clark, 1984). We infer that the terminal stages of hydrothermal activity at Toquepala contained a significant magmatic component with acid-generating volatiles and that the considerable extent of the late stage alteration and mineralization reflects the incursion of large volumes of groundwater.

The pervasive albite-sericite alteration developed locally in the deeper zones of the Toquepala Deposit is not present at El Salvador. This alteration type is similar to that described from the Park Premier (John, 1989) and Cabang Kiri (Lowder and Dow, 1978) Prospects and to the late stage albitic alteration at Yerington (Carten, 1986). John (1989) interpreted the albite-sericite association at Park Premier as the innermost and probably earliest and highest temperature assemblage of an extensive hydrolytic alteration zone. Similarly, this alteration may represent a deep and early stage in the development of late stage alteration which evolved to a more acidic state at shallower levels at Toquepala.

The exceptional scale of tourmaline stage brecciation at Toquepala is matched by the enormous scale of pebble breccia development of the late stage environment. Here again the geologic features of the pebble breccia dikes are essentially identical to those reported by Langerfeldt (summarized in Gustafson and Hunt, 1975) at El Salvador. Toquepala's 300-meter-wide pebble pipe preserved over a vertical distance of over 500 meters is exceeded in size only by the Braden Pipe at El Teniente, Chile (Howell and Molloy, 1960), which attains a diameter of approximately 1,230 meters. Oversize pebble breccia development was directly associated with intrusion of late latite porphyry at both Toquepala and El Teniente, and a phreatomagmatic origin (sensu Sillitoe, 1985) is strongly implied. Like the Toquepala Pepple Pipe, the Braden Pipe (Howell and Molloy, 1960) erupted through a tourmaline breccia body of which vestiges are preserved as the pre-pipe breccia of Howell and Molloy (1960) and which is directly analogous to the border facies of the Toquepala System. The pebble breccia nature of the Braden Pipe, not entirely clear from Howell and Molloy's (1960) description, has been confirmed by observations by D.A. Heatwole (written communication, 1984) and C.J. Hodgson (personal communication, 1983). In both deposits this stage of phreatomagmatic brecciation had a negative impact on the hypogene orebodies, reducing copper grades in large volumes of rock from greater than 0.8 percent to below 0.4 percent.

P-T conditions and classification of mineralization.

Recent experimentation and thermodynamic modeling have emphasized the important role of confining pressure in the partitioning of chlorine, iron, and many base and precious metals (copper, lead, zinc, gold, and silver) between felsic magmas and aqueous fluids in the second boiling environment (Whitney and others, 1985; Candela, 1989a and b; Shinohara and others, 1989; Cline and Bodnar, 1991; Webster, 1992; Williams and others, 1992). Fluid inclusion data suggest that the Toquepala veinlet systems were emplaced under exceptionally low pressures approaching those of epithermal mineralization. Pressures evolved from about 300 bars in the early stage to less than 60 bars in the late stage, and almost all copper and molybdenum were deposited at pressures below 100 bars; even if hydrostatic conditions are assumed for the early stage, depths exceeding 3 kilometers are precluded. This deposit therefore corresponds closely to the low-pressure clan of Candela (1989a) and Cline and Bodnar (1991). These workers emphasized that in deep (high-pressure) deposits the earliest fluids to exsolve from the melt are more voluminous and carry the great bulk of the chlorine and copper, while in shallow (low-pressure) systems the earliest fluids to exsolve are less voluminous and relatively chlorine- and copper-poor with the result that these elements are partitioned most efficiently into greater volumes of fluids exsolved at the end of crystallization. Furthermore, at low pressures molybdenum and boron are melt-compatible and achieve their strongest partitioning into vapor simultaneously with copper.

These relationships may help to explain some of the differences in the styles of mineralization documented at El Salvador and Toquepala. The high-pressure setting at El Salvador (600 to 1,000 bars) may have promoted the formation of A veins and other hydrothermal features to form some three-quarters of the hypogene copper orebody and precluded the subsequent major development of tourmaline breccia and B veins, which contribute less than one-quarter of the total copper budget. In contrast, the low pressure setting at Toquepala (less than 300 bars) may have inhibited a widespread copper-rich early stage and fostered later development of the enormous tourmaline breccia pipe complex and subsequent formation of the hypogene copper and molybdenum orebody. Both Toquepala and El Salvador share comparable late-stage features, suggesting that the difference in depth between these two systems did not have a profound effect upon the waning stages of hydrothermal activity.

CONCLUDING STATEMENT

The present investigation, undertaken 30 to 40 years after the initial investigations directed by Kenyon Richard and Harold Courtright (Richard, Courtright and others, 1951), has benefited from experience gained from 30 years of open pit mining and from the deep drill program (Stevenson, 1981). Our model for the hypogene mineralization at Toquepala preserves many of the features recorded by Richard and Courtright (1958a) but brings a new perspective to bear on the significance of several of the more striking geological units by providing for the first time evidence for a sequence of magmatic-hydrothermal events. In particular, we conclude that the great tourmaline and pebble breccia complexes which dominate the upper half of the Toquepala Deposit played merely passive or even negative roles in the concentration of copper and molybdenum, on the one hand constituting an explosive barren interlude in the orderly evolution of metal extraction in the second boiling environment and on the other excising part of the earlier formed orebody.

ACKNOWLEDGMENTS

Field and laboratory research were funded by grants from the Natural Sciences and Engineering Research Council of Canada to A.H.C. and were initiated through the good auspices of the late Frank Archibald, former Chairman of Southern Peru Copper Corporation. Field work would not have been possible without the unselfish assistance and advice of former SPCC mine geologists Armando Plazolles, Juan Torres, Jorge Manrique, and Enrique Sanca. Invaluable logistical help was provided by Juan Chiri and Grimaldo Alvarize. Frank Stevenson, SPCC Chief Geologist, and Charles Preble, Manager of the Toquepala operations in the early '80s and now SPCC President, did everything possible to facilitate our studies.

The senior author's work was partially funded by R. Samuel McLaughlin and Queen's University Graduate Awards. Discussions with Jay Hodgson, Edward Farrar, Bob Mason, Doug Archibald, Bob Seal, Alfonso Truda, Doug Hall, and Pam Scowen were invaluable, as was the logistical assistance of Roger Innis and Jerzy Advent (sectioning), Bob Foster and the late Frank Dunphy (rock analysis), Chris Peck and Ela Rusak (drafting), and Joan Charbonneau (manuscript preparation). The authors are particularly grateful for the amazing patience, forbearance, and skill of the volume's editor-in-chief, Frances Pierce.

Permission to publish this paper is granted by Southern Peru Copper Corporation.

REFERENCES

Agar, R.A., and Le Bel, L.M., 1985, The Linga super-unit: high-K diorites of the Arequipa segment, *in* Pitcher, W.S., Atherton, M.P., Cobbing, E.J., and Beckinsale, R.D., eds., Magmatism at a plate-edge: the Peruvian Andes: Glasgow, Blackie and Sons, p. 119-127.

Allman-Ward, P., Halls, C., Rankin, A., and Bristow, C., 1982, An intrusive hydrothermal breccia body at Wheal Remfry in the western part of the St. Austell granite pluton, Cornwall, England, *in* Evans, A.M., ed., Metallization associated with acid magmatism: Chichester, John Wiley and Sons Ltd., p. 1-28.

Arancibia, O.N., and Clark, A.H., 1990, Early magnetite-rich alteration/mineralization in the Island Copper porphyry copper-molybdenum-gold deposit, British Columbia [abs.]: Geological Association of Canada/Mineralogical Association of Canada, Program with Abstracts, v. 15, p. A4.

Arancibia, O.N., and Clark, A.H., (in press), Early magnetite-amphibole-plagioclase alteration-mineralization in the Island Copper porphyry copper-molybdenum-gold deposit, British Columbia: Economic Geology.

Barreiro, B.A., and Clark, A.H., 1984, Lead isotopic evidence for evolutionary changes in magma-crust interaction, Central Andes, southern Peru: Earth and Planetary Science Letters, v. 69, p. 30-42.

Barua, V., 1961, Reconocimiento geológico — Zona Tacna y Moquegua: Boletín de la Sociedad Geológica del Perú, v. 36, p. 35-59.

Beckinsale, R.D., Sanchez-Fernandez, A.W., Brook, M., Cobbing, E.J., Taylor, W.P., and Moore, N.D., 1985, Rb-Sr whole-rock isochron and K-Ar age determinations for the Coastal Batholith of Peru, *in* Pitcher, W.S., Atherton, M.P., Cobbing, E.J., and Beckinsale, R.D., eds., Magmatism at a plate edge: the Peruvian Andes: Glasgow, Blackie and Sons, p. 177-202.

Bellido B., E., 1979, Geología del cuadrángulo de Moquegua: Lima, Perú, Instituto Geológico Minero y Metalúrgico, Perú, Boletín 15, 78 p.

Bellido B., E., and Guevara, C., 1963, Geología de los cuadrángulos de Punta de Bombón y Clemesí: Lima, Perú, Comisión de la Carta Geológica Nacional Boletín, v. 2, no. 5, 92 p.

Bellido B., E., and Landa, C., 1965, Mapa geológico del cuadrángulo de Moquegua (1:100.000): Lima, Perú, Comisión de la Carta Geológica Nacional.

Boily, M., Brooks, C., and James, D.E., 1984, Geochemical characteristics of the late Mesozoic Andean volcanics, *in* Harmon, R.S., and Barriero, B.A., eds., Andean magmatism: chemical and isotopic constraints: Nantwich, U.K., Shiva Publishing Ltd., p. 190-202.

Boily, M., Ludden, J.N., and Brooks, C., 1990, Geochemical constraints on the magmatic evolution of the pre- and post-Oligocene volcanic suites of southern Peru: implications for the tectonic evolution of the Central Volcanic Zone: Geological Society of America Bulletin, v. 102, p. 1565-1579.

Bowman, J.R., Parry, W.T., Kropp, W.P., and Kryer, S.A., 1987, Chemical and isotopic evidence of hydrothermal solutions at Bingham, Utah: Economic Geology, v. 82, p. 395-428.

Burnham, C.W., 1967, Hydrothermal fluids at the magmatic stage, *in* Barnes, H.L., ed., Geochemistry of hydrothermal ore deposits (1st edition): New York, Holt, Rinehart, and Winston, Inc., p. 34-76.

Burnham, C.W., 1979, Magmas and hydrothermal fluids, *in* Barnes, H.L., ed., Geochemistry of hydrothermal ore deposits (2nd edition): New York, John Wiley and Sons, Ltd., p. 71-136.

Burnham, C.W., and Ohmoto, H., 1980, Late-stage processes of felsic magmatism, *in* Ishihara, S., and Takenouchi, S., eds., Granitic magmatism and related mineralization: Mining Geology Special Issue, no. 8, p. 1-11.

Candela, P.A., 1989a, Magmatic ore-forming fluids: thermodynamic and mass-transfer calculations of metal concentrations, *in* Whitney, J.A., and Naldrett, A.J., eds., Ore deposition associated with magmas: Reviews in Economic Geology no. 4, Society of Economic Geologists, p. 203-221.

Candela, P.A., 1989b, Felsic magmas, volatiles and metallogenesis, *in* Whitney, J.A., and Naldrett, A.J., eds., Ore deposition associated with magmas: Reviews in Economic Geology no. 4, Society of Economic Geologists, p. 222-233.

Cargill, D.G., Lamb, J., Young, M.J., and Rugg, E.S., 1976, Island Copper, *in* Sutherland Brown, A., ed., Porphyry deposits of the Canadian Cordillera: Canadian Institute of Mining and Metallurgy Special Volume 15, p. 206-218.

Carten, R.B., 1986, Sodium-calcium metasomatism chemical, temporal, and spatial relationships at the Yerington, Nevada, porphyry copper deposit: Economic Geology, v. 81, p. 1495-1519.

Carten, R.B., Geraghty, E.P., Walker, B.M., and Shannon, J.R., 1988, Cyclic development of igneous features and their relationship to high-temperature hydrothermal features in the Henderson porphyry molybdenum deposit, Colorado: Economic Geology, v. 83, p. 266-296.

Carten, R.B., Walker, B.M., Geraghty, E.P., and Gunow, A.J., 1988, Comparison of field-based studies of the Henderson porphyry molybdenum deposit, Colorado, with experimental and theoretical models of porphyry systems, *in* Taylor, R.P., and Strong, D.F., eds., Recent advances in the geology of granite-related mineral deposits: Canadian Institute of Mining and Metallurgy Special Volume 39, p. 351-366.

Chou, I.M., 1987, Phase relations in the system NaCl-KCl-H_2O: III. Solubility of halite in vapor-saturated liquids above 445°C and redetermination of phase equilibrium properties in the system NaCl-H_2O to 1000°C and 1000 bars: Geochimica et Cosmochimica Acta, v. 51, p. 1965-1975.

Clark, A.H., 1990, The slump breccias of the Toquepala porphyry Cu(-Mo) deposit, Peru: implications for fragment rounding in hydrothermal breccias: Economic Geology, v. 85, p. 1677-1685.

Clark, A.H., 1993, Are outsize porphyry copper deposits either anatomically or environmentally distinctive?, *in* Whiting, B.H., Mason, R., and Hodgson, C.J., eds., Giant ore deposits: Society of Economic Geologists Special Publication no. 2, p. 213-283.

Clark, A.H., Chen, Y., Langridge, R.J., and Farrar, E., in press, $^{40}Ar/^{39}Ar$ geochronology of batholith evolution and porphyry copper-molybdenum mineralization, Toquepala district, Moquegua, southeastern Peru:

Clark, A.H., Farrar, E., Kontak, D.J., Langridge, R.J., Arenas, M.J., France, L.J., McBride, S.L., Woodman, P.L., Wasteneys, H.A., Sandeman, H.A., and Archibald, D.A., 1990a, Geologic and geochronologic constraints on the metallogenic evolution of the Andes of southeastern Peru: Economic Geology, v. 85, p. 1520-1583.

Clark, A.H., Tosdal, R.M., Farrar, E., and Plazolles, A., 1990b, Geomorphological environment and age of supergene enrichment of the Cuajone, Quellaveco, and Toquepala porphyry copper deposits, southeastern Peru: Economic Geology, v. 85, p. 1604-1628.

Cline, J.S., and Bodnar, R.J., 1991, Can economic porphyry copper mineralization be generated by a typical calc-alkaline melt?: Journal of Geophysical Research, v. 96, no. B5, p. 8113-8126.

Crawford, M.L., 1981, Phase equilibria in aqueous fluid inclusions, *in* Hollister, L.S. and Crawford, M.L., eds., Short course in fluid inclusions: applications to petrology: Mineralogical Association of Canada, v. 6, p. 75-100.

Crawford, M.L., Kraus, D.W., and Hollister, L.S., 1979, Petrologic and fluid inclusion study of calc-silicate rocks, Prince Rupert, British Columbia: American Journal of Science, v. 9, p. 1135-1159.

Damiani, O., 1967, Algunos aspectos de la mineralización hipógena de Toquepala: Lima, Southern Peru Copper Corporation, unpublished company report, 34 p.

Damiani, O., 1969, Aplicación practica estudio de alteración-mineralización de la diorita de Toquepala: Arequipa, Universidad Nacional de San Agustín, B.Sc. thesis [unpublished], 40 p.

de Silva, S.L., and Francis, P.L., 1991, Volcanoes of the Andes: Berlin, Springer-Verlag, 216 p.

Dilles, J.H., and Einaudi, M.T., 1992, Wall-rock alteration and hydrothermal flowpaths about the Ann-Mason porphyry copper deposit, Nevada: a 6-km vertical reconstruction: Economic Geology, v. 87, p. 1963-2001.

Einaudi, M.T., 1982, Description of skarns associated with porphyry copper plutons, southwestern North America, *in* Titley, S.R., ed., Advances in geology of the porphyry copper deposits, Southwestern North America: Tucson, University of Arizona Press, p. 139-183.

Estrada, F., 1975, Geología de Quellaveco: Boletín de la Sociedad Geológica del Perú, v. 46, p. 65-86.

Fletcher, C.J.N., 1977, The geology, mineralization, and alteration of Ilkwang mine, Republic of Korea: A Cu-W-bearing tourmaline breccia pipe: Economic Geology, v. 72, p. 753-768.

Fox, P.E., Grove, E.W., Seraphim, R.H., and Sutherland Brown, A., 1976, Schaft Creek, *in* Sutherland Brown, A., ed., Porphyry deposits of the Canadian Cordillera: Canadian Institute of Mining and Metallurgy Special Volume 15, p. 219-226.

Freemark, T., 1977, A study of intrusive breccias at Toquepala, Peru, and their relation to porphyry copper formation: Kingston, Queen's University, B.Sc. thesis [unpublished], 49 p.

Gilmour, P., 1982, Grades and tonnages of porphyry copper deposits, *in* Titley, S.R., ed., Advances in geology of the porphyry copper deposits, Southwestern North America: Tucson, University of Arizona Press, p. 7-36.

Grant, J.N., Halls, C., Avila, S.W., and Avila, G., 1977, Igneous geology and the evolution of hydrothermal systems in some sub-volcanic tin deposits of Bolivia, *in* Volcanic processes in ore genesis: London, Institution of Mining and Metallurgy/Geological Society of London, p. 117-126.

Gustafson, L.B., 1978, Some major factors of porphyry copper genesis: Economic Geology, v. 73, p. 600-607.

Gustafson, L.B., and Hunt, J.P., 1975, The porphyry copper deposit at El Salvador, Chile: Economic Geology, v. 70, p. 857-912.

Haas, J.L., Jr., 1976, Physical properties of the coexisting phases and the thermochemical properties of the H_2O component in boiling NaCl solutions: U.S. Geological Survey Bulletin 1421-A, 73 p.

Hart, L.H., 1958, Geology of Toquepala, Peru — discussion: Mining Engineering, v. 10, p. 699-700.

Hearwole, D.A., 1973, Occurrence and distribution of tourmaline in the El Salvador orebody, El Salvador, Chile: Unpublished company report, The Anaconda Company, 29 p.

Hollister, V.F., 1979, Porphyry copper-type deposits of the Cascade volcanic arc, Washington: Minerals Science and Engineering, v. 11, no. 1, p. 22-35.

Howell, F.H., and Molloy, J.S., 1960, Geology of the Braden orebody, Chile, South America: Economic Geology, v. 55, p. 863-905.

Hudson, D.M., 1977, Geology and alteration of the Wedekind and part of the Peavine districts, Washoe County, Nevada: Reno, Nevada, University of Nevada, M.S. thesis [unpublished], 101 p.

James, D.E., Brooks, C., and Cuyobumba, A., 1974, Strontium isotopic composition and K-Rb-Sr geochemistry of Mesozoic volcanic rocks of the Central Andes: Carnegie Institute of Washington Yearbook, v. 73, p. 970-983.

Jenks, W.F., 1948, Geología de la Hoja de Arequipa: Instituto Geología del Perú, Boletín 9, 204 p.

John, D.A., 1989, Evolution of hydrothermal fluids in the Park Premier stock, central Wasatch Mountains, Utah: Economic Geology, v. 84, p. 879-902.

Keith, J.D., Shanks, W.C., III, Archibald, D.A., and Farrar, E., 1986, Volcanic and intrusive history of the Pine Grove Porphyry-Molybdenum system, southwestern Utah: Economic Geology, v. 81, p. 553-577.

Klinck, B.A., Ellison, R.A., and Hawkins, M.P., compilers, 1986, The geology of the Cordillera Occidental and Altiplano west of Lake Titicaca, southern Peru: Lima, Peru, British Geological Survey and Instituto Geologico, Minero y Metalúrgico, 353 p.

Laharie, R., 1973, Geomorfología y volcanismo en los Andes del Sur del Perú: Arequipa, Perú, Tercer ciclo de conferencias de geomorfología, 72 p.

Langerfeldt, H., 1964, Pebble dikes at El Salvador: El Salvador, Chile, Andes Copper Mining Company, unpublished company report.

Lemeyre, J., and Bowden, P., 1982, Classification of plutonic rocks: discrimination of various granitic series by their modal composition: Journal of Volcanology and Geothermal Research, v. 14, p. 169-186.

Llambias, E.J., and Malvicini, Lidia, 1969, The geology and genesis of the Bi-Cu mineralized breccia pipe, San Francisco de los Andes, San Juan, Argentina: Economic Geology, v. 64, p. 271-286.

Lowder, G.G., and Dow, J.A.S., 1978, Geology and exploration of porphyry copper deposits in North Sulawesi, Indonesia: Economic Geology, v. 73, p. 628-644.

Manrique, J., and Plazolles, A., 1975, Geología de Cuajone: Boletín de la Sociedad Geológica del Perú, v. 46, p. 137-150.

Marocco, R., and Noblet, C., 1990, Sedimentation, tectonism and volcanism relationships in two Andean basins of southern Peru: Geologische Rundschau, v. 79, p. 111-120.

Mendívil, S., 1965, Geología de los cuadrángulos de Maure y Antajave: Comisión de la Carta Geológia Nacional, Perú, Boletín 10, 99 p.

Mendoza, J., 1980, Estudio mineralógico de muestras del yacimiento de Toquepala: Lima, Southern Peru Copper Corporation, unpublished report, 44 p.

Meyer, C., and Hemley, J.J., 1967, Wall rock alteration, *in* Barnes, H.L., ed., Geochemistry of hydrothermal ore deposits (1st edition): New York, Holt, Rinehart, and Winston, Inc., p. 166-235.

Meyer, Charles, Shea, E.P., Goddard, C.C., Jr., Zeihen, L.G., Guilbert, J.M., Miller, R.N., McAleer, J.F., Brox, G.B., Ingersoll, R.G., Jr., Burns, G.J., and Wigal, Thomas, 1968, Ore deposits at Butte, Montana, *in* Ridge, J.D., ed., Ore deposits of the United States, The Graton-Sales Volume: New York, The American Institute of Mining, Metallurgical, and Petroleum Engineers, Inc., p. 1373-1416.

Nash, J.T., 1976, Fluid-inclusion petrology — data from porphyry copper deposits and application to exploration: U.S. Geological Survey Professional Paper 907-D, 15 p.

Phillips, W.J., 1973, Mechanical effects of retrograde boiling and its probable importance in the formation of some porphyry ore deposits: London, Transactions of the Institution of Mining and Metallurgy, Section B: Applied Earth Science, v. 82, p. B90-B98.

Pichavant, M., 1981, An experimental study of the effect of boron on a water-saturated haplogranite at 1 kbar pressure; geological applications: Contributions to Mineralogy and Petrology, v. 76, p. 430–439.

Pichavant, M., 1987, Effects of B and H_2O on liquidus phase relations in the haplogranite system at 1 kbar: American Mineralogist, v. 72, p. 1056-1070.

Pitcher, W.S., 1985, A multiple and composite batholith, *in* Pitcher, W.S., Atherton, M.P., Cobbing, E.J., and Beckinsale, R.D., eds., Magmatism at a plate edge: the Peruvian Andes: Glasgow, Blackie and Sons, p. 93-101.

Pitcher, W.S., Atherton, M.P., Cobbing, E.J., and Beckinsale, R.D., eds., 1985, Magmatism at a plate edge: the Peruvian Andes: Glasgow, Blackie and Sons, 328 p.

Plazolles, A., 1981, Zona de yeso-anhidrita en el yacimiento de Toquepala: Lima, Southern Peru Copper Corporation, unpublished company report, 20 p.

Potter, R.W., II, 1977, Pressure corrections for fluid-inclusion homogenization temperatures based on the volumetric properties of the system NaCl-H_2O: Journal of Research of the U.S. Geological Survey, v. 5, p. 603-607.

Richard, K., and Courtright, J.H., 1958a, Geology of Toquepala, Peru: Mining Engineering, v. 10, p. 262-266.

Richard, K., and Courtright, J.H., 1958b, Geology of Toquepala, Peru — discussion: Mining Engineering, v. 10, p. 700.

Richard, K., Courtright, J.H., and Staff, 1951, Maps, Toquepala deposit area: Lima, Peru, Southern Peru Copper Corporation, unpublished geologic reports.

Roedder, E., 1967, Fluid inclusions as samples of ore fluids, *in* Barnes, H.L., ed., Geochemistry of hydrothermal ore deposits (1st edition): New York, Holt, Rinehart, and Winston, Inc., p. 515-574.

Roedder, E., 1971, Fluid inclusion studies on the porphyry-type ore deposits at Bingham, Utah; Butte, Montana; and Climax, Colorado: Economic Geology, v. 66, p. 98-120.

Roedder, E., 1979, Fluid inclusions as samples of ore fluids, *in* Barnes, H.L., ed., Geochemistry of hydrothermal ore deposits (2nd edition): New York, John Wiley and Sons, Ltd., p. 684-737.

Roedder, E., and Bodnar, R.J., 1980, Geologic pressure determinations from fluid inclusion studies: Annual Review of Earth and Planetary Science, v. 8, p. 263-301.

Schwartz, M.O., 1982, The porphyry copper deposit at La Granja, Peru: Economic Geology, v. 77, p. 482–488.

Sébrier, M., Fornari, M., Vatin-Perignon, N., Vivier, G., and Cabrera, J., 1983, Nuevas edades radiométricas del volcanismo Cenozoico del Sur del Perú: implicancias en la tectorogénesis andina [abs.]: Sociedad Geológica del Perú, V Congreso Peruano Geología, Lima, Libro de Resumenes, p. GR-16.

Shanks, T., 1977, Fluid inclusions in the Toquepala porphyry copper deposit: a reconnaissance study: Kingston, Queen's University, B.Sc. thesis [unpublished], 49 p.

Shaver, S.A., 1984, The Hall (Nevada Moly) molybdenum deposit, Nye County, Nevada: geology, alteration, mineralization, and geochemical dispersion: Stanford, California, Stanford University, Ph.D. thesis [unpublished], 261 p.

Sheppard, S.M.F., and Gustafson, L.B., 1976, Oxygen and hydrogen isotopes in the porphyry copper deposit at El Salvador, Chile: Economic Geology, v. 71, p. 1549-1559.

Sheppard, S.M.F., Nielson, R.L., and Taylor, H.P., Jr., 1969, Oxygen and hydrogen isotope ratios of clay minerals from porphyry copper deposits: Economic Geology, v. 64, p. 755-777.

Sheppard, S.M.F., Nielson, R.L., and Taylor, H.P., Jr., 1971, Hydrogen and oxygen isotope ratios in minerals from porphyry copper deposits: Economic Geology, v. 66, p. 515-542.

Shinohara, H., Iiyama, J.T., and Matsuo, S., 1989, Partition of chlorine compounds between silicate melt and hydrothermal solutions: I. Partition of NaCl-KCl: Geochimica et Cosmochimica Acta, v. 53, p. 2617-2630.

Sillitoe, R.H., 1973, Geology of the Los Pelambres porphyry copper deposit, Chile: Economic Geology, v. 68, p. 1-10.

Sillitoe, R.H., 1985, Ore-related breccias in volcanoplutonic ores: Economic Geology, v. 80, p. 1467-1514.

Sillitoe, R.H., and Gappe, I.M., Jr., 1984, Philippine porphyry copper deposits: geologic setting and characteristics: United Nations Development Program, Committee for Co-ordination of Joint Prospecting for Mineral Resources in Asian Offshore Areas (CCOP), Technical Publication 14, ESCAP, Bangkok, 89 p.

Sillitoe, R.H., Jaramillo, L., and Castro, H., 1984, Geologic exploration of a molybdenum rich porphyry copper deposit at Mocoa, Colombia: Economic Geology, v. 79, p. 106-123.

Sillitoe, R.H., and Sawkins, F.J., 1971, Geologic, mineralogic, and fluid inclusion studies relating to the origin of copper-bearing tourmaline breccia pipes, Chile: Economic Geology, v. 66, p. 1028-1041.

Steefel, C.I., and Atkinson, W.W., Jr., 1984, Hydrothermal andalusite and corundum in the Elkhorn district, Montana: Economic Geology, v. 79, p. 573-579.

Stevenson, F.B., 1981, Exploration of the Toquepala deep Orebody — 3100 to 2695 Levels: Lima, Peru, Southern Peru Copper Corporation, unpublished company report.

Stevenson, F.B., and Damiani, O., 1968, Interpretación estructural del deposito de Toquepala: Lima, Peru, Southern Peru Copper Corporation, unpublished company report, 27 p.

Streckeisen, A., 1976, To each rock its proper name: Earth Science Reviews, v. 12, p. 181-217.

Taylor, R.P., Jr., 1974, The application of oxygen and hydrogen isotope studies to problems of hydrothermal alteration and ore deposition: Economic Geology, v. 69, p. 843-883.

Tosdal, R.M., Farrar, E., and Clark, A.H., 1981, K-Ar geochronology of the late Cenozoic volcanic rocks of the Cordillera Occidental, southern most Peru: Journal of Volcanology and Geothermal Research, v. 10, p. 157-173.

Tosdal, R.M., Clark, A.H., and Farrar, E., 1984, Cenozoic polyphase landscape and tectonic evolution of the Cordillera Occidental southernmost Peru: Geological Society of America Bulletin, v. 95, p. 1318-1332.

Walker, V.A., 1979, Relationships among several breccia pipes and a lead-silver vein in the Copper Creek Mining District, Pinal County, Ari-

zona: Tucson, Arizona, University of Arizona, M.S. thesis [unpublished], 163 p.

Warnaars, F.W., Holmgren, D.C., and Barassi, F.S., 1985, Porphyry copper and tourmaline breccias of Los Bronces — Río Blanco, Chile: Economic Geology, v. 80, p. 1544–1565.

Webster, J.D., 1992, Fluid-melt interactions involving Cl-rich granites: experimental study from 2 to 8 kbar: Geochimica et Cosmochimica Acta, v. 56, p. 659–678.

Whitney, J.A., Hemley, J.J., and Simon, F.O., 1985, The concentration of iron in chloride solutions equilibrated with synthetic granitic compositions; the sulfur-free system: Economic Geology, v. 80, p. 444–460.

Williams, T.J., Candela, P.R., and Piccoli, P.M., 1992, The partitioning of copper between a high-silica rhyolite and a chloride-bearing, [illegible]-phase aqueous mixture; comparison of experimental results at 1 kbar, 800°C, and ½ kbar, 850°C [abs.]: EOS, Transactions of the American Geophysical Union, v. 73, no. 43, p. 606.

Wilson, J.J., and Garcia, W., 1962, Geología de los cuadrángulos de Pachia y Palca: Comisión de la Carta Geológica Nacional Perú Boletín, v. II, no. 4, 82 p.

Zweng, P.L., 1984, Evolution of the Toquepala porphyry Cu(-Mo) deposit, Peru: Kingston, Queen's University, M.S. thesis [unpublished], 131 p.